



RS2

Joint Analysis

Verification Manual

Table of Contents

Updates	6
1. Goodman and Bray Block Toppling Example #1	7
1.1. Introduction.....	7
1.2. Problem Description	7
1.3. Geometry and Properties	7
1.4. Results	9
2. Alejano and Alonso Block Toppling	12
2.1. Introduction.....	12
2.2. Problem Description	12
2.3. Geometry and Properties	12
2.4. Results	13
3. Lorig and Varona Forward Block Toppling	15
3.1. Introduction.....	15
3.2. Problem Description	15
3.3. Geometry and Properties	15
3.4. Results	16
4. Lorig and Varona Flexural Toppling	19
4.1. Introduction.....	19
4.2. Problem Description	19
4.3. Geometry and Properties	19
4.4. Results	20
5. Lorig and Varona Backward Block Toppling	24
5.1. Introduction.....	24
5.2. Problem Description	24
5.3. Geometry and Properties	24
5.4. Results	25
6. Lorig and Varona Plane Failure with Daylighting Discontinuities	28
6.1. Introduction.....	28
6.2. Problem Description	28
6.3. Geometry and Properties	28
6.4. Results	29
7. Lorig and Varona Plane Failure with Non-Daylighting Discontinuities.....	32

7.1. Introduction.....	32
7.2. Problem Description.....	32
7.3. Geometry and Properties	32
7.4. Results	33
8. Flexural Toppling in Base Friction Model	36
8.1. Introduction.....	36
8.2. Problem Description.....	36
8.3. Geometry and Properties	36
8.4. Results	37
9. Alejano et al. Bilinear Slab Failure Example 1a	42
9.1. Introduction.....	42
9.2. Problem Description.....	42
9.3. Geometry and Properties	43
9.4. Results	43
10. Alejano et al. Bilinear Slab Failure Example 1b	47
10.1. Introduction.....	47
10.2. Problem Description.....	47
10.3. Geometry and Properties	48
10.4. Results	48
11. Alejano et al. Ploughing Sliding Slab Failure.....	52
11.1. Introduction.....	52
11.2. Problem Description.....	52
11.3. Geometry and Properties	53
11.4. Results	53
12. Alejano et al. Ploughing Toppling Slab Failure	57
12.1. Introduction.....	57
12.2. Problem Description.....	57
12.3. Geometry and Properties	58
12.4. Results	59
13. Alejano et Al. Ploughing Sliding Slab Failure	62
13.1. Introduction.....	62
13.2. Problem Description.....	62
13.3. Geometry and Properties	63
13.4. Results	63

14. Alejano et al. Ploughing Sliding Slab Failure.....	65
14.1. Introduction.....	65
14.2. Problem Description.....	65
14.3. Geometry and Properties.....	66
14.4. Results.....	66
15. Alejano et Al. Partially Joint - Controlled Footwall Slope Failure.....	68
15.1. Introduction.....	68
15.2. Problem Description.....	68
15.3. Geometry and Properties.....	69
15.4. Results.....	69
16. Barla et al. Partially Joint - Controlled Footwall Slope Failure.....	72
16.1. Introduction.....	72
16.2. Problem Description.....	72
16.3. Geometry and Properties.....	73
16.4. Results.....	73
17. Step-Path Failure with En-Echelon Joints.....	77
17.1. Introduction.....	77
17.2. Problem Description.....	77
17.3. Geometry and Properties.....	77
17.4. Results.....	78
18. Step-Path Failure with Continuous Joints.....	82
18.1. Introduction.....	82
18.2. Problem Description.....	82
18.3. Geometry and Properties.....	82
18.4. Results.....	83
19. Bi-Planar Step-Path Failure.....	86
19.1. Introduction.....	86
19.2. Problem Description.....	86
19.3. Geometry and Properties.....	86
19.4. Results.....	87
20. Hammah and Yacoub Slope with Voronoi Joints.....	90
20.1. Introduction.....	90
20.2. Problem Description.....	90
20.3. Geometry and Properties.....	90

20.4. Results	91
21. Shallow Excavation - Tunnel	95
21.1. Introduction.....	95
21.2. Problem Description.....	95
21.3. Geometry and Properties	95
21.4. Results	96
22. Joint Constitutive Model: Hyperbolic Softening.....	100
22.1. Introduction.....	100
22.2. Formulation and Problem description	100
22.3. Results	101
23. Joint Constitutive Model: Mohr Coulomb with Residual Strength and Dilation	103
23.1. Introduction.....	103
23.2. Formulation and Problem Description.....	103
23.2.1. Formulation.....	103
23.2.2. Problem Description	104
23.2.3. Dilation.....	104
23.2.4. Directional Dilation.....	105
23.3. Result and Discussion.....	105
23.3.1. Dilation.....	105
23.3.2. Directional Dilation.....	106
Bibliography	107

Updates

Most of models involving complicated joint networks needs to be carefully investigated and adjusted the convergence criteria (number of iterations and tolerance) so that the results are realistic especially with shear strength reduction analysis. In some cases, an excessive number of iterations were employed resulting a very long computation time.

A new algorithm has been introduced into the RS2 program to improve the convergence of joint network models. The program will automatically calculate the stiffness of the joint as soon as a joint violates the strength criteria. Using the new algorithm together with the accelerate stiffness results in a robust and fast calculation scheme for joint network model. The convergence parameters under *Advanced SSR Settings* are now able to match the convergence parameters under *Stress Analysis Settings* with 0.001 tolerance and 500 maximum numbers of iteration. Under *SSR Settings*, the new convergence type "*Absolute Force & Energy*" is added, and with this new convergence type, the option of "*Accelerate initial stiffness*" under *Stress Analysis* needs to be checked and defined with a min Alpha of 0.2 and a Max Alpha of 5. Please note that all of the settings are the default settings as shown when you open RS2 program. The following examples compare the results from previous results and the updated algorithm.

1. Goodman and Bray Block Toppling Example #1

1.1. Introduction

This verification looks at Example 1 in the paper:

Goodman, R. E., & Bray, J. W. (1976). Toppling of Rock Slopes. *Rock Engineering for Foundations and Slopes* (pp. 201 - 234). New York: American Society of Civil Engineers.

1.2. Problem Description

Four analyses of block toppling were performed in RS2. The analyses comprised of computing the factor of safety for examples 1a and 1b and the same examples with higher friction (page 222 of the paper), named examples 1c and 1d here. All examples include a stabilizing force at the toe of the slope. In the case of examples 1a and 1b, this force is the force required for limit equilibrium (FS=1) as computed by the Goodman and Bray method.

1.3. Geometry and Properties

Table 1.1: *Material Properties*

Analysis	ϕ' (deg.)	Force on Toe Block (kN)	γ (kN/m ³)
Example 1a	38.15	0.5	25.0
Example 1b	33.02	2013	25.0
Example 1c	38.66	0.5	25.0
Example 1d	38.66	2013	25.0

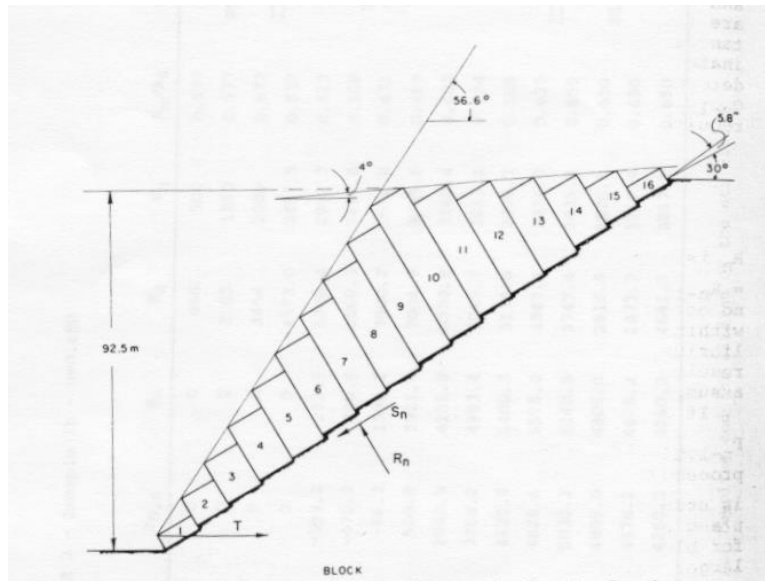


Figure 1.1: Geometry (Goodman and Bray, 1976)

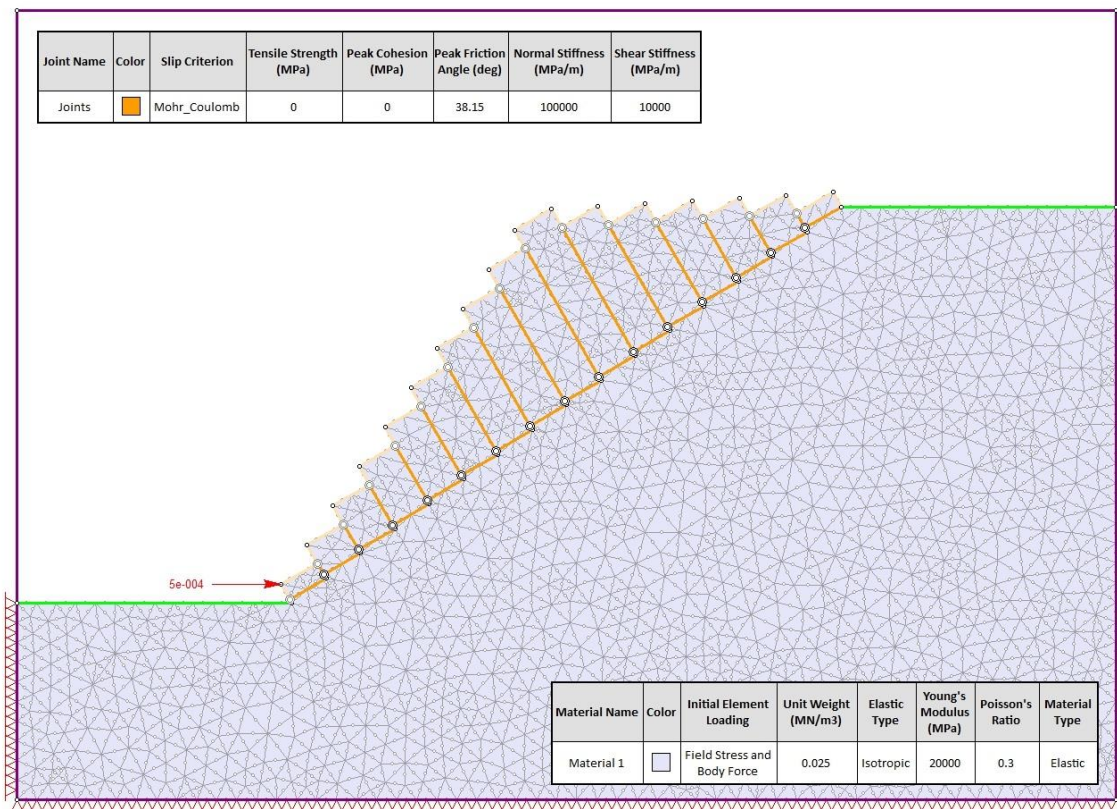


Figure 1.2: RS2 Model of Example 1a

1.4. Results

Table 1.2: *Factors of Safety*

Analysis	RS2 with joint improvement	RS2 without joint improvement	Goodman	UDEC
Example 1a	0.97	0.99	1.0	0.99
Example 1b	0.94	0.97	1.0	0.99
Example 1c	0.99	1.01	1.02	1.01
Example 1d	1.16	1.19	1.23	1.22

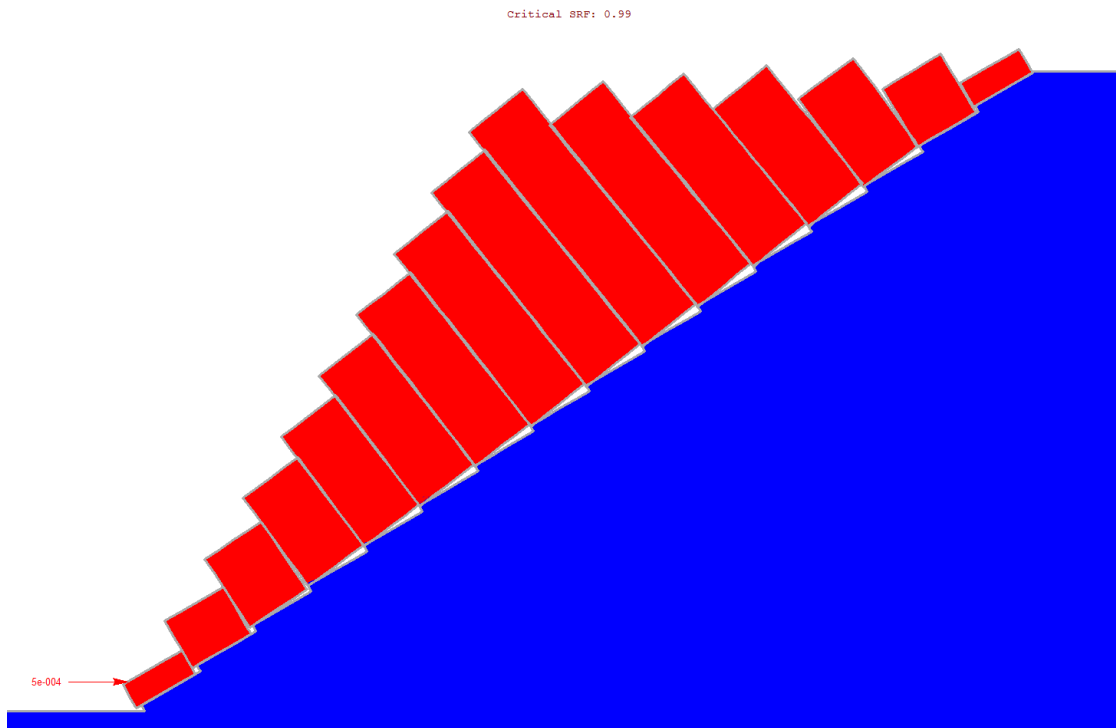


Figure 1.3a: Deformed Shape of Example 1a (RS2)

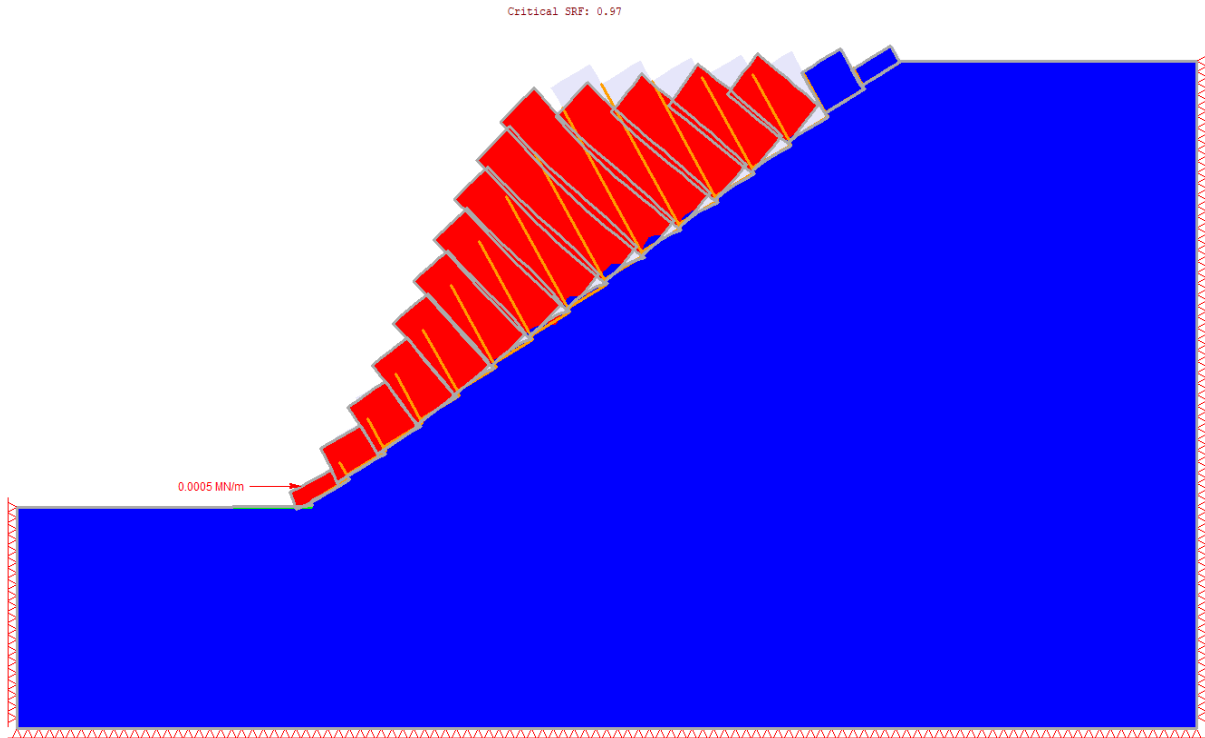


Figure 1.4: Deformed Shape of Example 1a (RS2-Joint convergence improved)

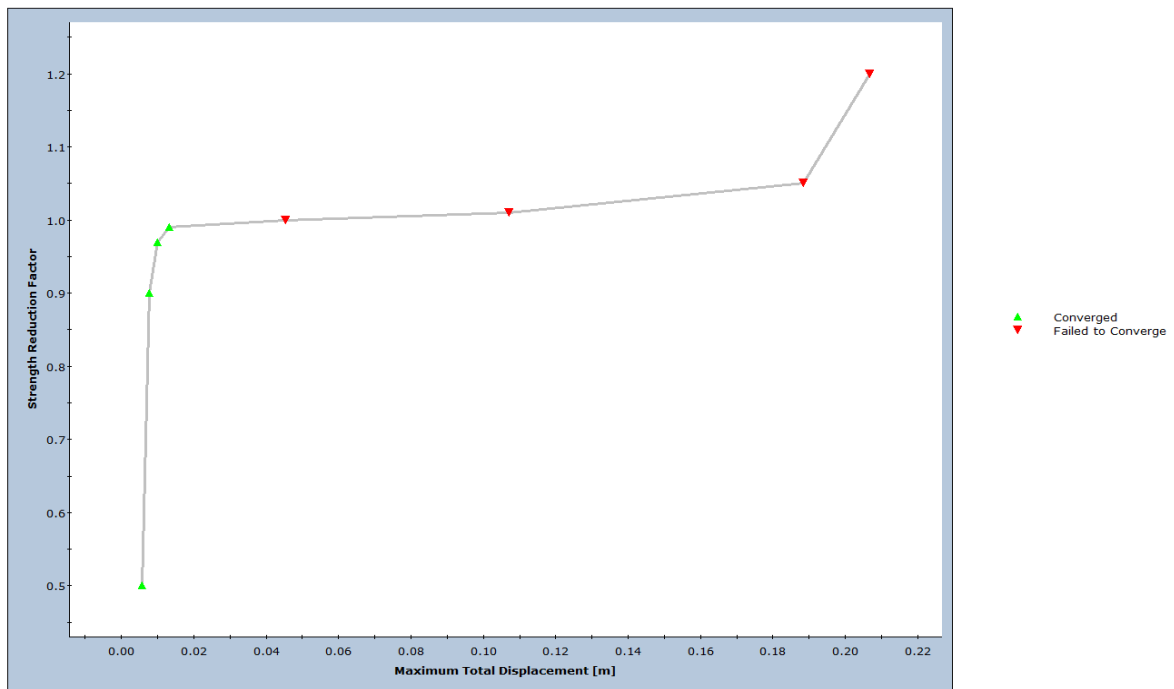


Figure 1.5: Shear Strength Reduction Plot (RS2)

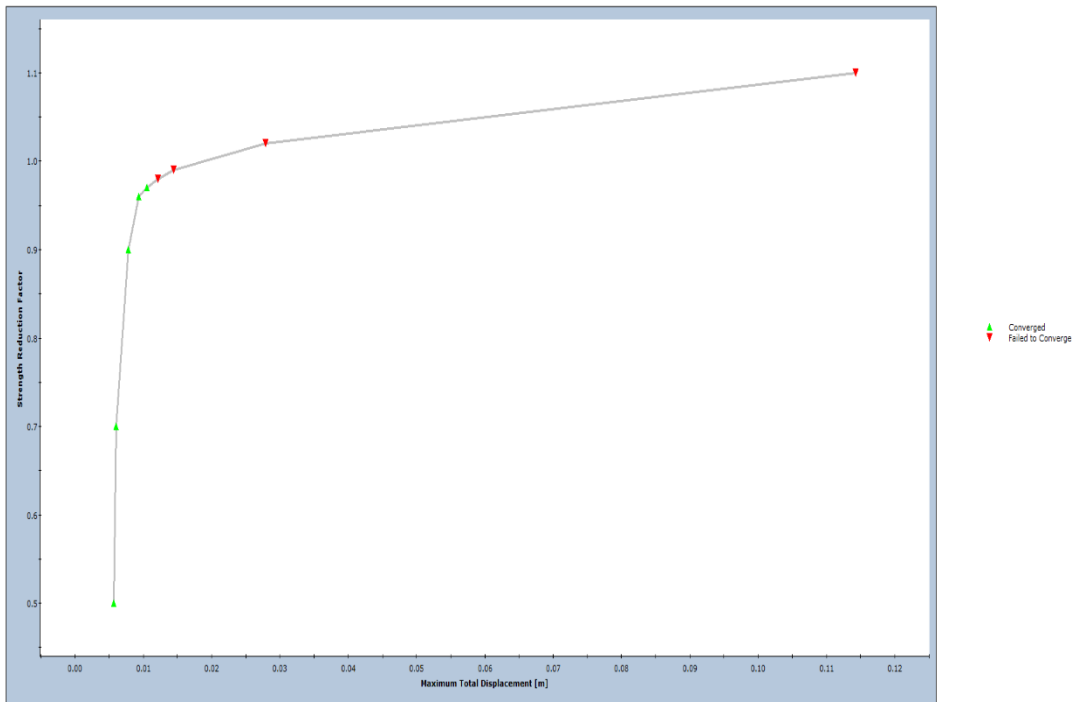


Figure 1.6: Shear Strength Reduction Plot (RS2-Joint convergence improved)

2. Alejano and Alonso Block Toppling

2.1. Introduction

This verification looks at the block toppling example from:

Alejano, L. R., & Alonso, E. (2005). Application of the 'Shear and Tensile Strength Reduction Technique' to Obtain Factors of Safety of Toppling and Footwall Rock slopes. *Eurock: Impact of Human Activity on the Geological Environment*.

2.2. Problem Description

An analysis of block toppling was performed in RS2 and was verified using Goodman and Bray's limit-equilibrium method and UDEC results from the paper.

2.3. Geometry and Properties

Table 2.1: Material Properties

Slope Height (m)	Slope Angle (deg)	Joint Angle (deg)	Step Surface (deg)	ϕ' (deg)	γ (kN/m ³)
9.85	58.65	64	30	31	25.0

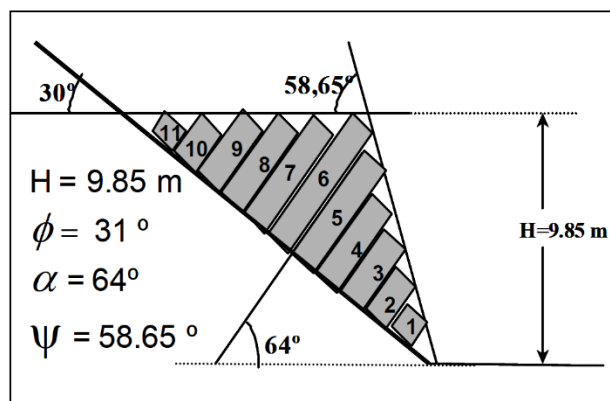


Figure 2.1: Goodman & Bray Geometry (Alejano & Alonso, 2005)

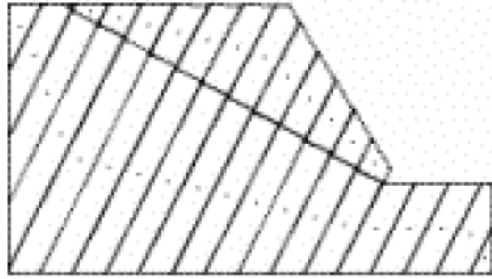


Figure 2.2: UDEC Geometry (Alejano & Alonso, 2005)

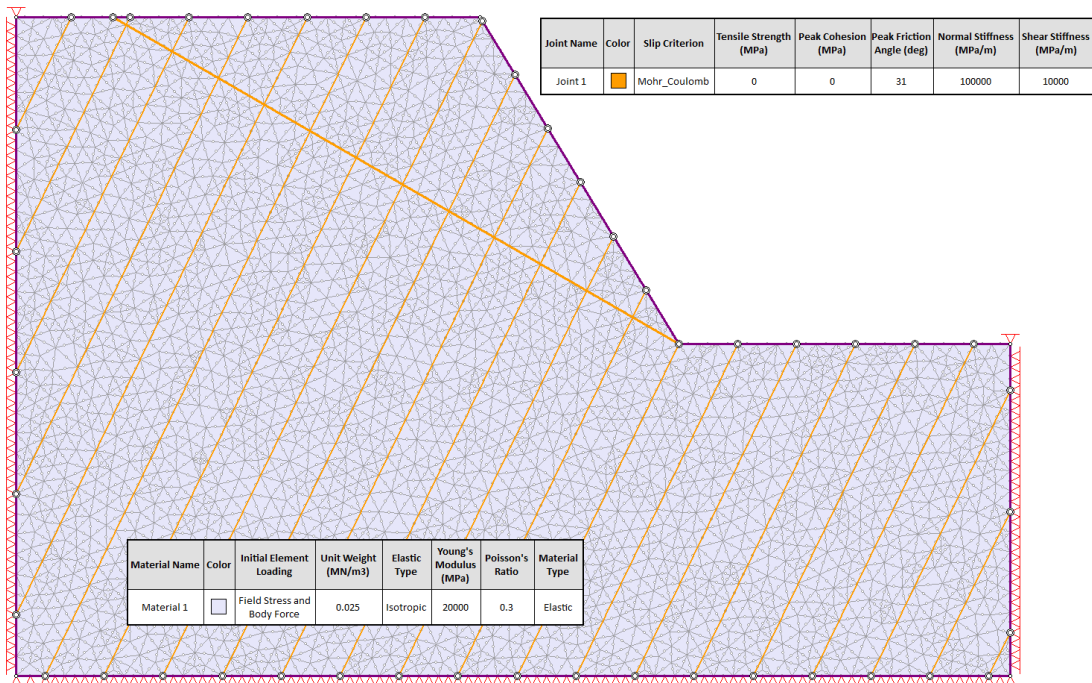


Figure 2.3: RS2 Geometry and Properties

2.4. Results

Table 2.2: Factor of Safety

Factor of Safety – RS2 with joint improvement	Factor of Safety - RS2 without joint improvement	Factor of Safety - UDEC	Factor of Safety - Goodman
0.82	0.86	0.87	0.76

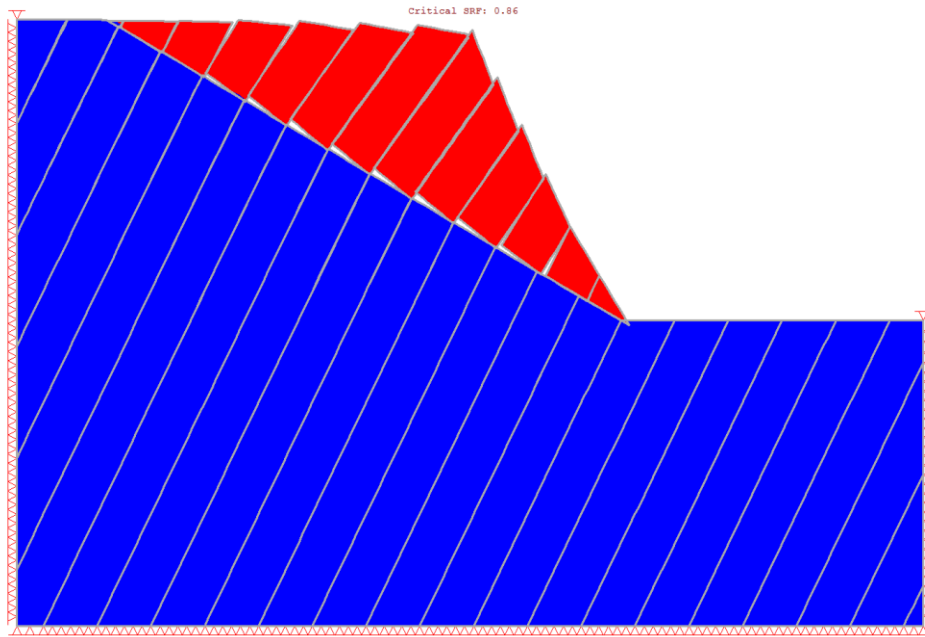


Figure 2.4: Deformed Shape (RS2)

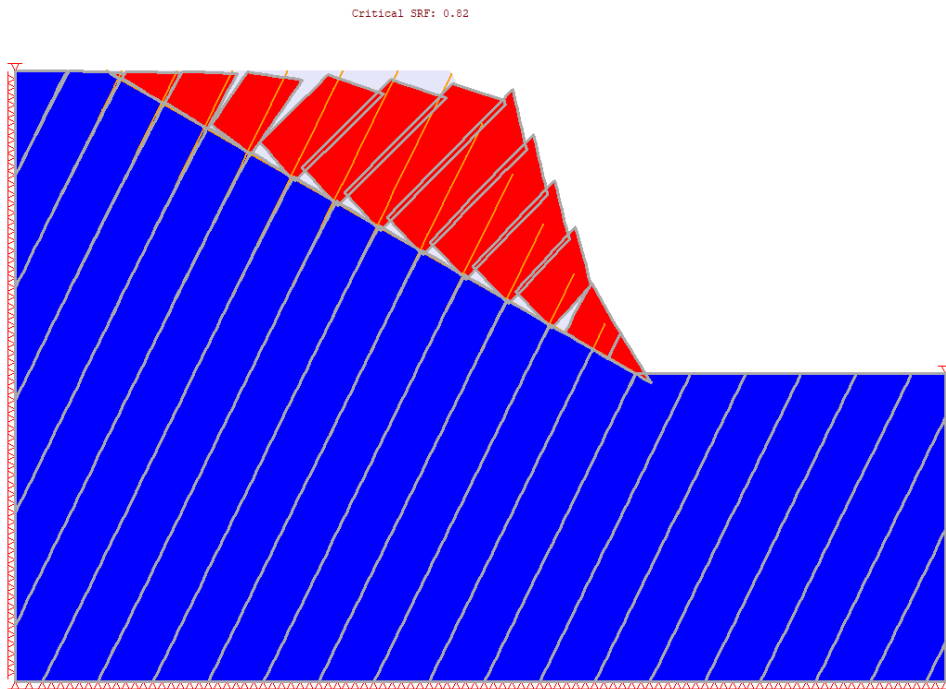


Figure 2.5: Deformed Shape (RS2-Joint convergence improved)

3. Lorig and Varona Forward Block Toppling

3.1. Introduction

This verification looks at the forward block toppling example from:

Lorig, L., & Varona, P. (2004). Toppling Failure - Block and Flexural. In D. C. Wyllie, & C. W. Mah, *Rock Slope Engineering Civil and Mining 4th Edition* (pp. 234-238). New York: Spon Press Taylor & Francis Group.

3.2. Problem Description

An analysis of forward block toppling was performed in RS2 and was verified using UDEC results provided in the reference.

3.3. Geometry and Properties

Table 3.1: Material Properties

Slope Height (m)	Slope Angle (deg)	Joint Angle (deg)	ϕ' joint (deg)	σ_t (rock) (MPa)	γ (kN/m ³)
260	55	70 and 160	40	0	26.1

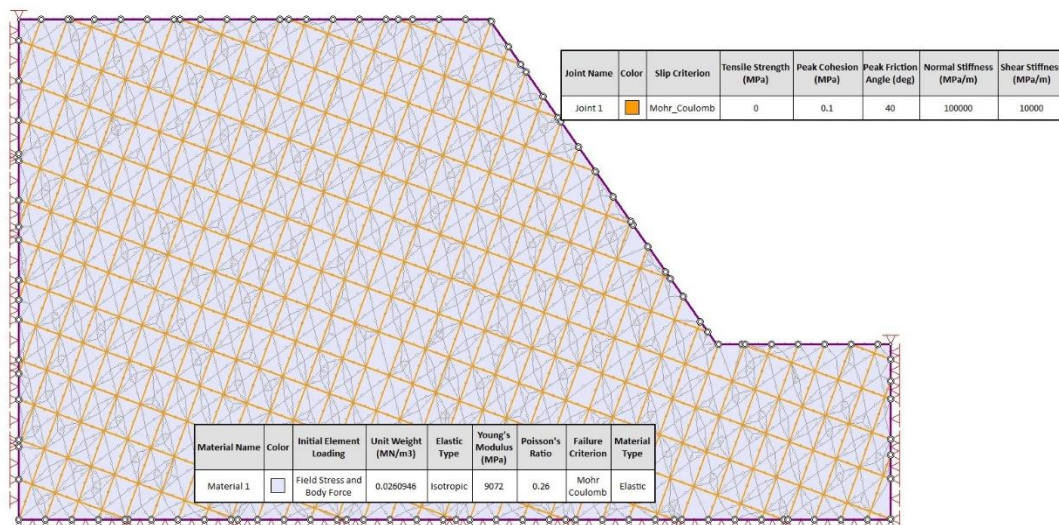


Figure 3.1: RS2 Geometry and Properties

3.4. Results

Table 3.2: Factor of Safety

Factor of Safety – RS2 with joint improvement	Factor of Safety – RS2 without joint improvement	Factor of Safety – UDEC
1.09	1.12	1.13

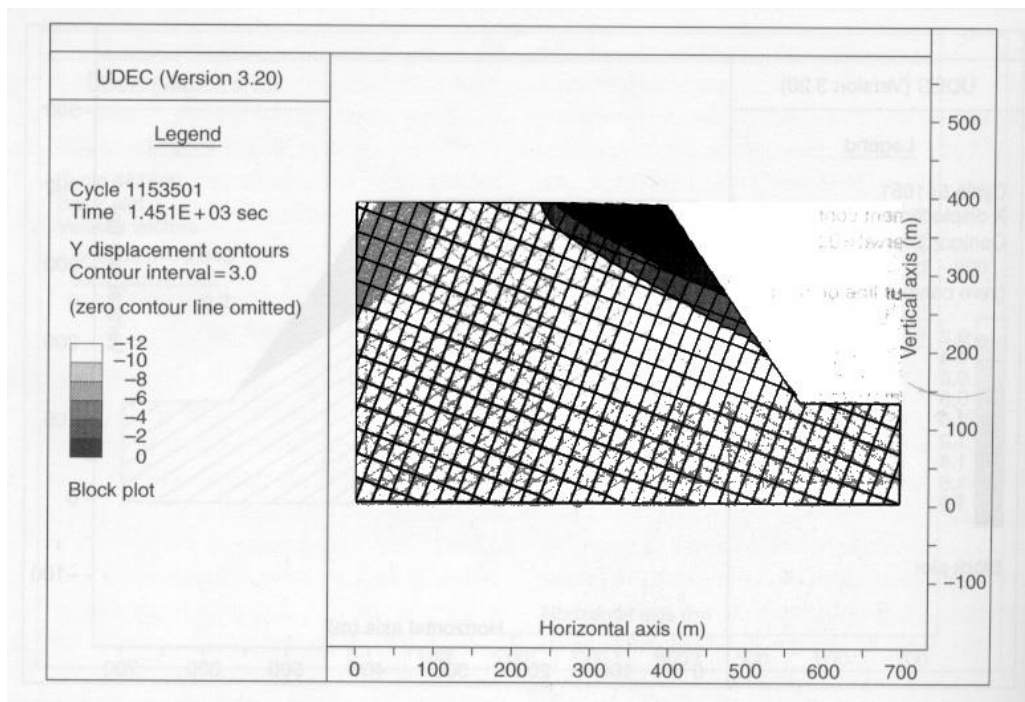


Figure 3.2: UDEC Geometry and Results (Lorig & Varona, 2004)

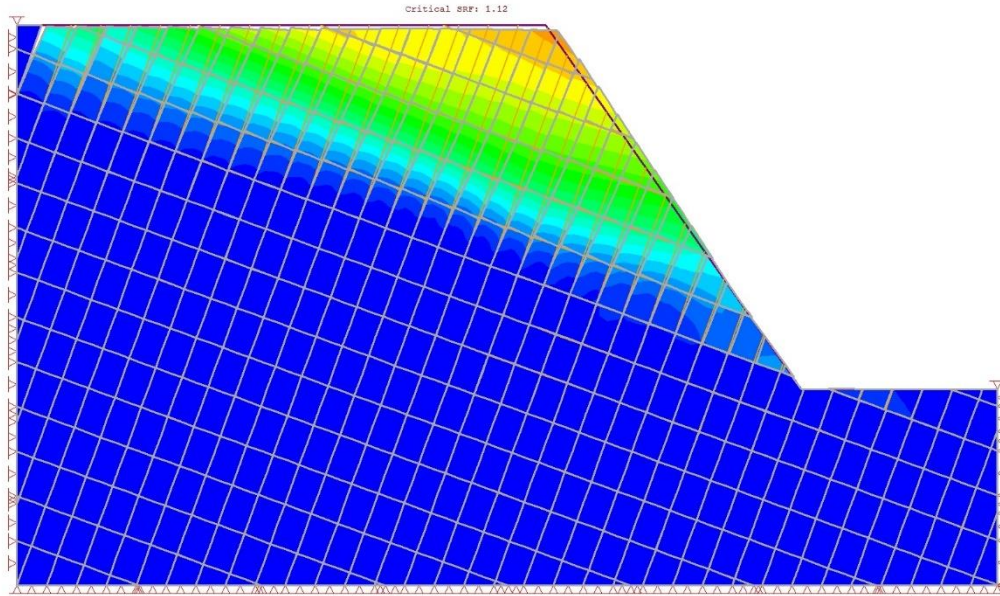


Figure 3.3: Total Displacement at SRF = 1.12 (RS2)

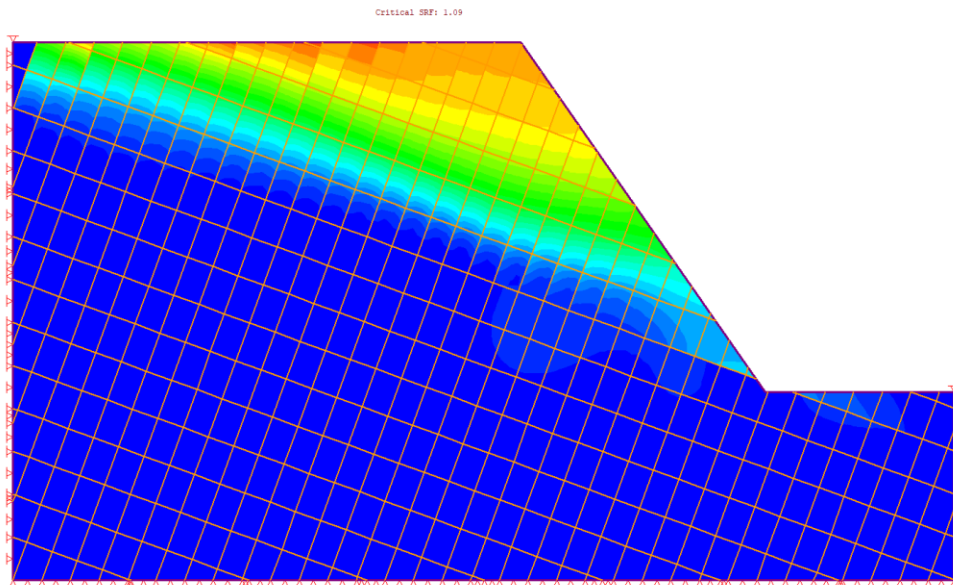


Figure 3.4: Total Displacement at SRF = 1.09 (RS2-Joint convergence improved)

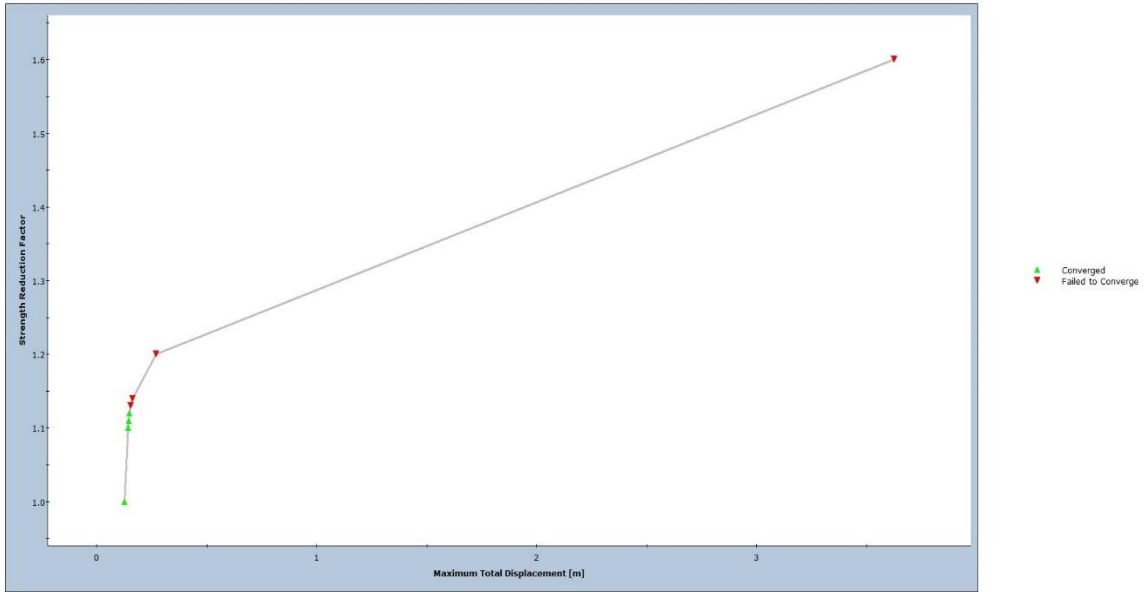


Figure 3.5: Shear Strength Reduction Plot (RS2)

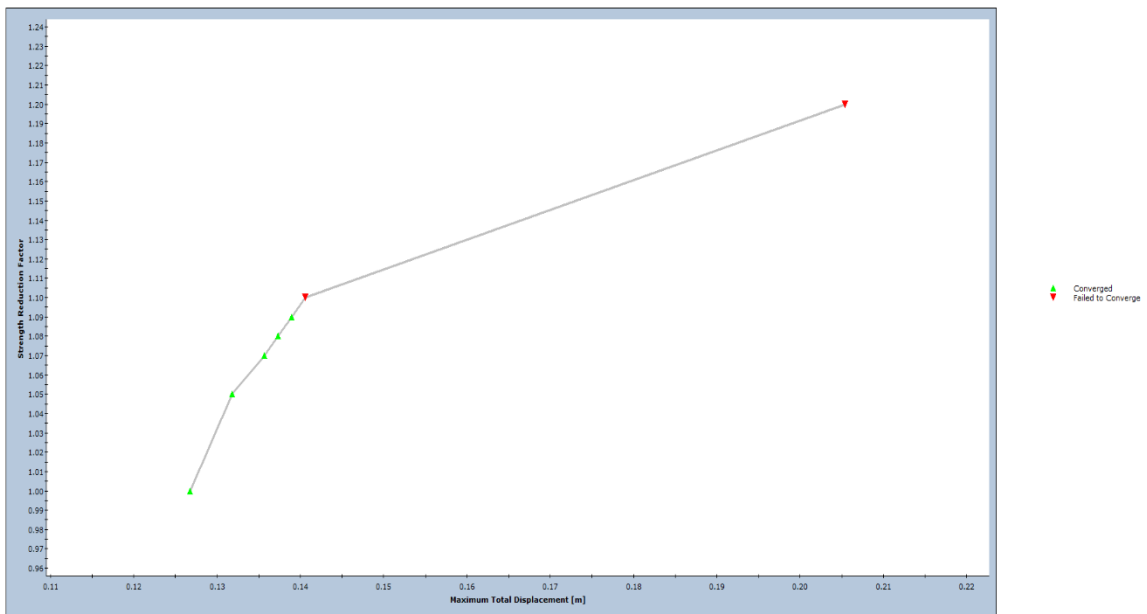


Figure 3.6: Shear Strength Reduction Plot (RS2-Joint convergence improved)

4. Lorig and Varona Flexural Toppling

4.1. Introduction

This verification looks at the flexural toppling example from:

Lorig, L., & Varona, P. (2004). Toppling Failure - Block and Flexural. In D. C. Wyllie, & C. W. Mah, *Rock Slope Engineering Civil and Mining 4th Edition* (pp. 234-238). New York: Spon Press Taylor & Francis Group.

4.2. Problem Description

An analysis of flexural toppling was performed in RS2 and was verified using UDEC results provided in the reference.

4.3. Geometry and Properties

Table 4.1: Material Properties

Slope Height (m)	Slope Angle (deg)	Joint Angle (deg)	ϕ' joint (deg)	σ_t (rock) (MPa)	γ (kN/m ³)
260	55	70	40	0	26.1

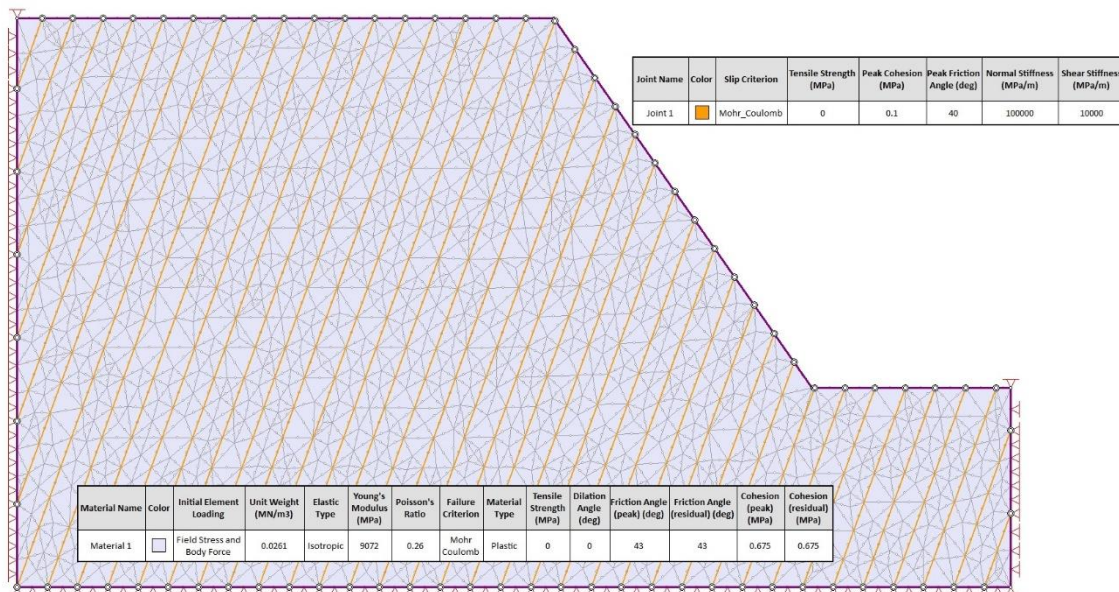


Figure 4.1: RS2 Geometry and Properties

4.4. Results

Table 4.2: Factor of Safety

Factor of Safety – RS2 with joint improvement	Factor of Safety – RS2 without joint improvement	Factor of Safety – UDEC
1.27	1.19	1.3

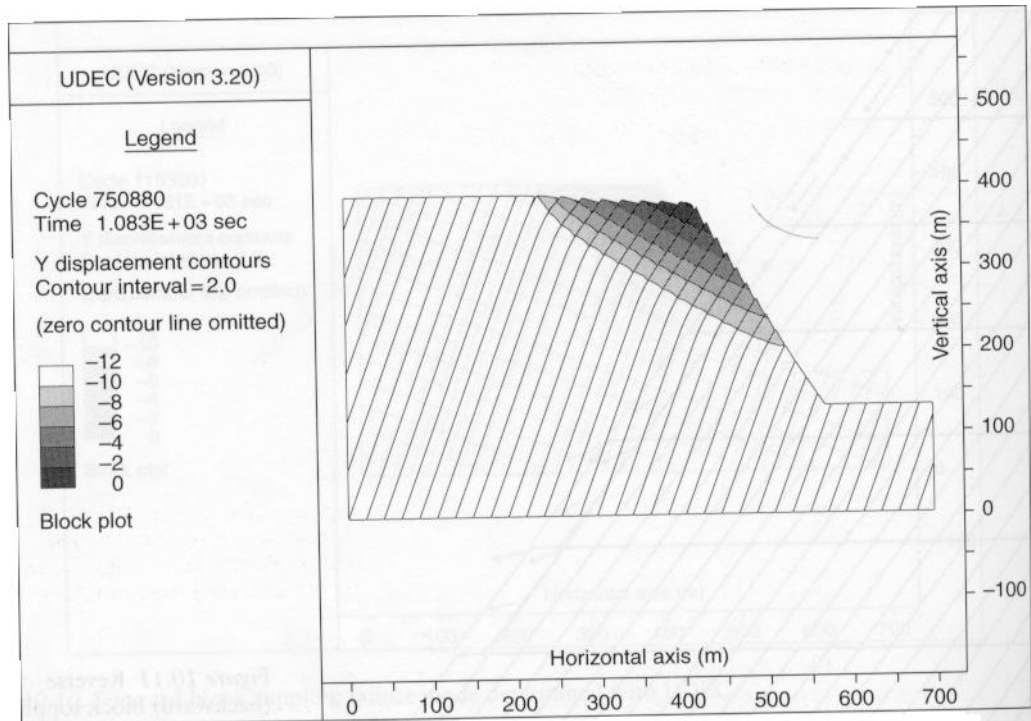


Figure 4.2: UDEC Geometry and Results (Lorig & Varona, 2004)

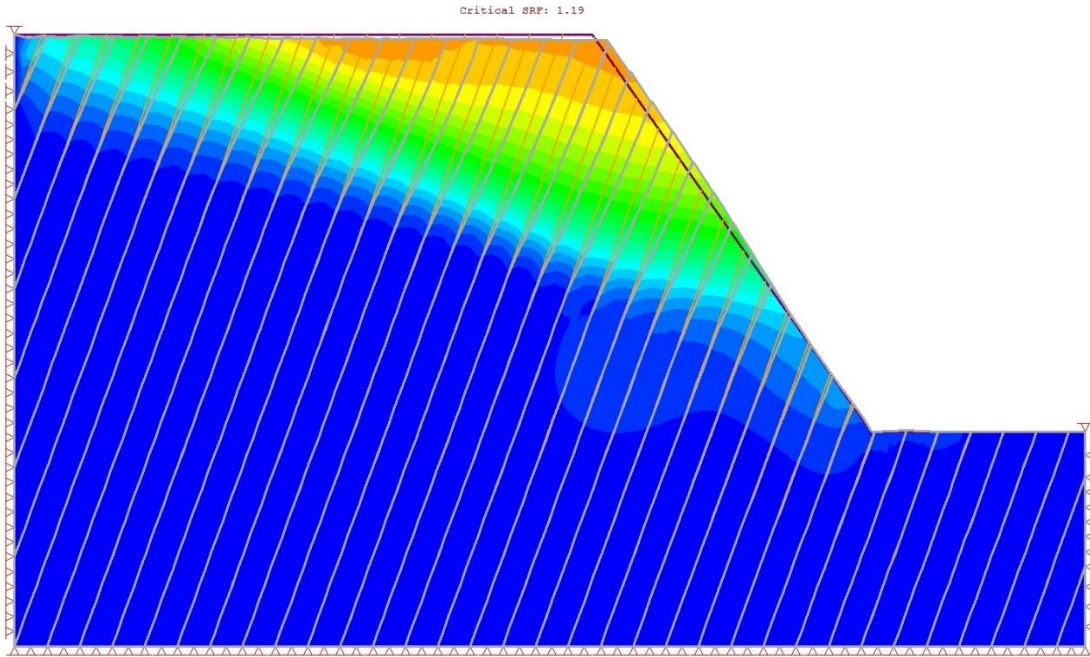


Figure 4.3: Total Displacement at SRF = 1.19 (RS2)

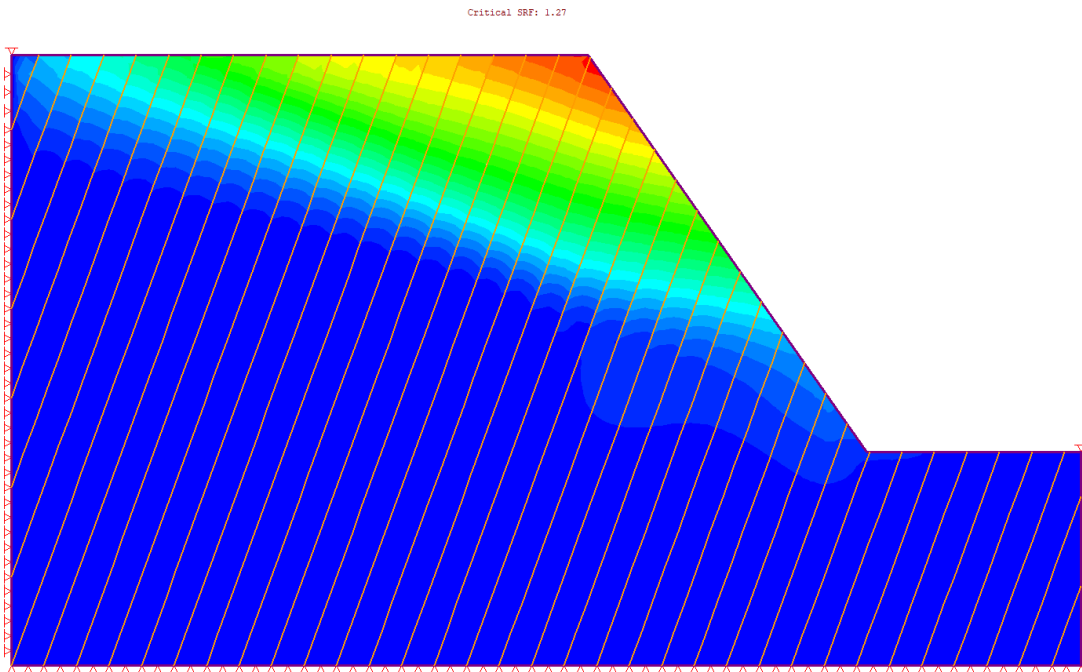


Figure 4.4: Total Displacement at SRF = 1.27 (RS2-Joint convergence improved)

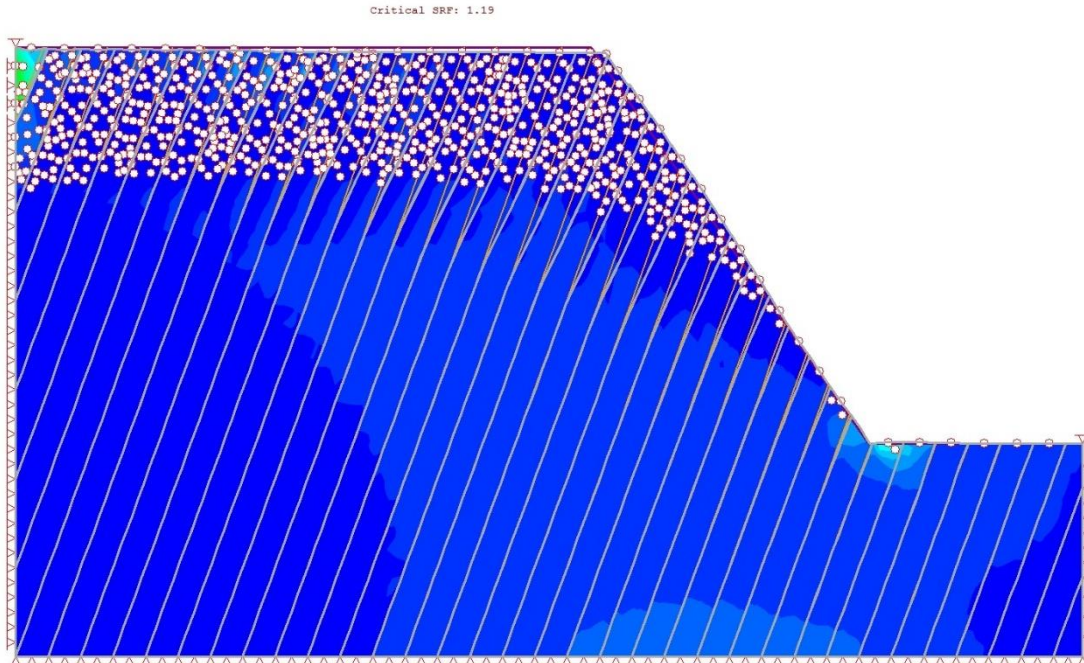


Figure 4.5: Tensile failure at SRF = 1.19 (RS2)

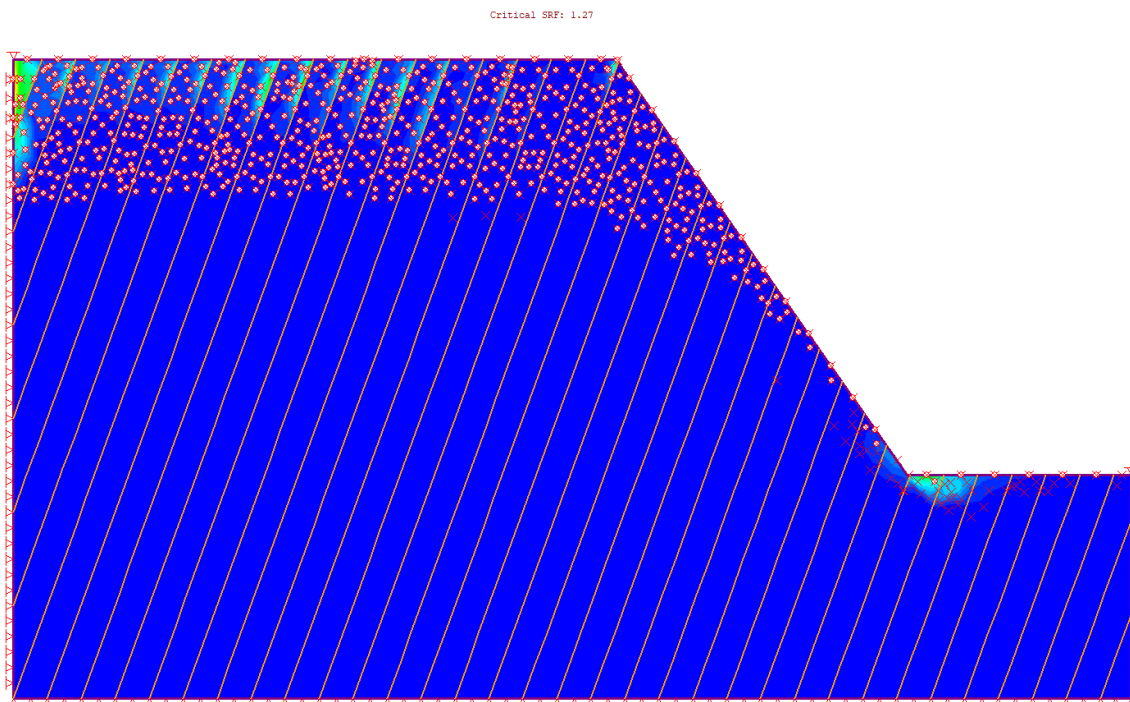


Figure 4.6: Tensile failure at SRF = 1.27 (RS2-Joint convergence improved)

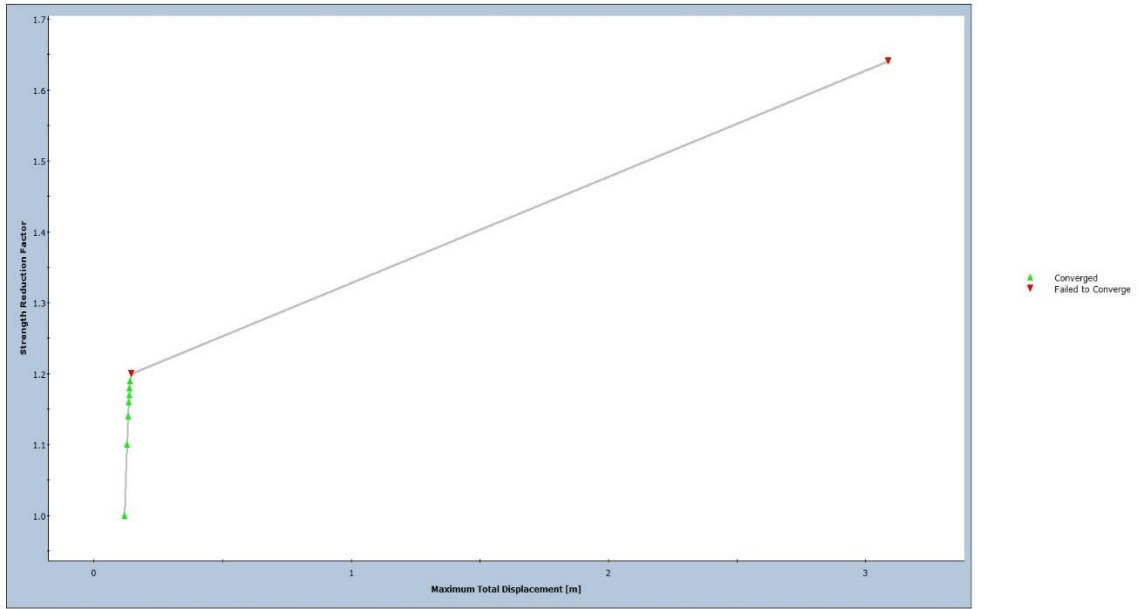


Figure 4.7: Shear Strength Reduction Plot (RS2)

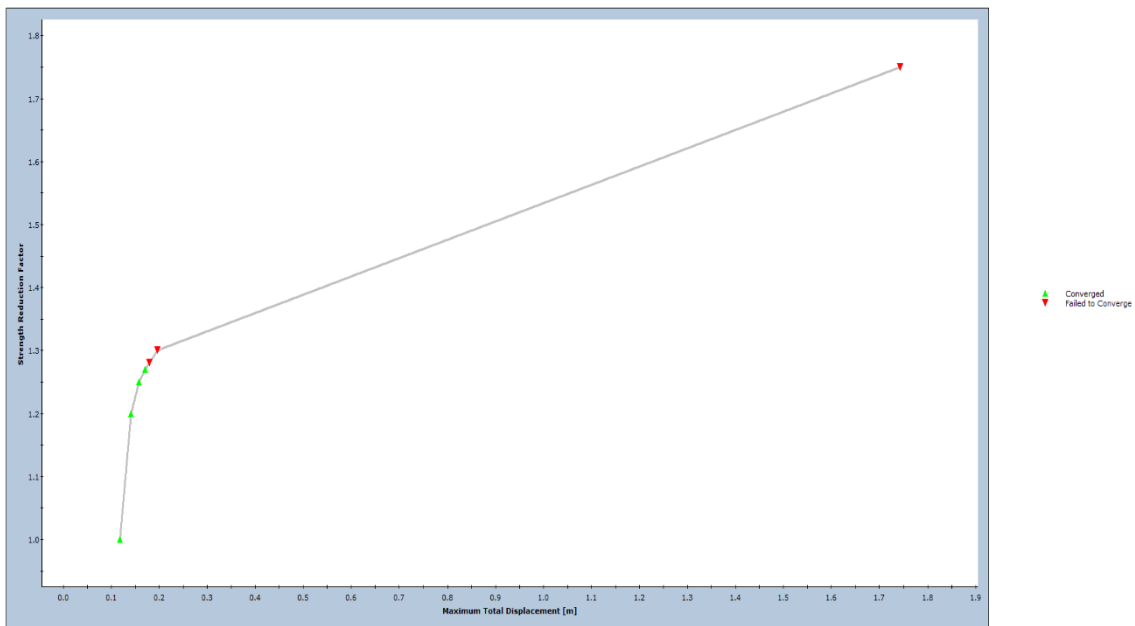


Figure 4.8: Shear Strength Reduction Plot (RS2-Joint convergence improved)

5. Lorig and Varona Backward Block Toppling

5.1. Introduction

This verification looks at the backward block toppling example from:

Lorig, L., & Varona, P. (2004). Toppling Failure - Block and Flexural. In D. C. Wyllie, & C. W. Mah, *Rock Slope Engineering Civil and Mining 4th Edition* (pp. 234-238). New York: Spon Press Taylor & Francis Group.

5.2. Problem Description

An analysis of backward block toppling was performed in RS2 and was verified using UDEC results provided in the reference.

5.3. Geometry and Properties

Table 5.1: Material Properties

Slope Height (m)	Slope Angle (deg)	Joint Angle (deg)	ϕ' joint (deg)	σ_t (rock) (MPa)	γ (kN/m ³)
260	55	55 and 0	40	0	26.1

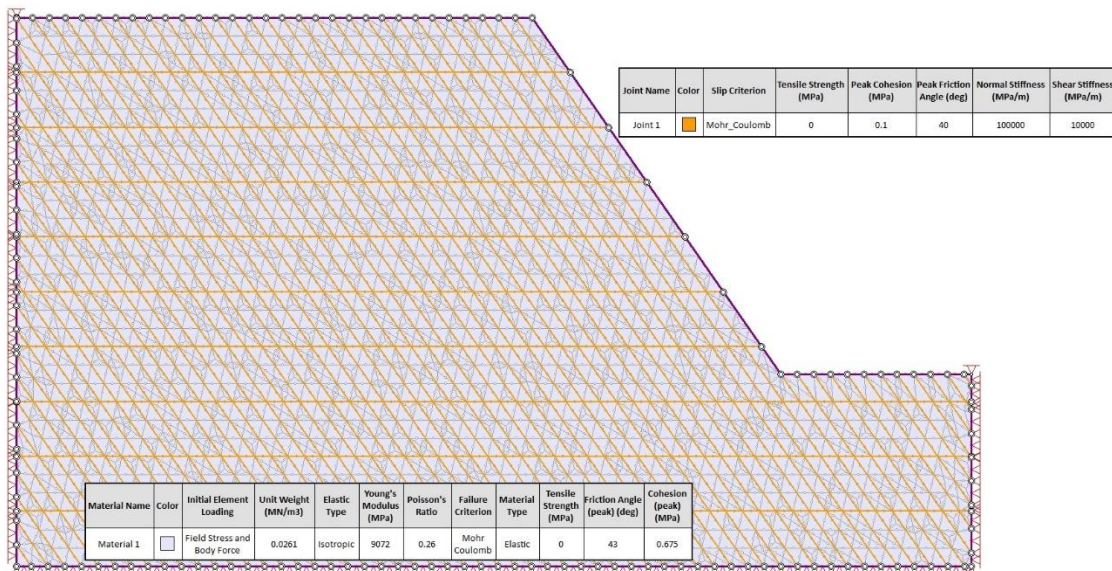


Figure 5.1: RS2 Geometry and Properties

5.4. Results

Table 5.2: Factor of Safety

Factor of Safety – RS2 with joint improvement	Factor of Safety – RS2 without joint improvement	Factor of Safety – UDEC
1.86	1.65	1.7

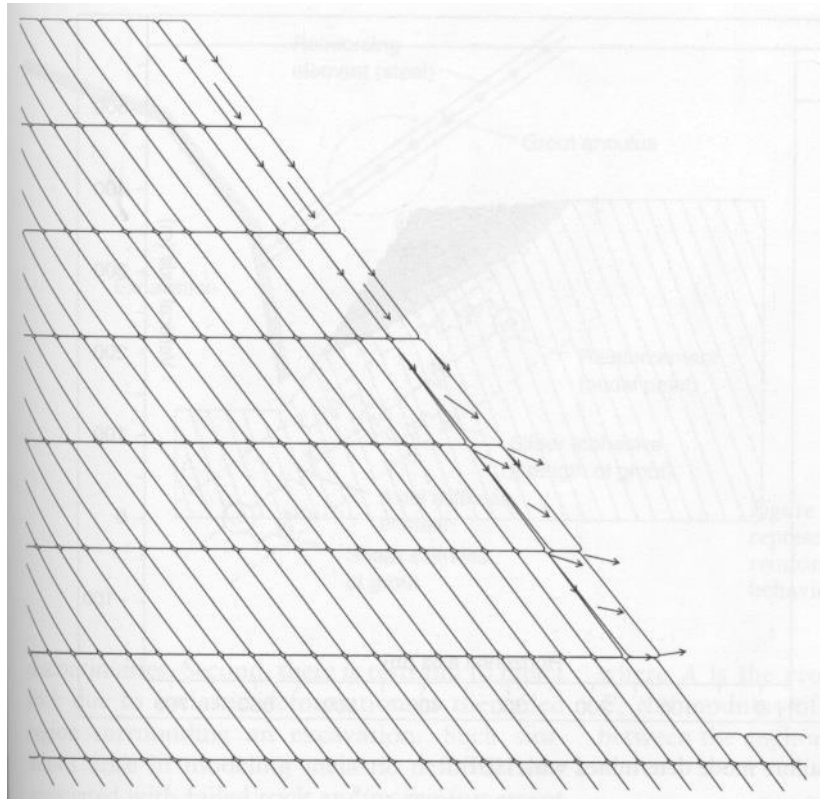


Figure 5.2: UDEC Geometry and Results (Lorig & Varona, 2004)

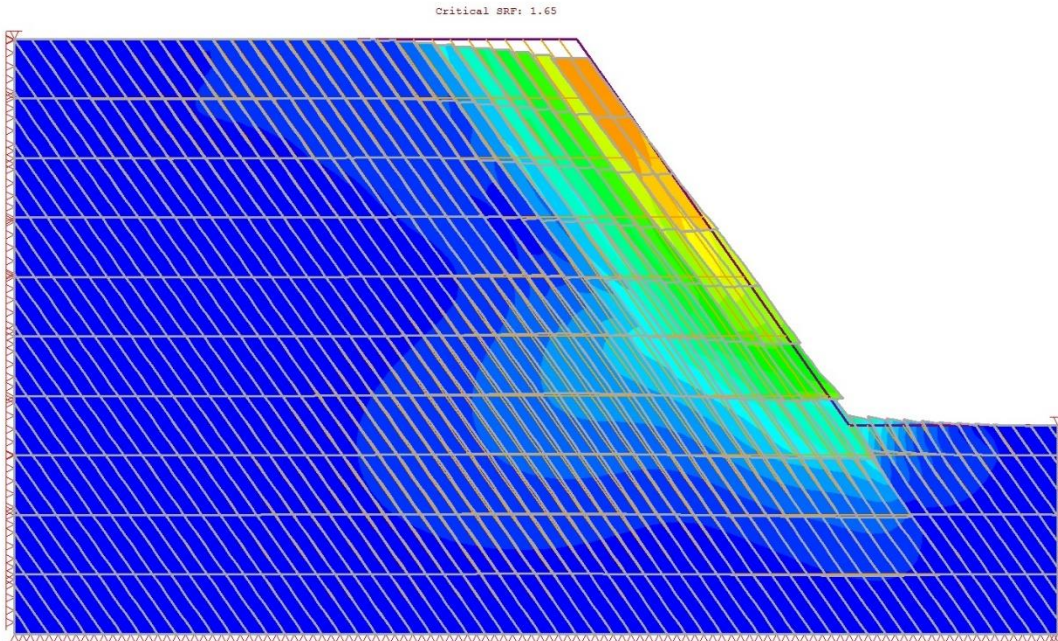


Figure 5.3: Total Displacement at SRF = 1.65 (RS2)

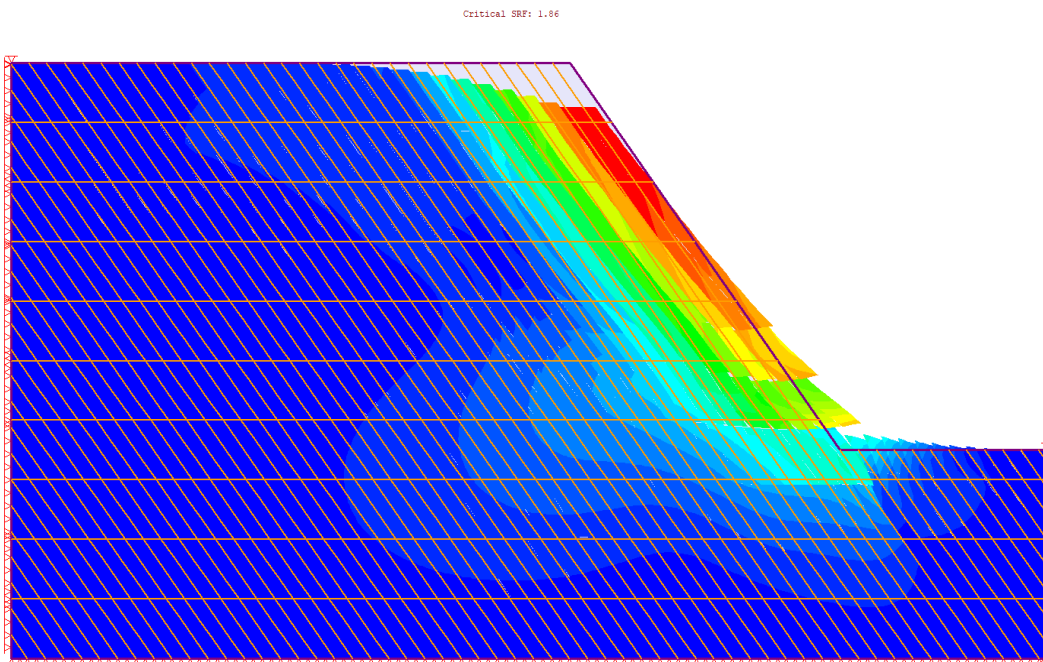


Figure 5.4: Total Displacement at SRF = 1.86 (RS2-Joint convergence improved)

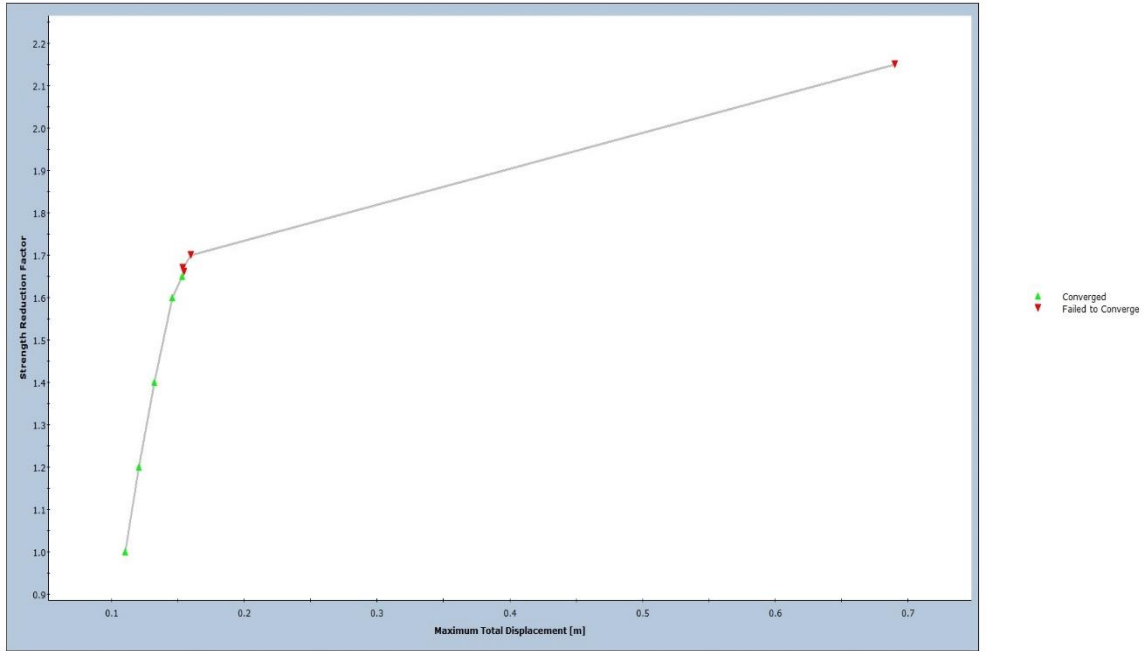


Figure 5.5: Shear Strength Reduction Plot (RS2)

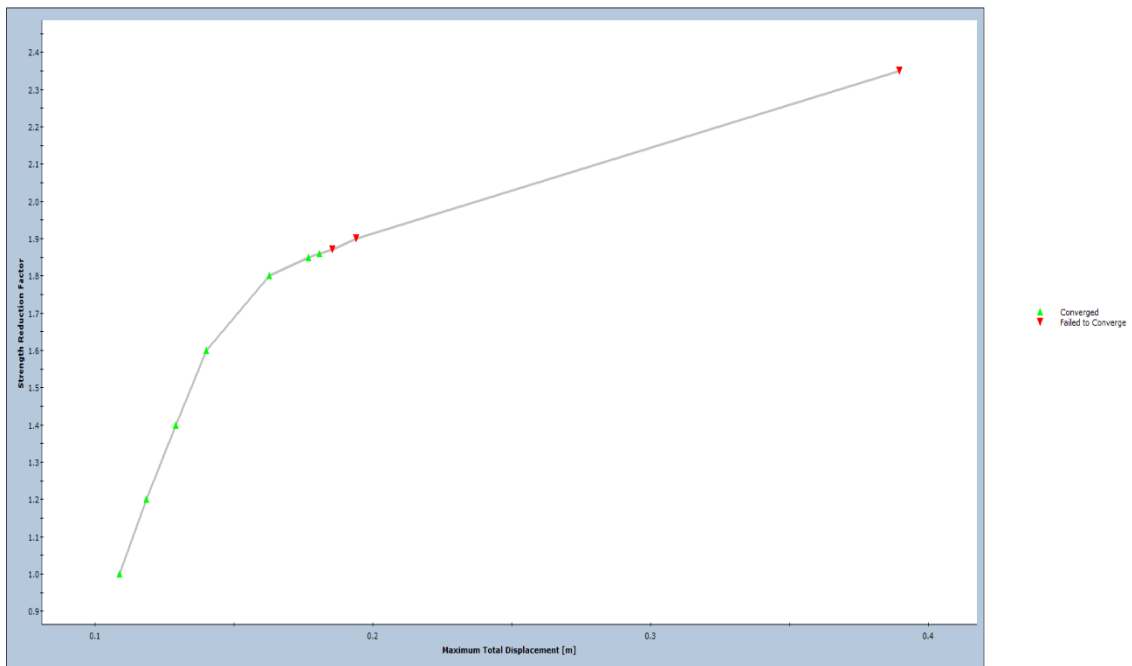


Figure 5.6: Shear Strength Reduction Plot (RS2-Joint convergence improved)

6. Lorig and Varona Plane Failure with Daylighting Discontinuities

6.1. Introduction

This verification looks at the plane failure example from:

Lorig, L., & Varona, P. (2004). Plane Failure - Daylighting and Non-Daylighting. In D. C. Wyllie, & C. W. Mah, *Rock Slope Engineering Civil and Mining 4th Edition* (pp. 233-235). New York: Spon Press Taylor & Francis Group.

6.2. Problem Description

An analysis of plane failure with daylighting discontinuities was performed in RS2 and verified using UDEC results provided in the reference.

6.3. Geometry and Properties

Table 6.1: Material Properties

Slope Height (m)	Slope Angle (deg)	Joint Angle (deg)	ϕ' joint (deg)	σ_t (rock) (MPa)	γ (kN/m ³)
260	55	35	40	0	26.1

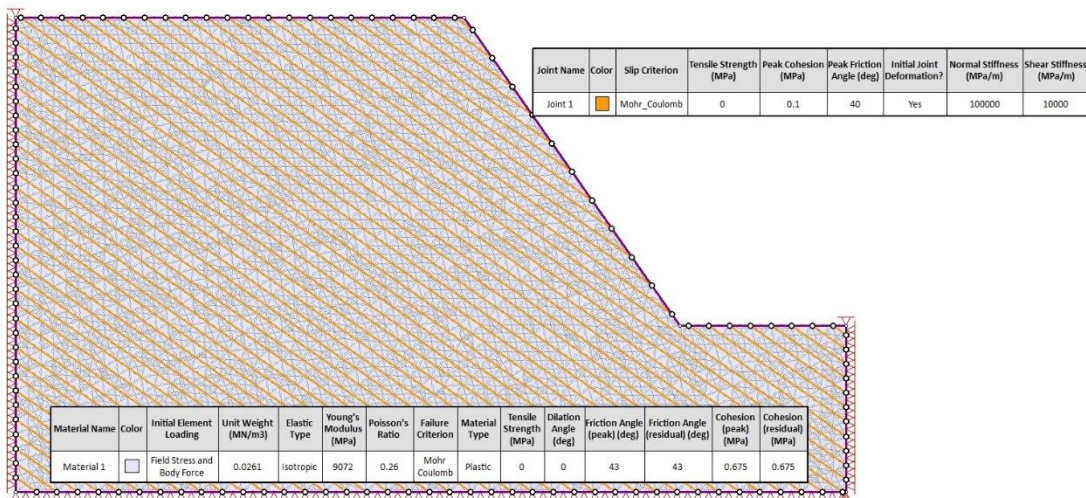


Figure 6.1: RS2 Geometry and Properties

6.4. Results

Table 6.2: Factor of Safety

Factor of Safety – RS2 with joint improvement	Factor of Safety – RS2 without joint improvement	Factor of Safety – UDEC
1.31	1.25	1.27

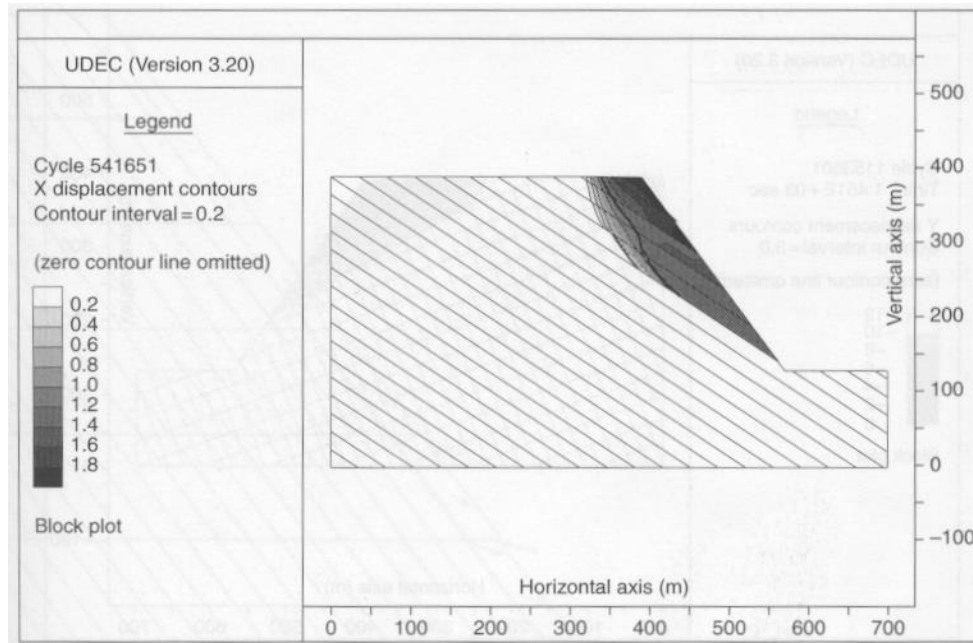


Figure 6.2: UDEC Geometry and Results (Lorig & Varona, 2004)

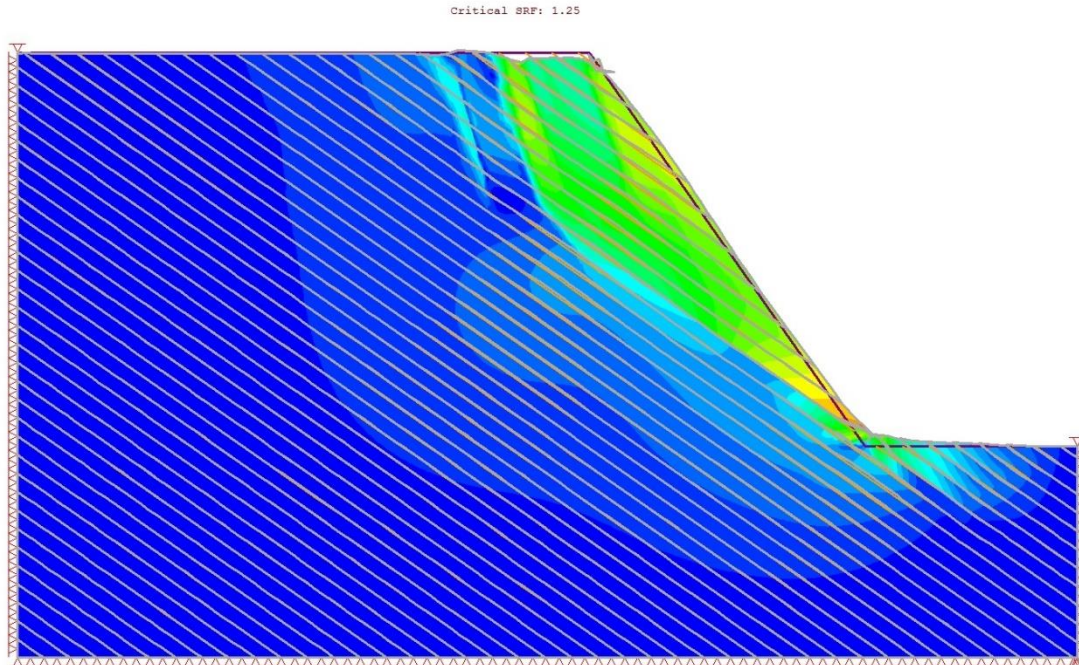


Figure 6.3: Total Displacement at SRF = 1.25 (RS2)

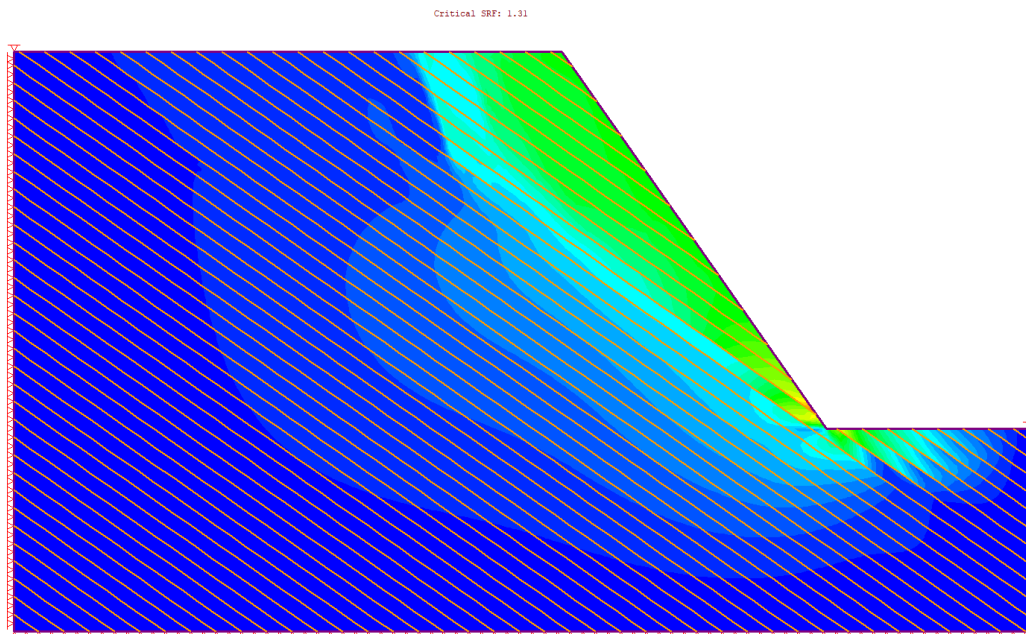


Figure 6.4: Total Displacement at SRF = 1.31 (RS2-Joint convergence improved)

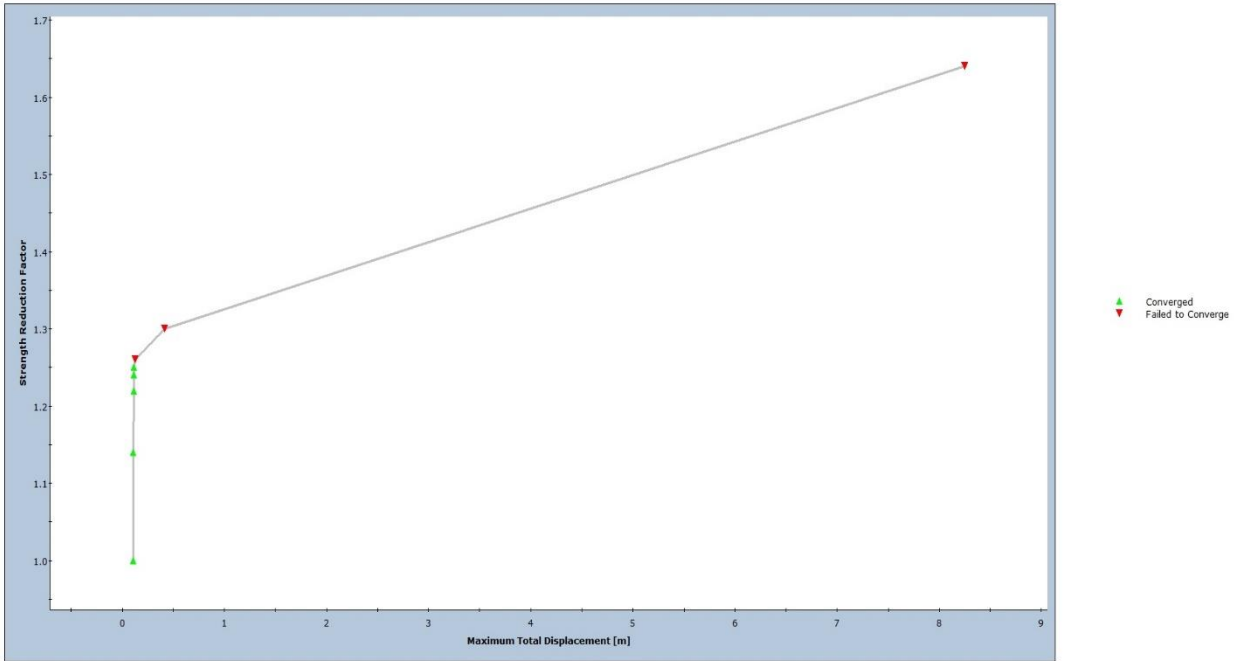


Figure 6.5: Shear Strength Reduction Plot (RS2)

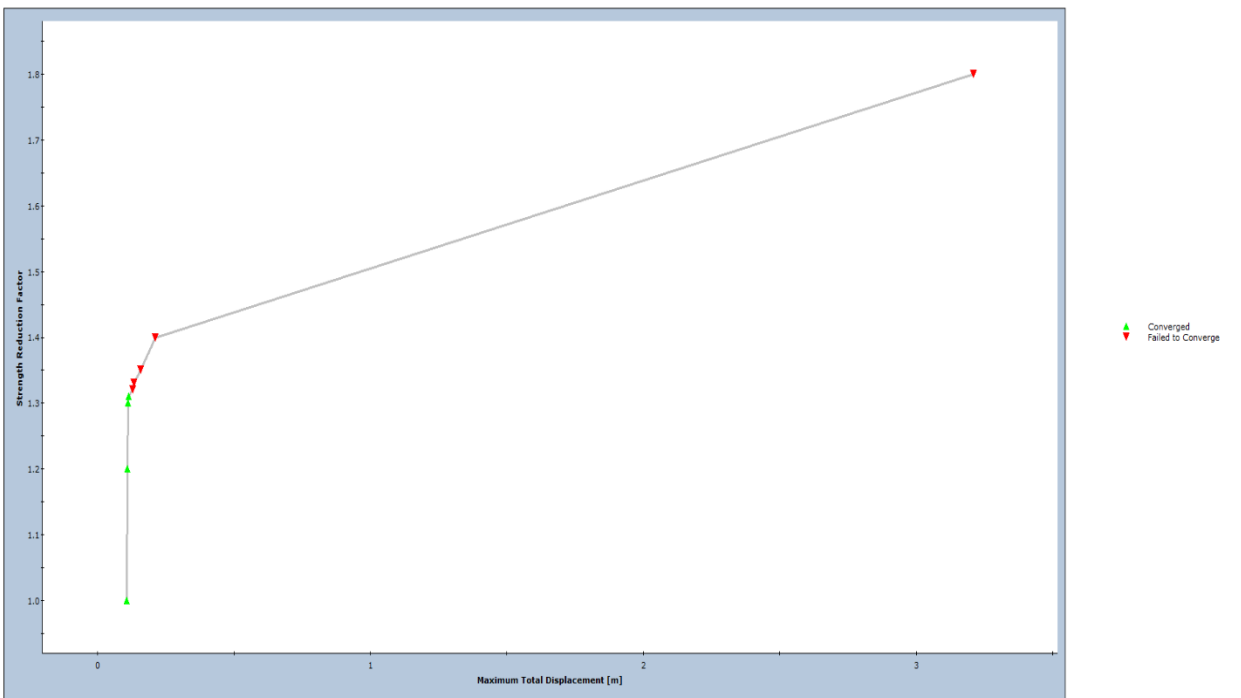


Figure 6.6: Shear Strength Reduction Plot (RS2-Joint convergence improved)

7. Lorig and Varona Plane Failure with Non-Daylighting Discontinuities

7.1. Introduction

This verification looks at the plane failure example from:

Lorig, L., & Varona, P. (2004). Plane Failure - Daylighting and Non-Daylighting. In D. C. Wyllie, & C. W. Mah, *Rock Slope Engineering Civil and Mining 4th Edition* (pp. 233-235). New York: Spon Press Taylor & Francis Group.

7.2. Problem Description

An analysis of plane failure with non-daylighting discontinuities was performed in RS2 and verified using UDEC results provided in the reference.

7.3. Geometry and Properties

Table 7.1: Material Properties

Slope Height (m)	Slope Angle (deg)	Joint Angle (deg)	ϕ' joint (deg)	σ_t (rock) (MPa)	γ (kN/m ³)
260	5	70	40	0	26.1

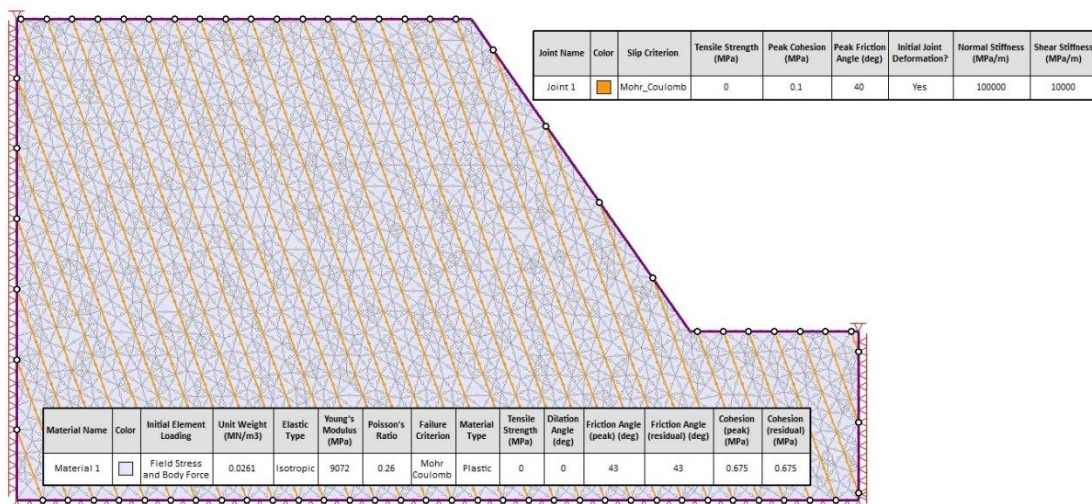


Figure 7.1: RS2 Geometry and Properties

7.4. Results

Table 7.2: Factor of Safety

Factor of Safety – RS2 with joint improvement	Factor of Safety – RS2 without joint improvement	Factor of Safety – UDEC
1.59	1.57	1.5

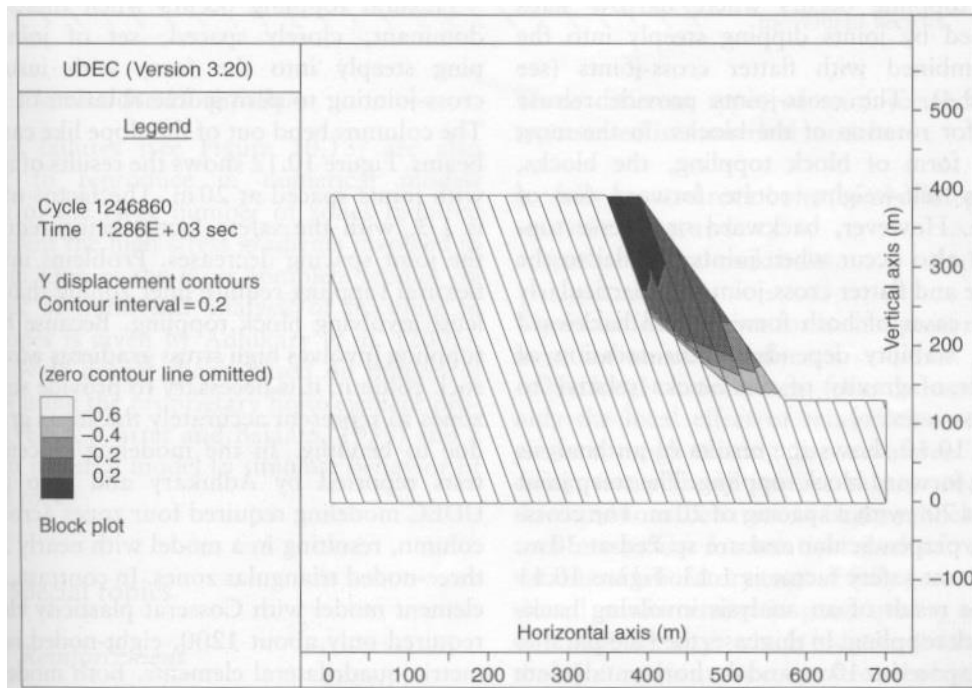


Figure 7.2: UDEC Geometry and Results (Lorig & Varona, 2004)

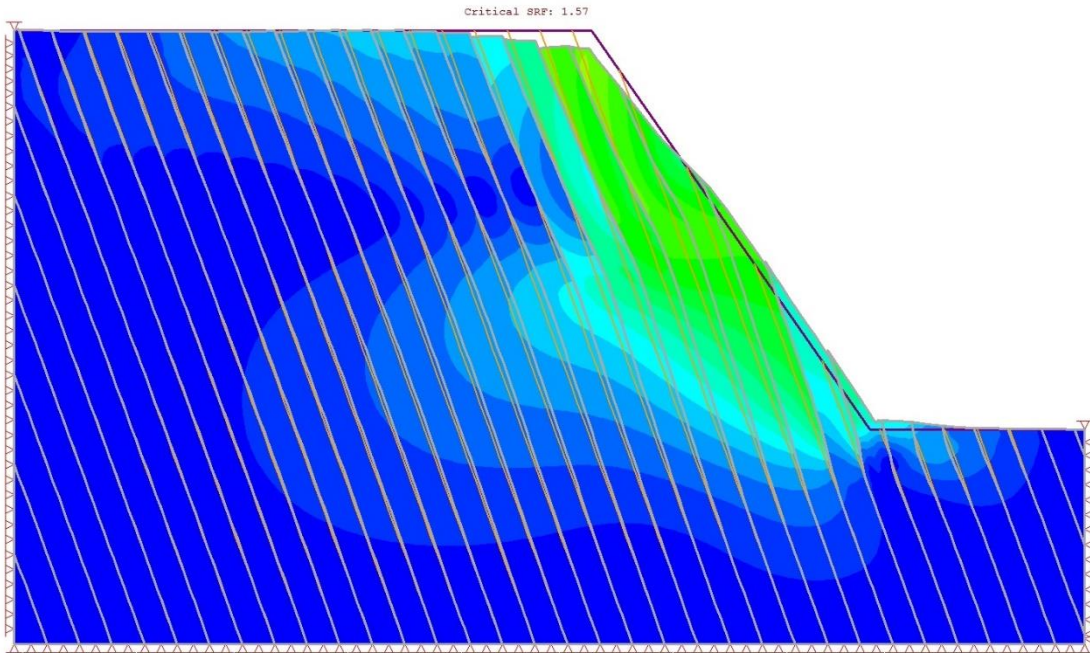


Figure 7.3: Total Displacement at SRF = 1.57 (RS2)

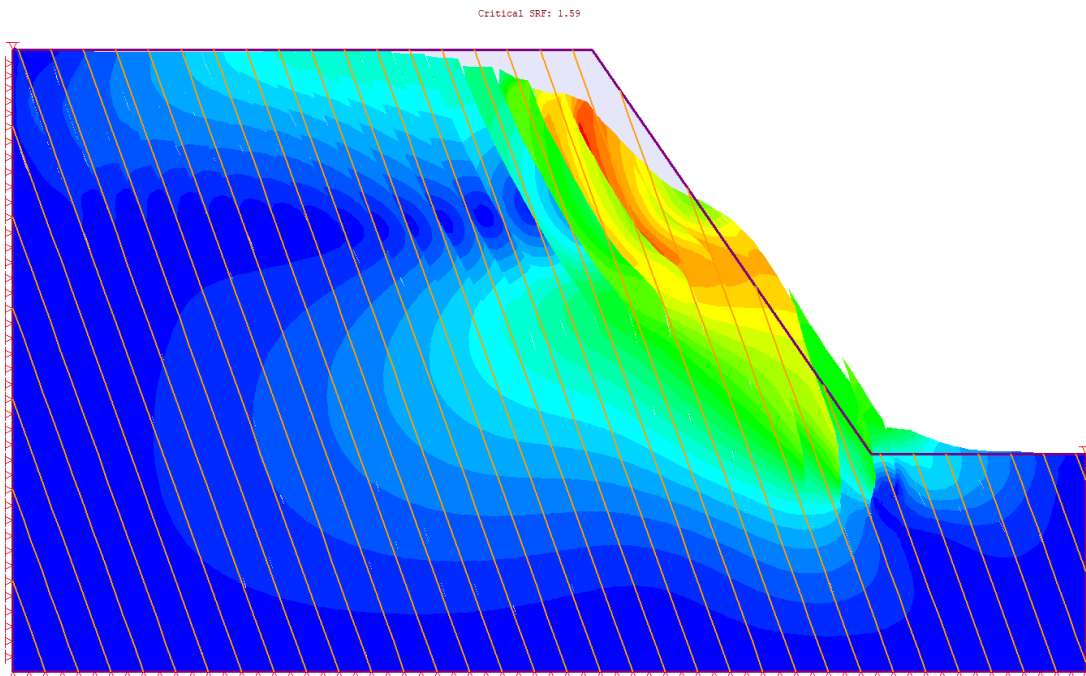


Figure 7.4: Total Displacement at SRF = 1.59 (RS2-Joint convergence improved)

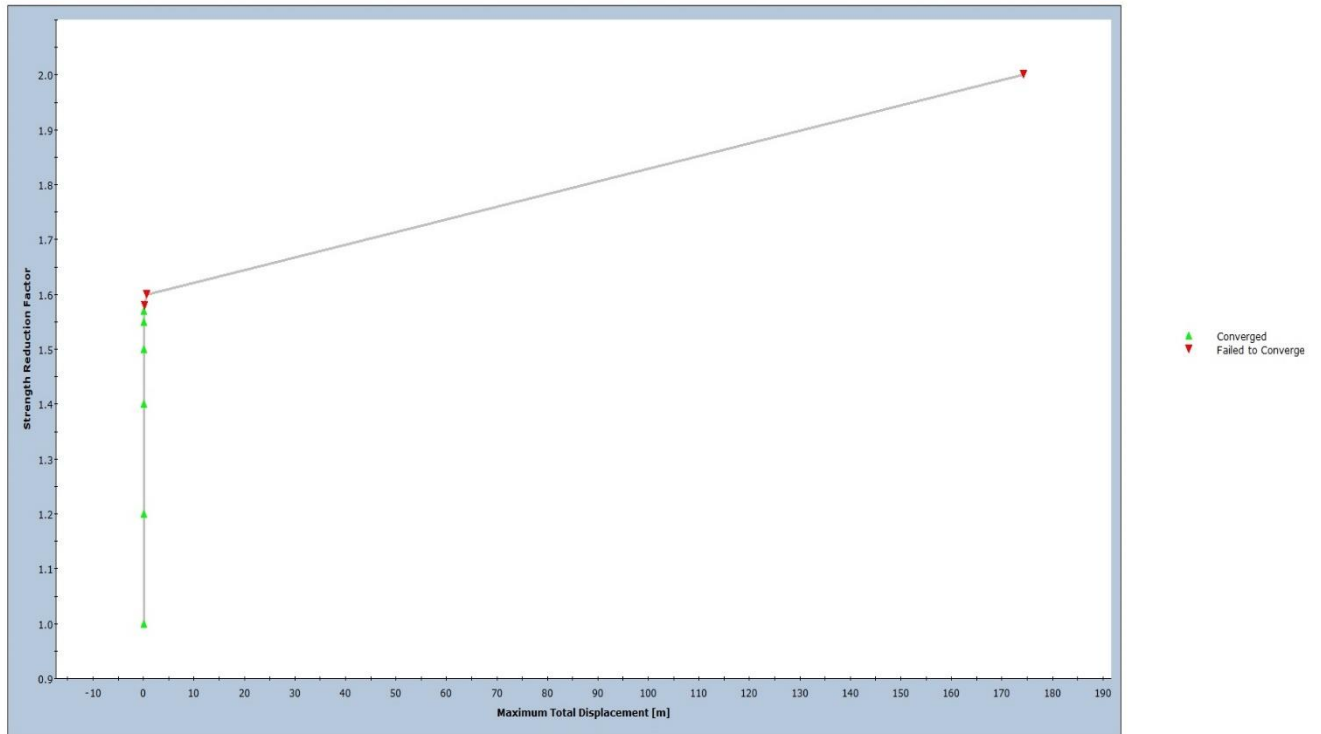


Figure 7.5: Shear Strength Reduction Plot (RS2)

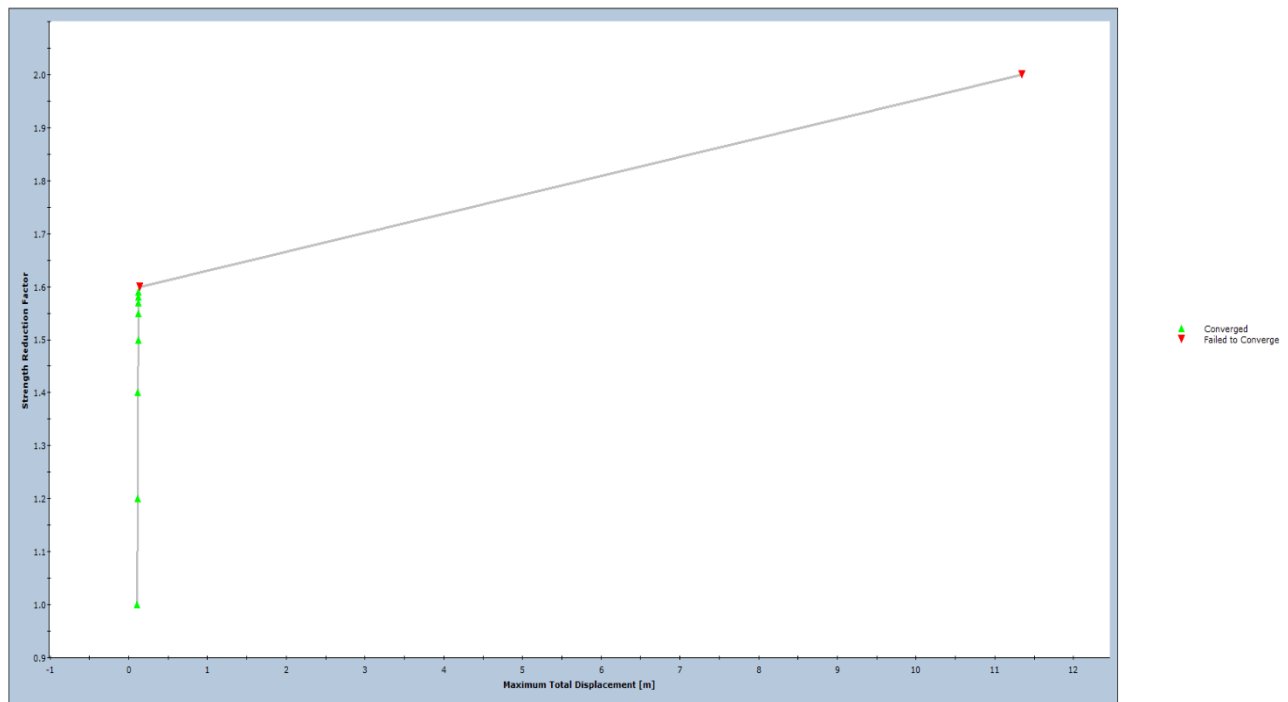


Figure 7.6: Shear Strength Reduction Plot (RS2-Joint convergence improved)

8. Flexural Toppling in Base Friction Model

8.1. Introduction

This verification looks at the base friction example from:

Pritchard, M. A., & Savigny, K. W. (1990). Numerical Modelling of Toppling. *Canadian Geotechnical Journal*, 823-834.

8.2. Problem Description

A small-scale base friction table model of flexural toppling was reproduced in both RS2 and UDEC. The software models were up-scaled 100 times from the base friction model.

8.3. Geometry and Properties

Table 8.1: Material Properties

Slope Height (m)	Slope Angle (deg)	Joint Angle (deg)	ϕ' joint (deg)	σ_t (rock) (MPa)	γ (kN/m ³)
30.5	78	60	39	0	25.506

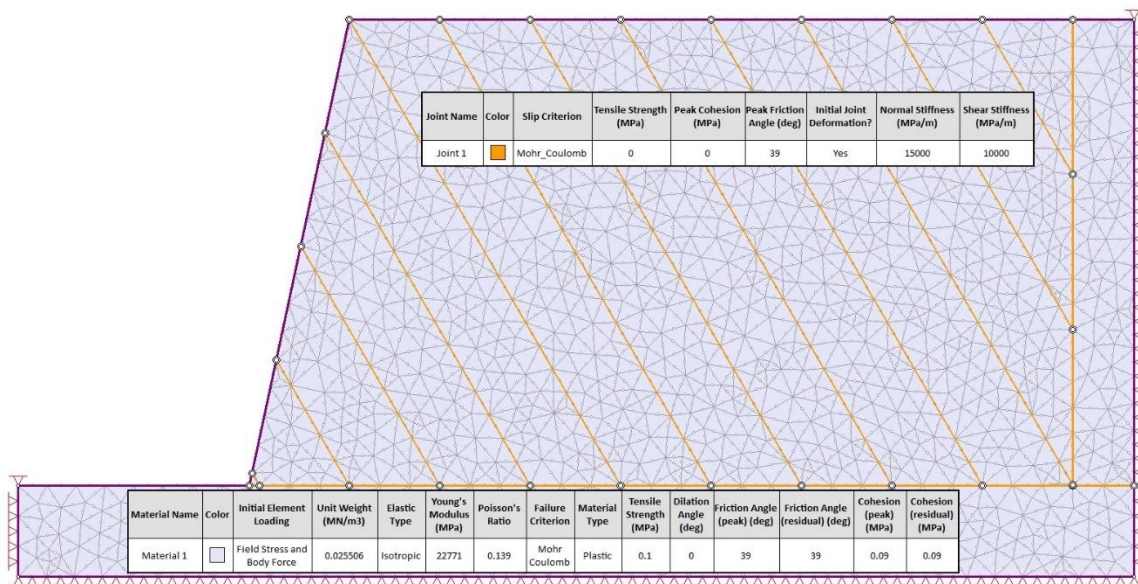


Figure 8.1: RS2 Geometry and Properties

8.4. Results

Table 8.2: Factor of Safety

Factor of Safety – RS2 with joint improvement	Factor of Safety – RS2 without joint improvement	Factor of Safety – UDEC
0.75	0.75	0.76

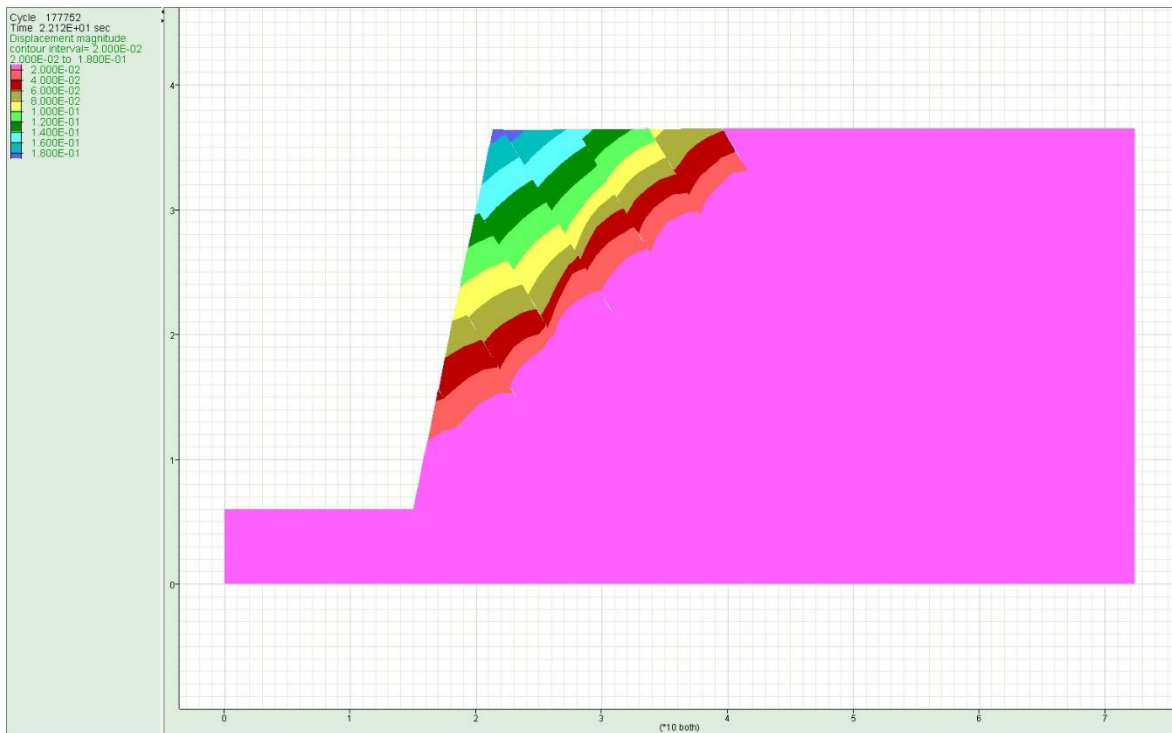


Figure 8.2: Displacement during Slope Deformation (UDEC)

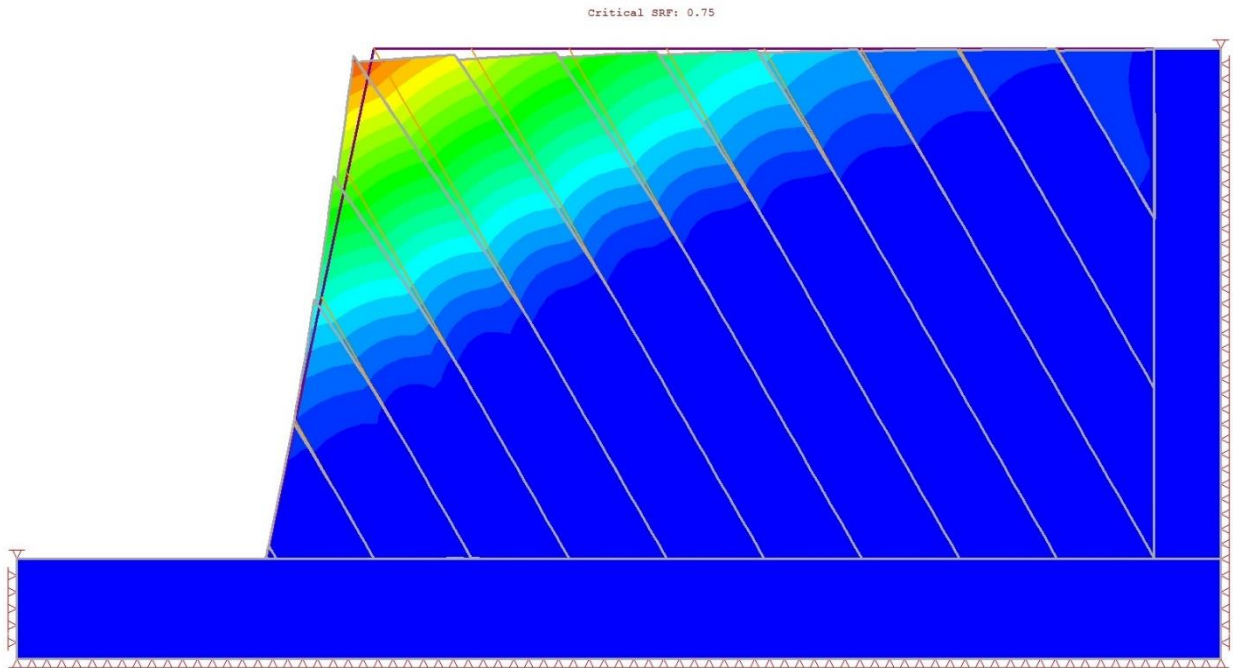


Figure 8.3: Total Displacement at SRF = 0.75 (RS2)

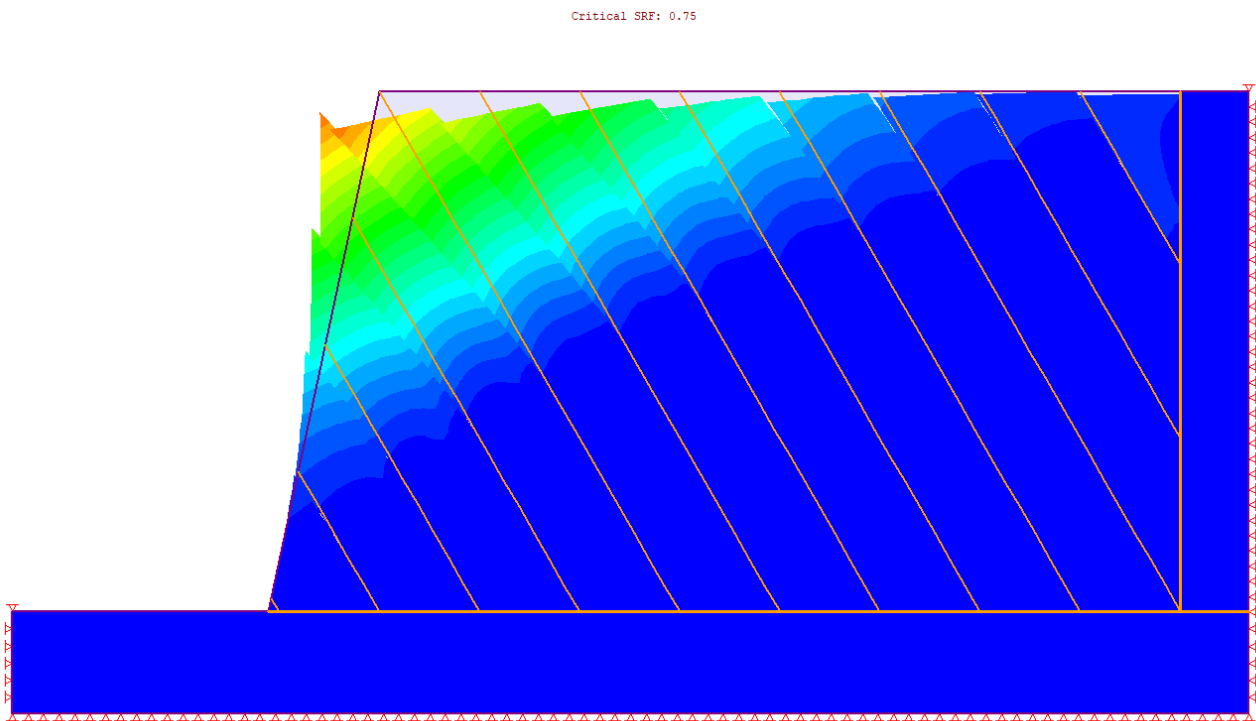


Figure 8.4: Total Displacement at SRF = 0.75 (RS2-Joint convergence improved)

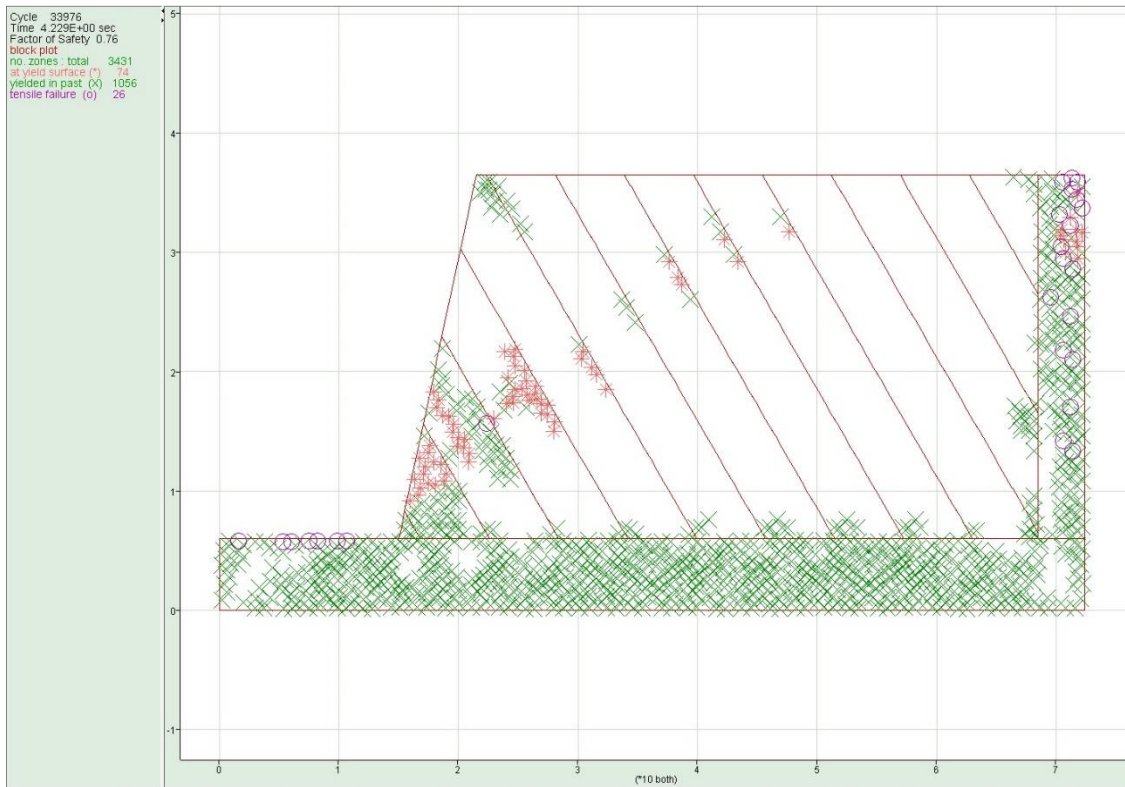


Figure 8.5: Plasticity Indicators (UDEEC)

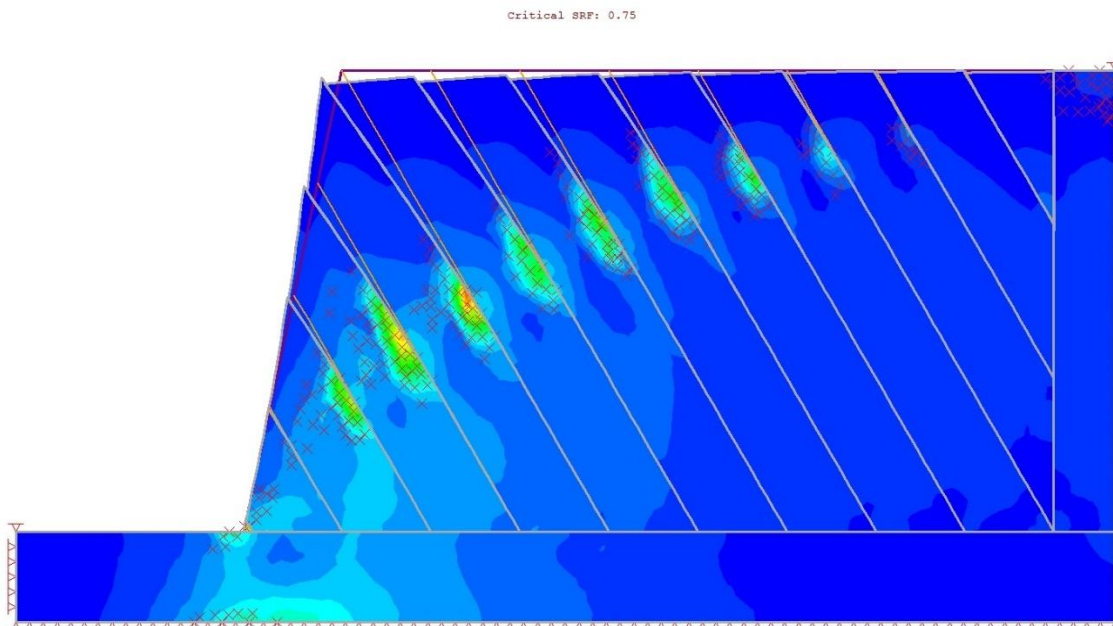


Figure 8.6: Elements Yielding by Shear at SRF = 0.75 (RS2)

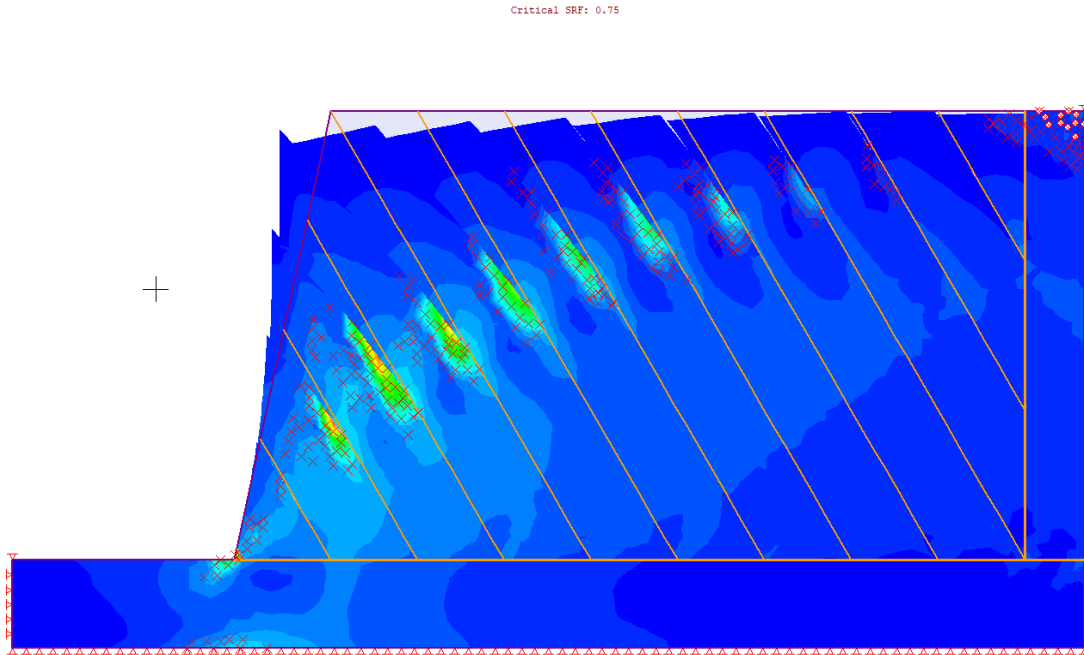


Figure 8.7: Elements Yielding by Shear at SRF = 0.75 (RS2-Joint convergence improved)

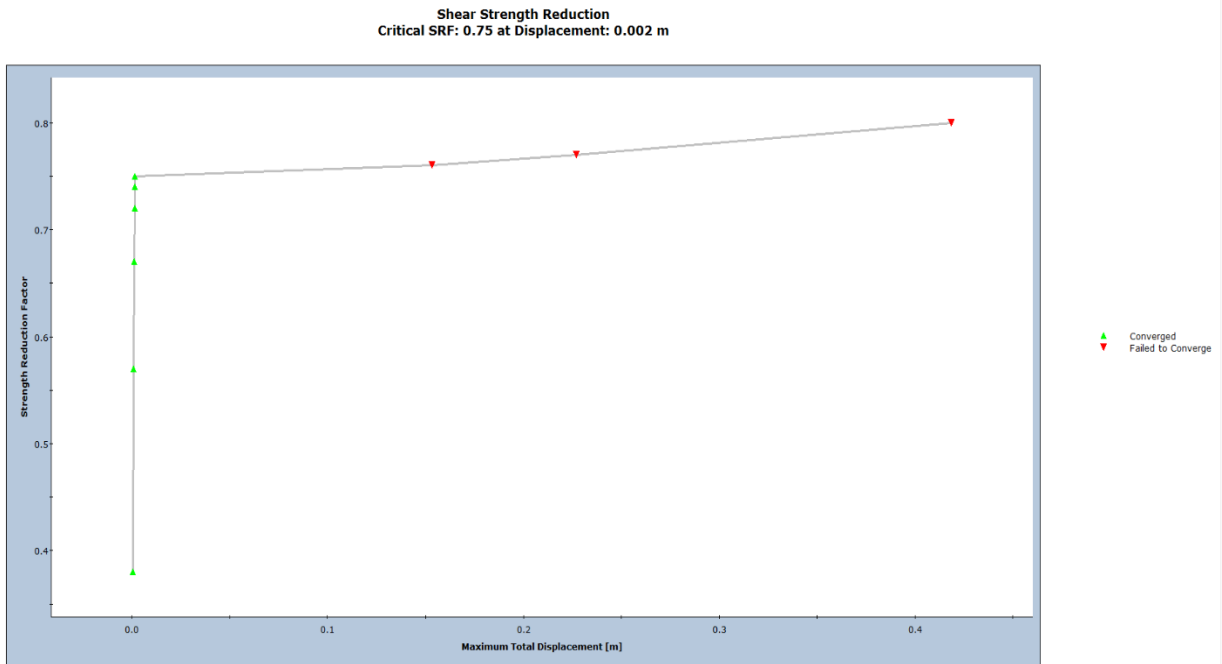


Figure 8.8: Shear Strength Reduction plot (RS2)

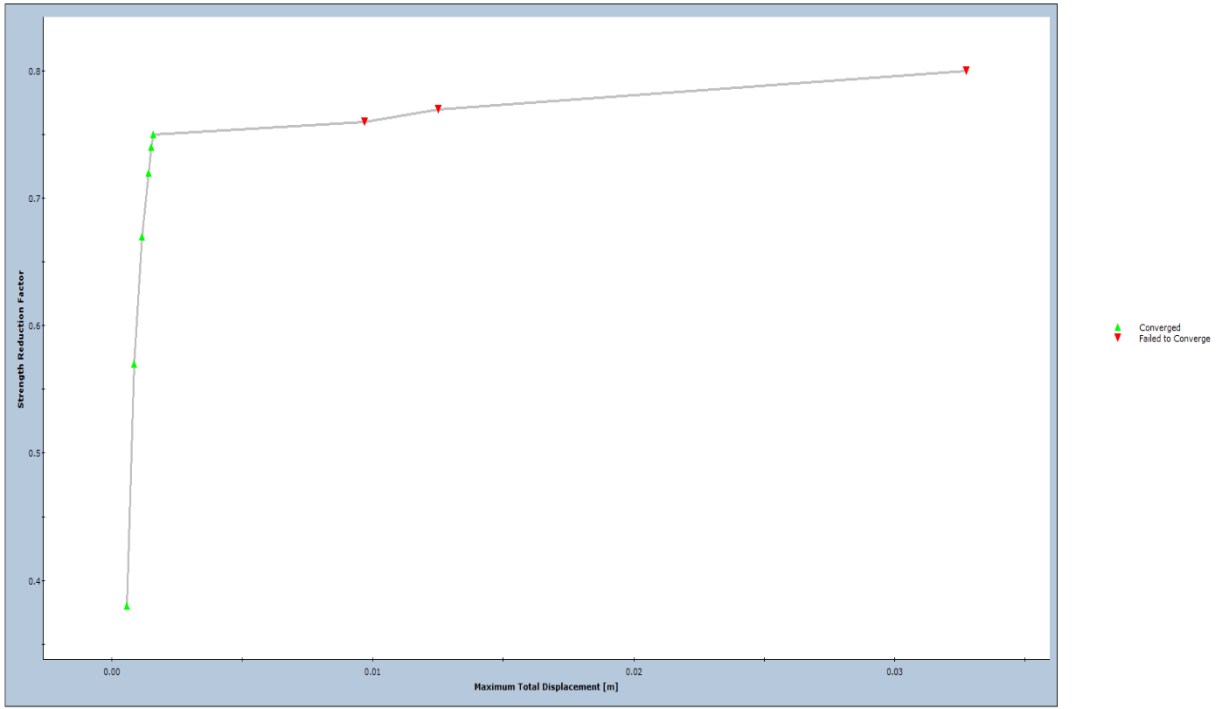


Figure 8.9: Shear Strength Reduction plot (RS2-Joint convergence improved)

9. Alejano et al. Bilinear Slab Failure Example 1a

9.1. Introduction

This verification looks at the bilinear slab failure example from:

Alejano, L. R., Ferrero, A. M., Ramirez-Oyanguren, P., & Alvarez Fernandez, M. I. (2011). Comparison of Limit-Equilibrium, Numerical and Physical Models of Wall Slope Stability. *International Journal of Rock Mechanics and Mining Sciences*, 16-26.

9.2. Problem Description

An analysis of bilinear slab failure was performed using RS2 and was verified using limit-equilibrium and UDEC-SSRT results provided in section 4.2.1 of the reference. Bilinear slab failure occurs when there is sliding along a basal plane in combination with sliding along a secondary shallow dipping joint undercut by the slope face (Figure 9.1). Note that rigid blocks were used in the UDEC model. To reproduce the model in RS2, an artificially high modulus of 2×10^8 MPa was given to the material. With such a high modulus, the tolerance for convergence also had to be reduced.

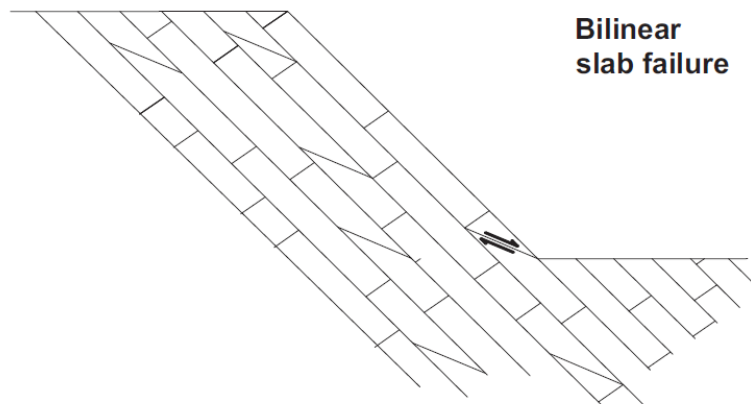


Figure 9.1: Bilinear Slab Failure (Alejano et al., 2011)

9.3. Geometry and Properties

Table 9.1: Material Properties

Slope Height (m)	Slope Angle (deg)	Joint Angle (deg)	ϕ' joint (deg)	Bedding Spacing (m)	ϕ' Bedding (deg)	γ (kN/m ³)
50	50	30	40	3	30	25.0

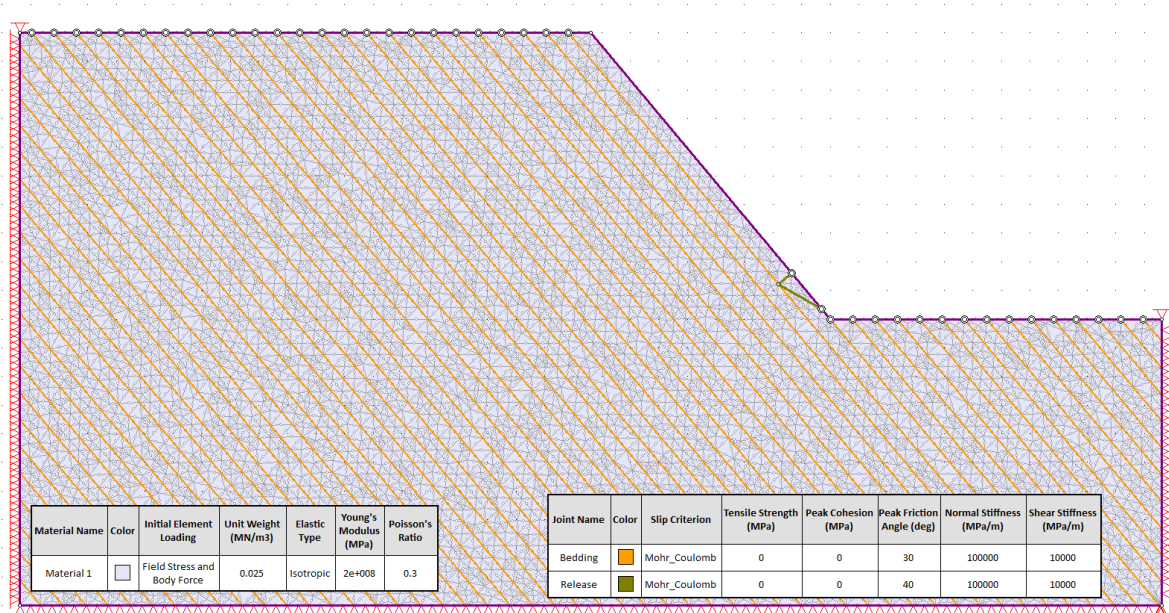


Figure 9.2: RS2 Geometry and Properties

9.4. Results

Table 9.2: Factor of Safety

Factor of Safety – RS2 with joint improvement	Factor of Safety – RS2 without joint improvement	Factor of Safety – UDEC	Factor of Safety – LE
1.09	1.01	1.03	0.40 -1.45

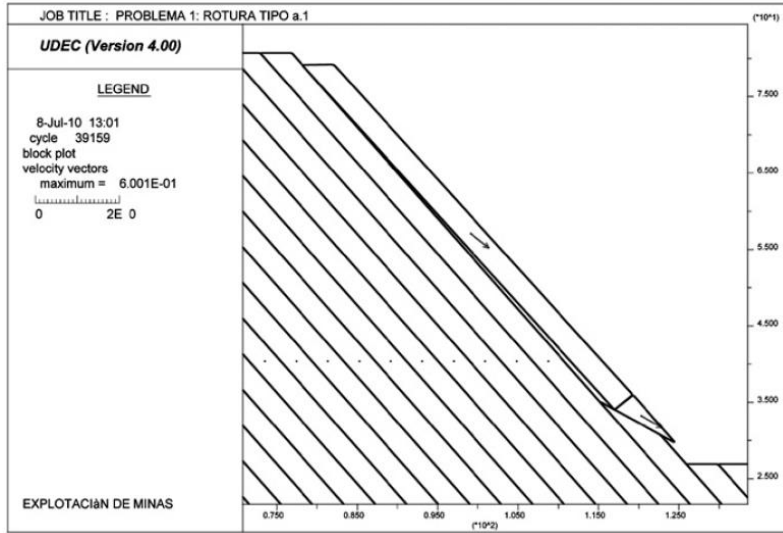


Figure 9.3: UDEC Model and Results (Alejano et al., 2011)

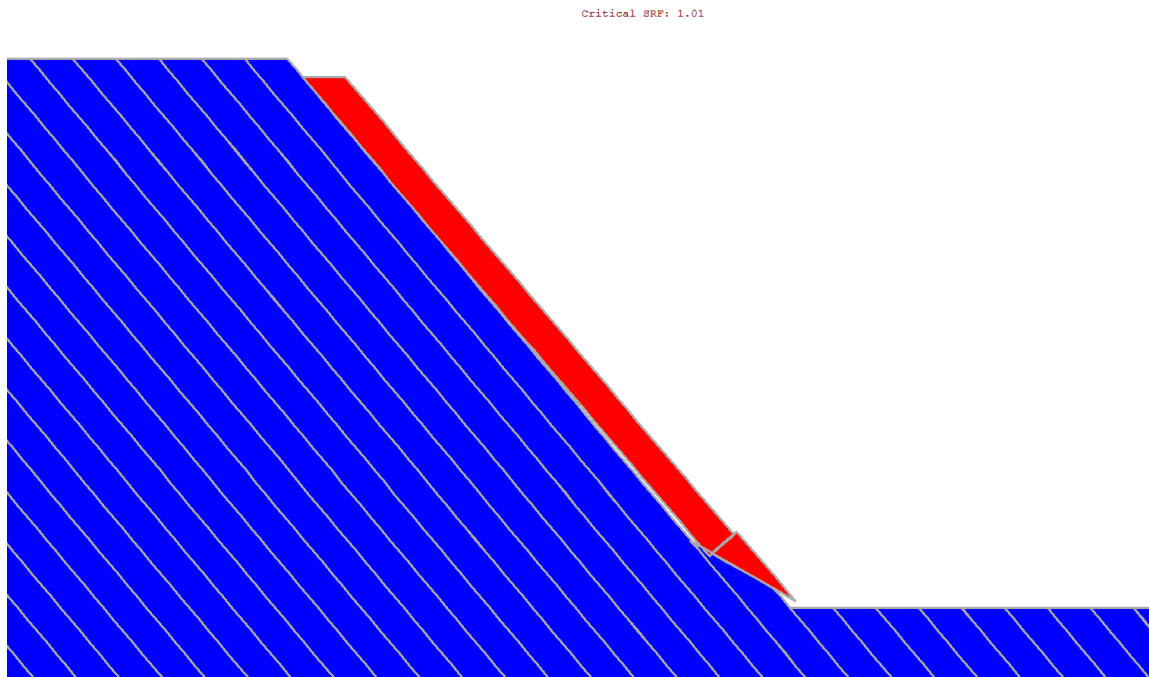


Figure 9.4: RS2 Deformed Shape

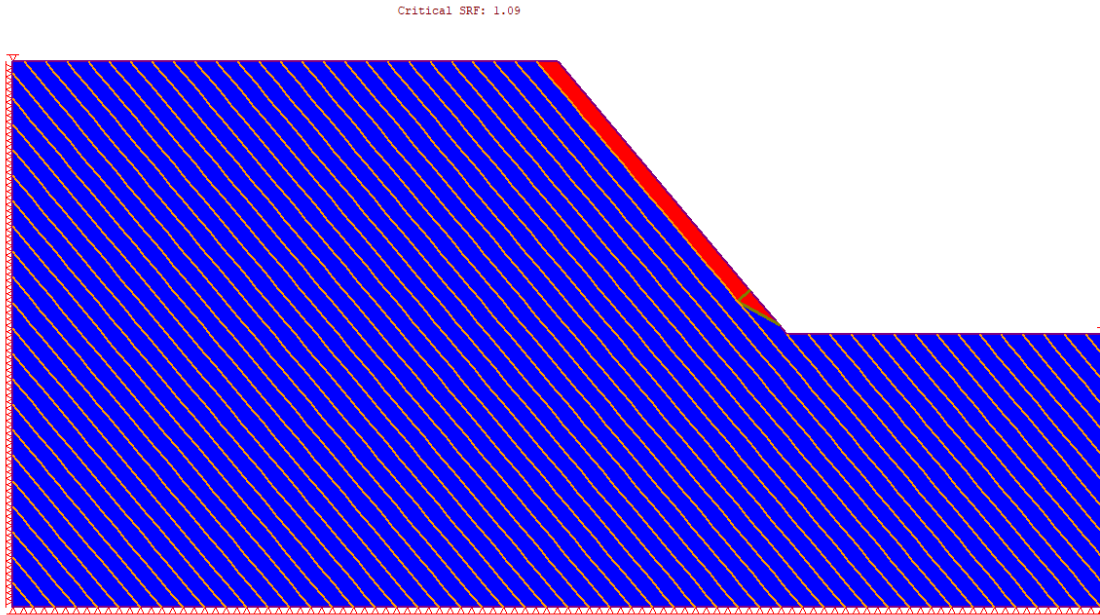


Figure 9.5: RS2-Joint convergence improved Deformed Shape

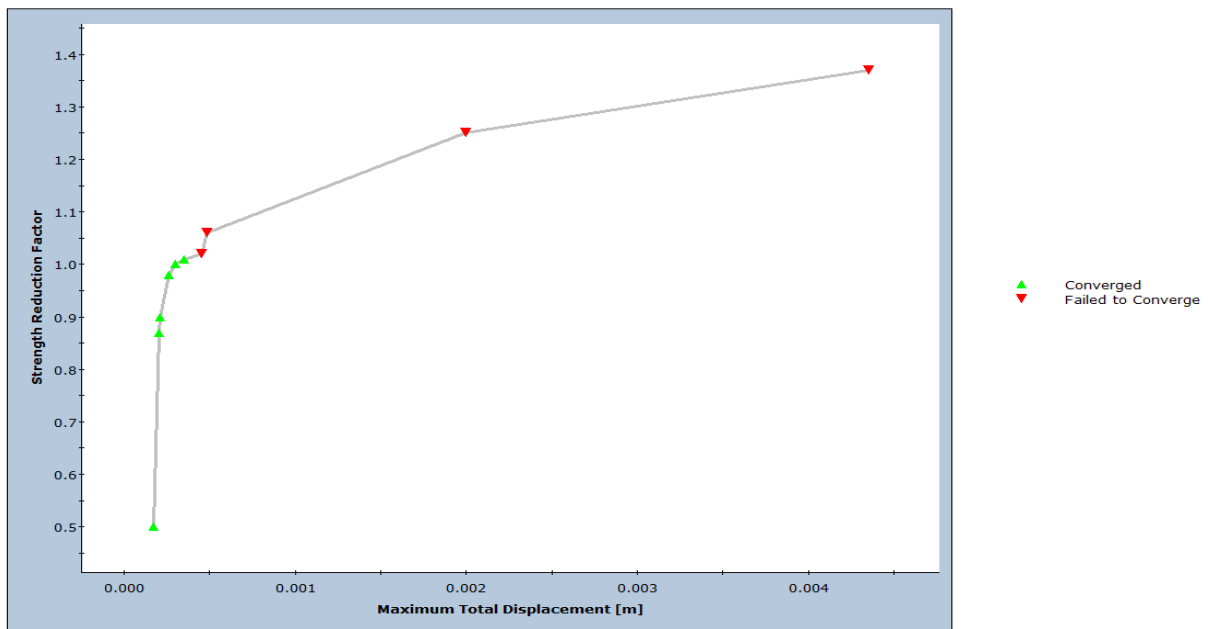


Figure 9.6: Shear Strength Reduction Plot (RS2)

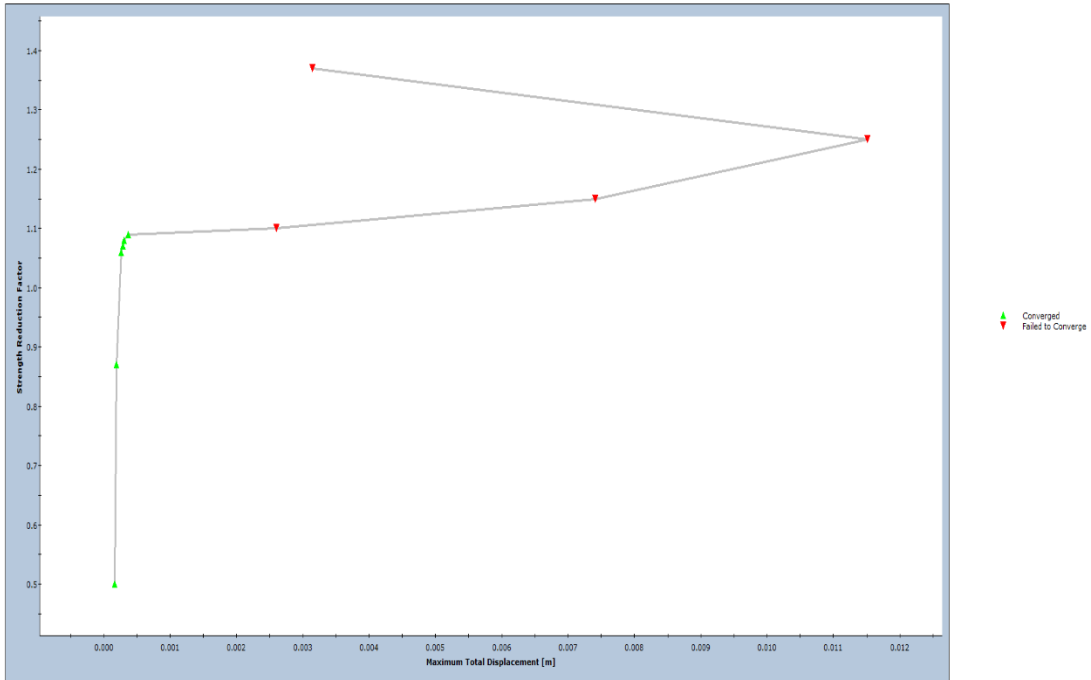


Figure 9.7: Shear Strength Reduction Plot (RS2-Joint convergence improved)

10. Alejano et al. Bilinear Slab Failure Example 1b

10.1. Introduction

This verification looks at the bilinear slab failure example from:

Alejano, L. R., Ferrero, A. M., Ramirez-Oyanguren, P., & Alvarez Fernandez, M. I. (2011). Comparison of Limit-Equilibrium, Numerical and Physical Models of Wall Slope Stability. *International Journal of Rock Mechanics and Mining Sciences*, 16-26.

10.2. Problem Description

An analysis of bilinear slab failure was performed using RS2 and was verified using limit-equilibrium and UDEC-SSRT results provided in section 4.2.1 of the reference. Bilinear slab failure occurs when there is sliding along a basal plane in combination with sliding along a secondary shallow dipping joint undercut by the slope face (Figure 10.1). The only difference between example 1a and 1b in the paper is that in example 1b the normal joint is moved upslope 5m. Note that rigid blocks were used in the UDEC model. To reproduce the model in RS2, an artificially high modulus of 2×10^8 MPa was given to the material. With such a high modulus, the tolerance for convergence also had to be reduced.

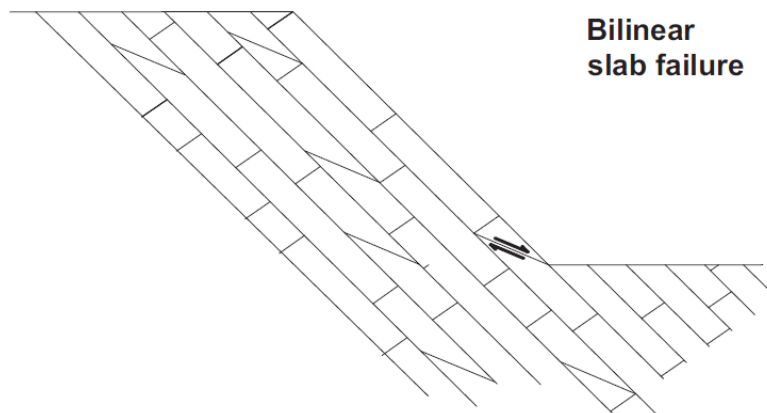


Figure 10.1: Bilinear Slab Failure (Alejano et al., 2011)

10.3. Geometry and Properties

Table 10.1: Material Properties

Slope Height (m)	Slope Angle (deg)	Joint Angle (deg)	ϕ' joint (deg)	Bedding Spacing (m)	ϕ' Bedding (deg)	γ (kN/m ³)
50	50	30	40	3	30	25.0

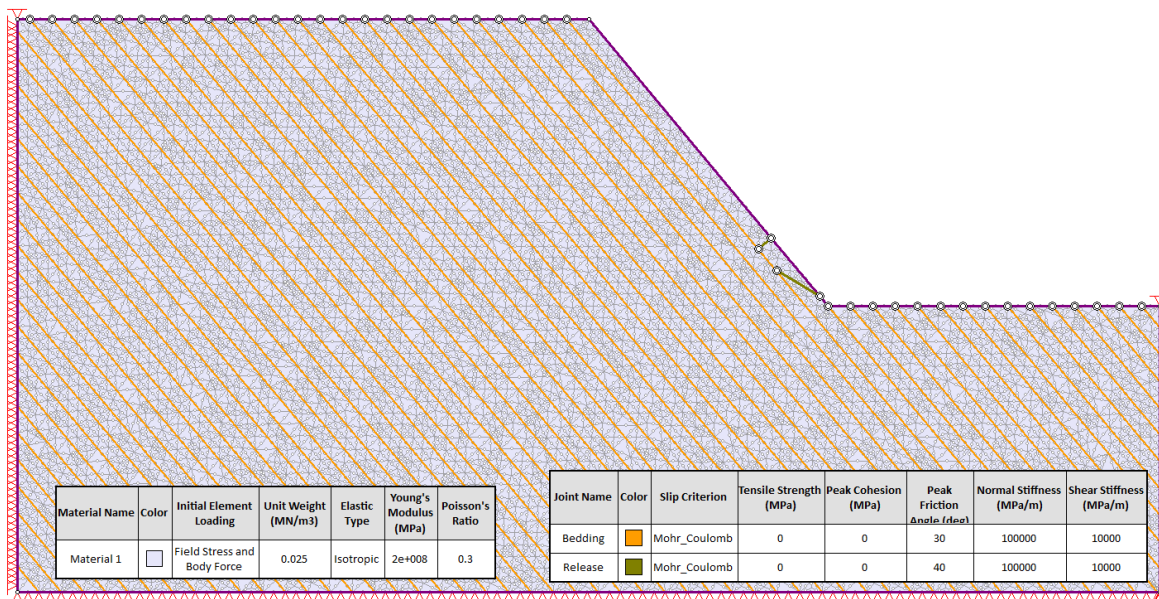


Figure 10.2: RS2 Geometry and Properties

10.4. Results

Table 10.2: Factor of Safety

Factor of Safety – RS2 with joint improvement	Factor of Safety – RS2 without joint improvement	Factor of Safety – UDEC	Factor of Safety – LE
1.08	0.92	1.03	0.43-1.45

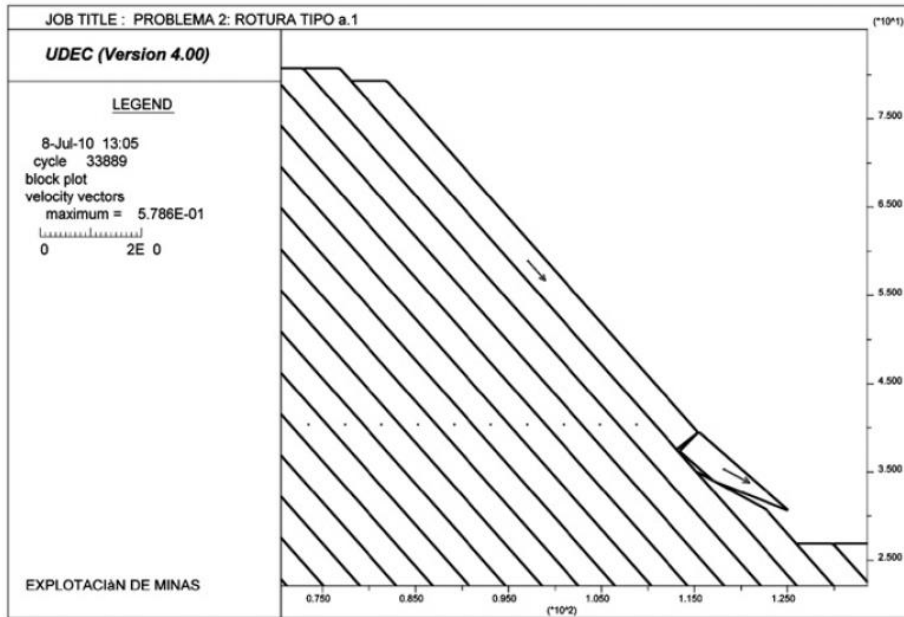


Figure 10.3: UDEC Model and Results (Alejano et al., 2011)

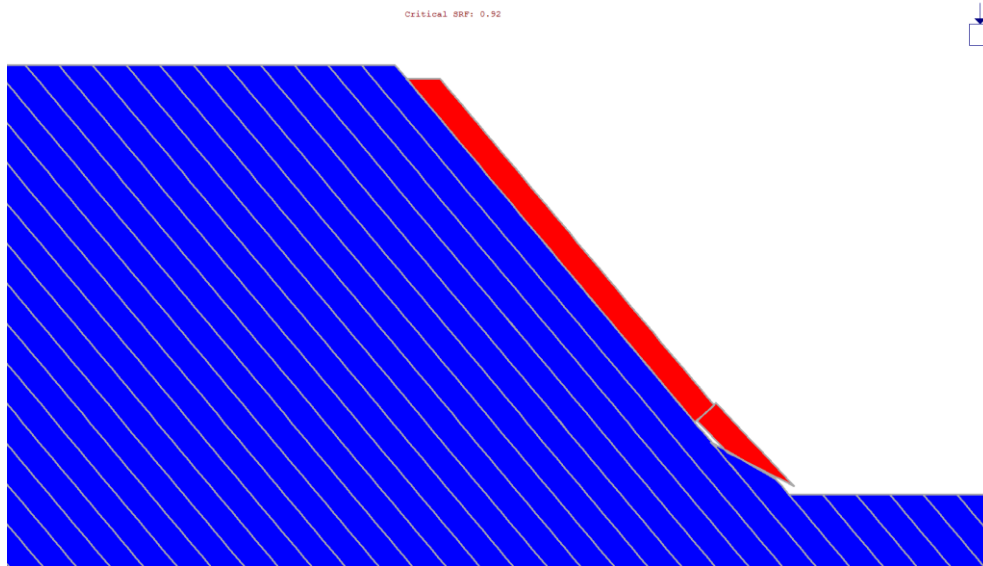


Figure 10.4: RS2 Deformed Shape

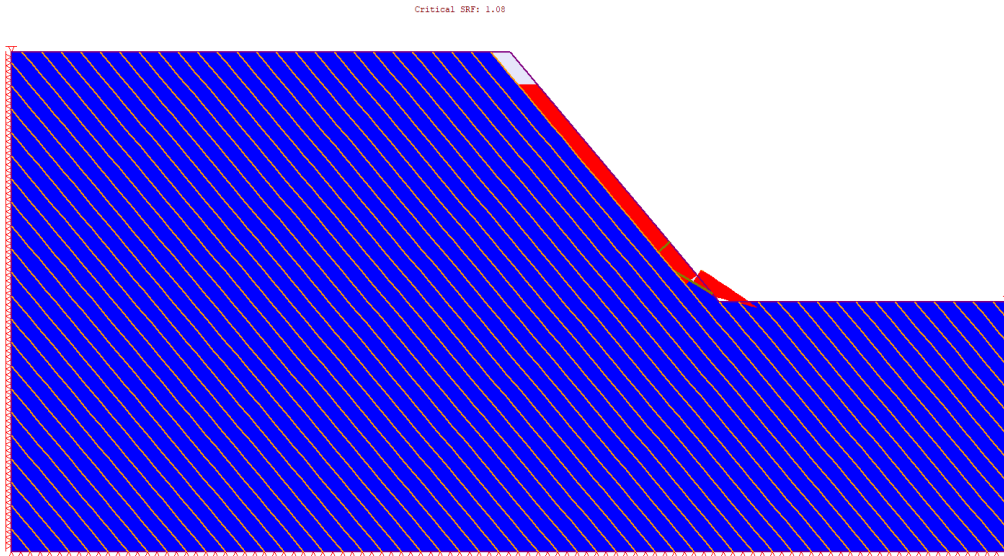


Figure 10.5: RS2-Joint convergence improved Deformed Shape

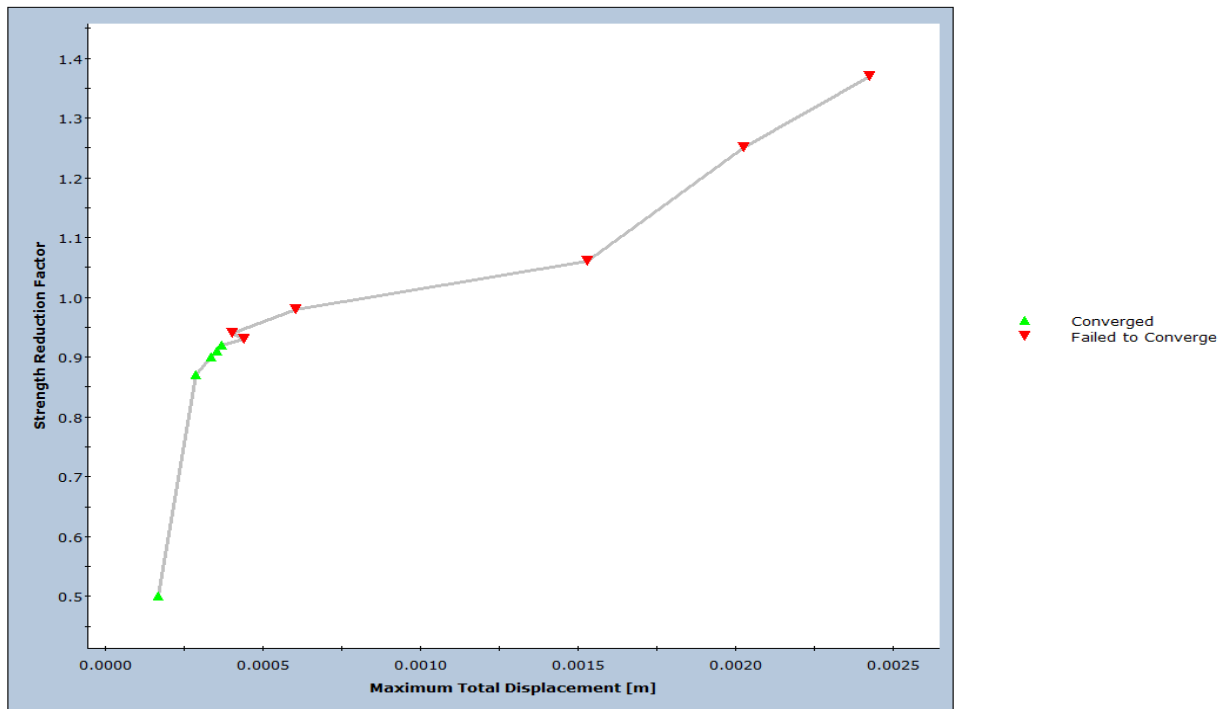


Figure 10.6: Shear Strength Reduction plot (RS2)

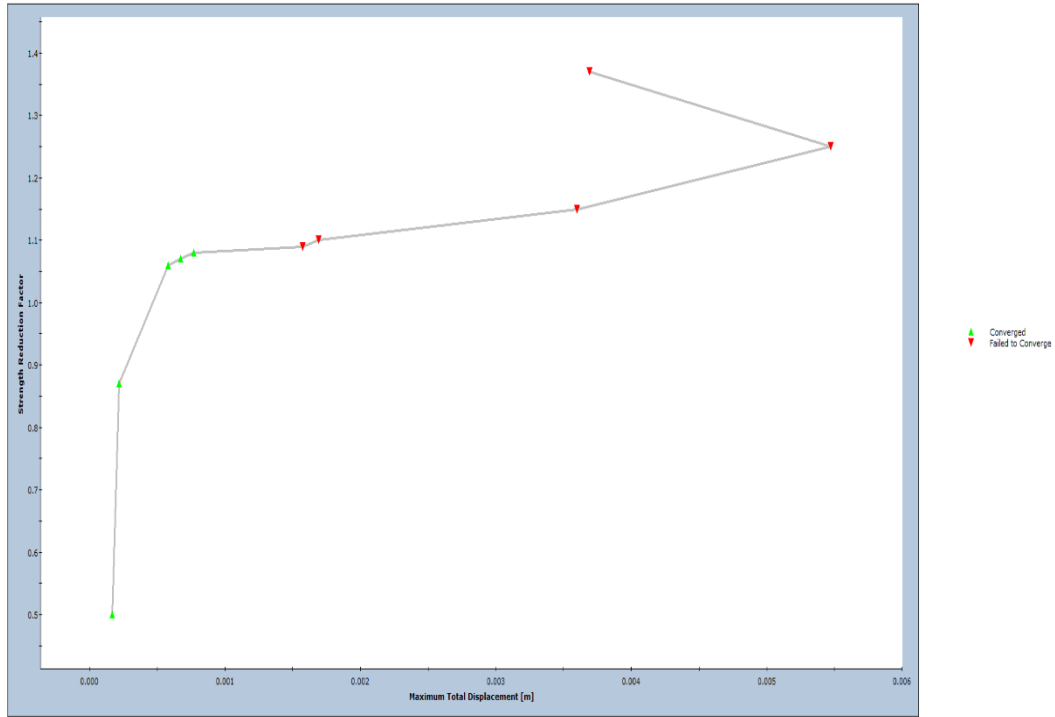


Figure 10.7: Shear Strength Reduction plot (RS2-Joint convergence improved)

11. Alejano et al. Ploughing Slab Failure

11.1. Introduction

This verification looks at the bilinear slab failure example from:

Alejano, L. R., Ferrero, A. M., Ramirez-Oyanguren, P., & Alvarez Fernandez, M. I. (2011). Comparison of Limit-Equilibrium, Numerical and Physical Models of Wall Slope Stability. *International Journal of Rock Mechanics and Mining Sciences*, 16-26.

11.2. Problem Description

An analysis of ploughing sliding slab failure was performed using RS2 and was verified using limit-equilibrium and UDEC-SSRT results provided in section 4.2.2 of the reference. Ploughing slab failure takes place when sliding along a primary discontinuity combines with sliding along a joint striking sub-parallel to the slope face, causing the toe block to be lifted and eventually rotated out of the slope. Note that rigid blocks were used in the UDEC model. To reproduce the model in RS2, an artificially high modulus of 2×10^8 MPa was given to the material. With such a high modulus, the tolerance for convergence also had to be reduced.

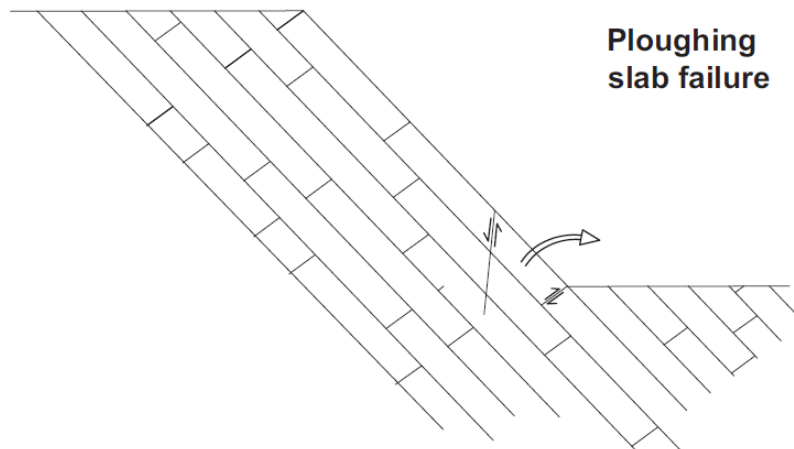


Figure 11.1: Ploughing Slab Failure (Alejano et al., 2011)

11.3. Geometry and Properties

Table 11.1: Material Properties

Slope Height (m)	Slope Angle (deg)	Joint Angle (deg)	ϕ' joint (deg)	Bedding Spacing (m)	ϕ' Bedding (deg)	γ (kN/m ³)
25	50	85	20	1.5	30	25.0

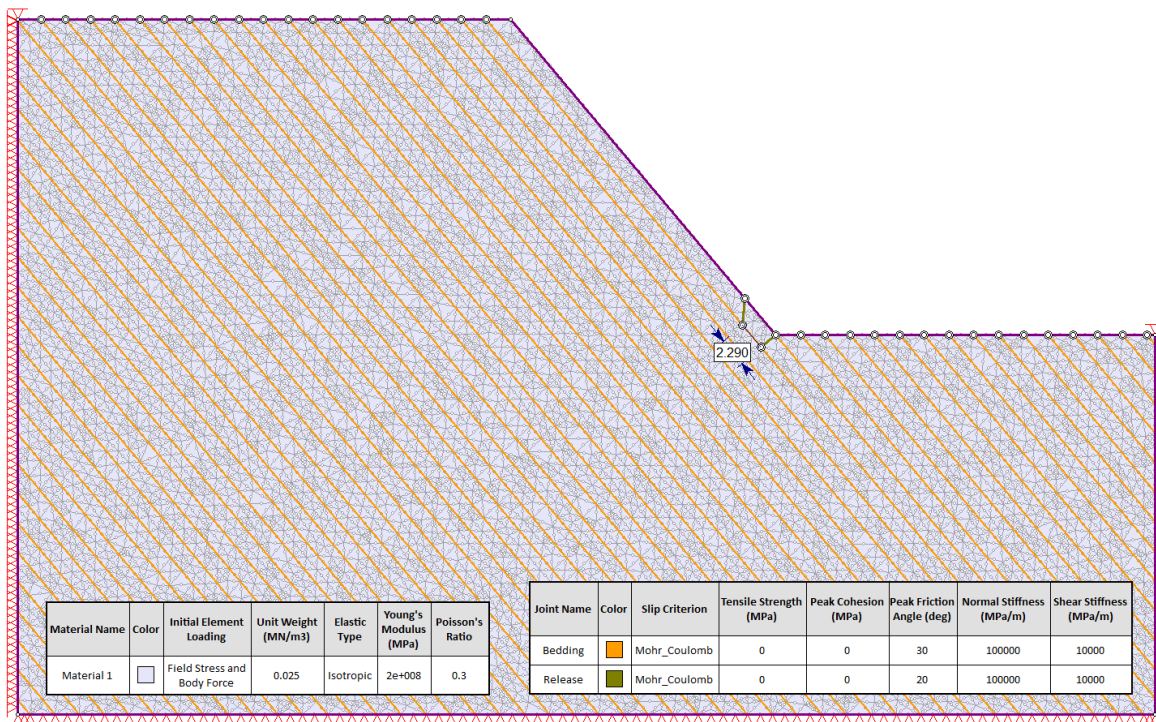


Figure 11.2: RS2 Geometry and Properties

11.4. Results

Table 11.2: Factor of Safety

Factor of Safety – RS2 with joint improvement	Factor of Safety – RS2 without joint improvement	Factor of Safety – UDEC	Factor of Safety – LE
1.3	1.22	1.21	1.75

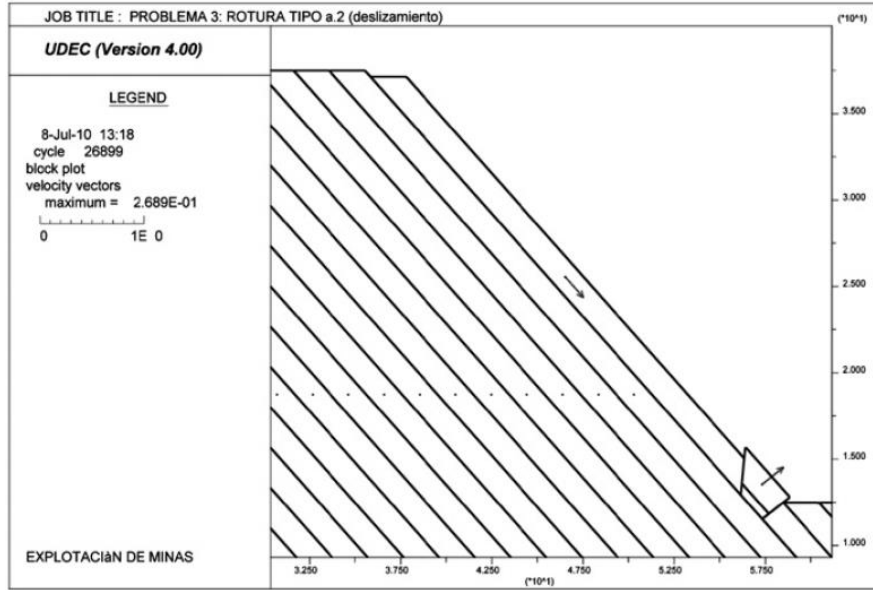


Figure 11.3: UDEC Model and Results (Alejano et al., 2011)

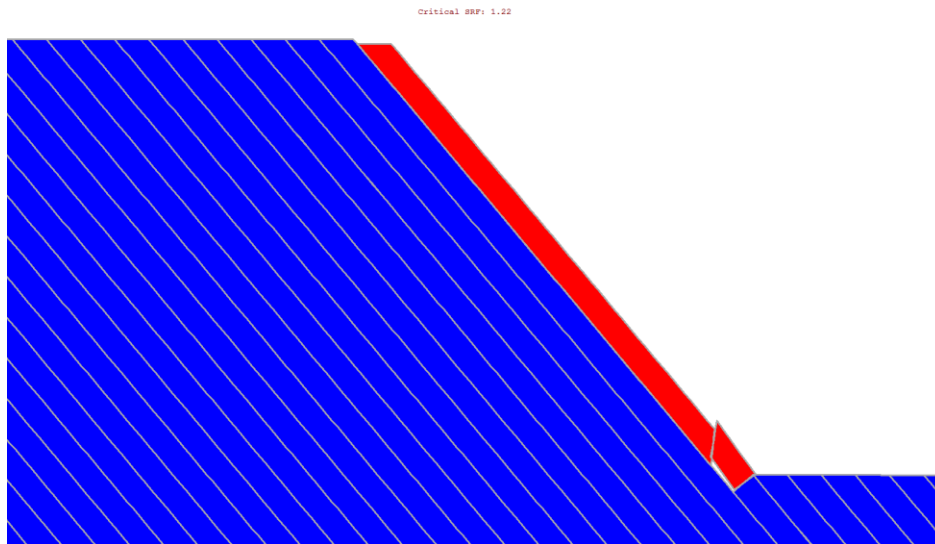


Figure 11.4: RS2 Deformed Shape

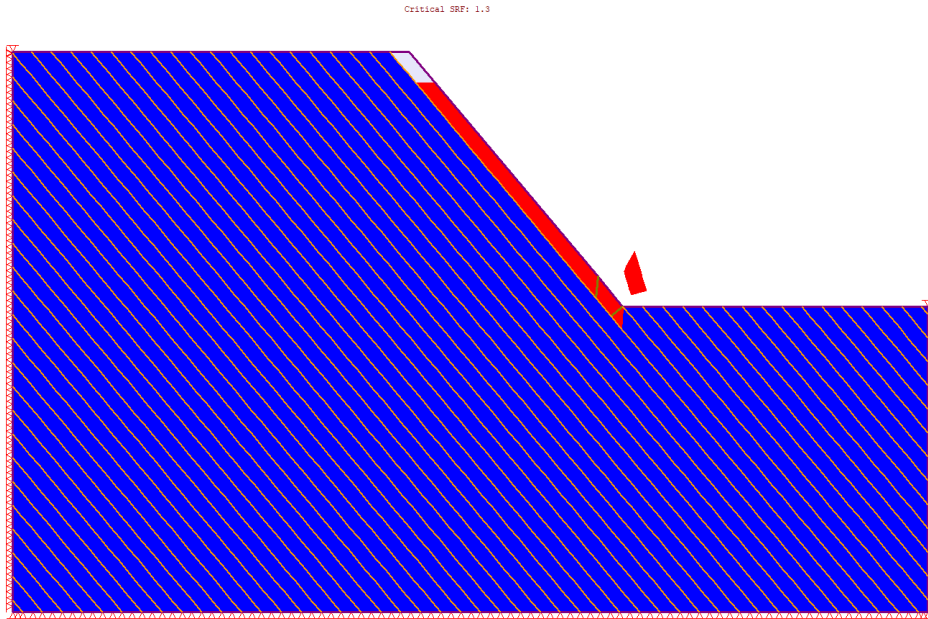


Figure 11.5: RS2-Joint convergence improved Deformed Shape

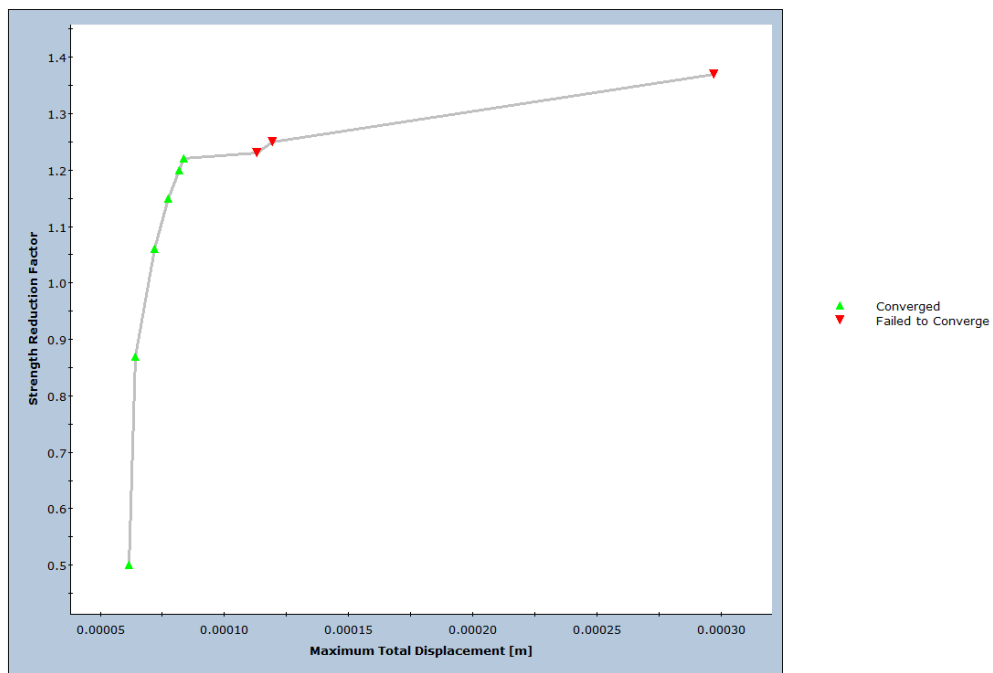


Figure 11.6: Shear Strength Reduction Plot (RS2)

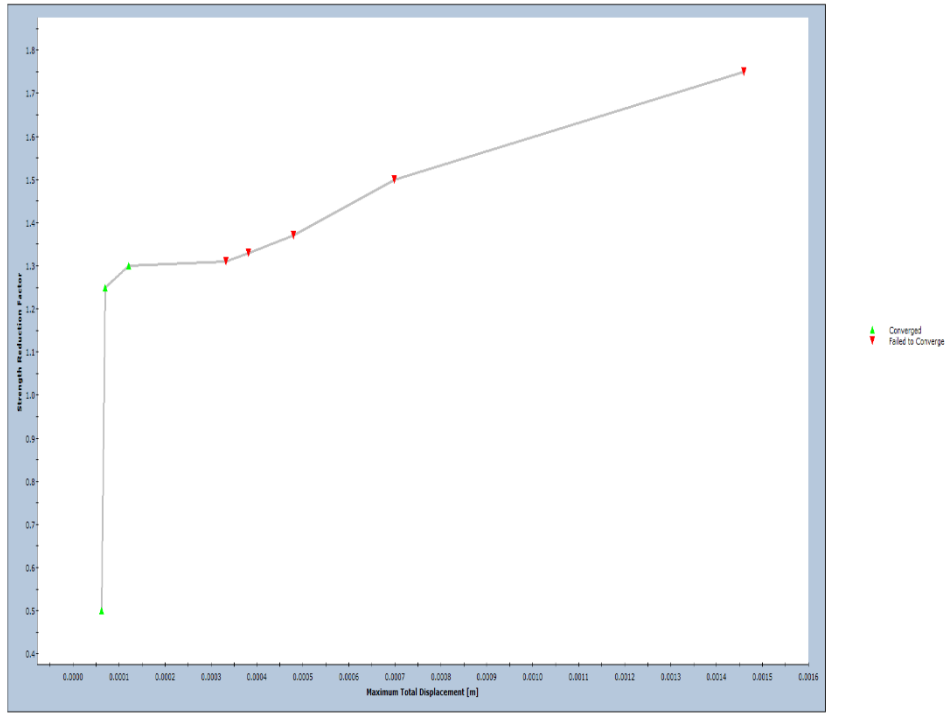


Figure 11.7: Shear Strength Reduction Plot (RS2-Joint convergence improved)

12. Alejano et al. Ploughing Toppling Slab Failure

12.1. Introduction

This verification looks at the bilinear slab failure example from:

Alejano, L. R., Ferrero, A. M., Ramirez-Oyanguren, P., & Alvarez Fernandez, M. I. (2011). Comparison of Limit-Equilibrium, Numerical and Physical Models of Wall Slope Stability. *International Journal of Rock Mechanics and Mining Sciences*, 16-26.

12.2. Problem Description

An analysis of ploughing toppling slab failure was performed using RS2 and was verified using limit-equilibrium and UDEC-SSRT results provided in section 4.2.3 of the reference. Ploughing slab failure takes place when sliding along a primary discontinuity combines with sliding along a joint striking sub-parallel to the slope face, causing the toe block to be lifted and eventually rotated out of the slope. Note that rigid blocks are used in the UDEC model. To reproduce the model in RS2, an artificially high modulus of 2×10^8 MPa was given to the material. With such a high modulus, the tolerance for convergence also had to be reduced.

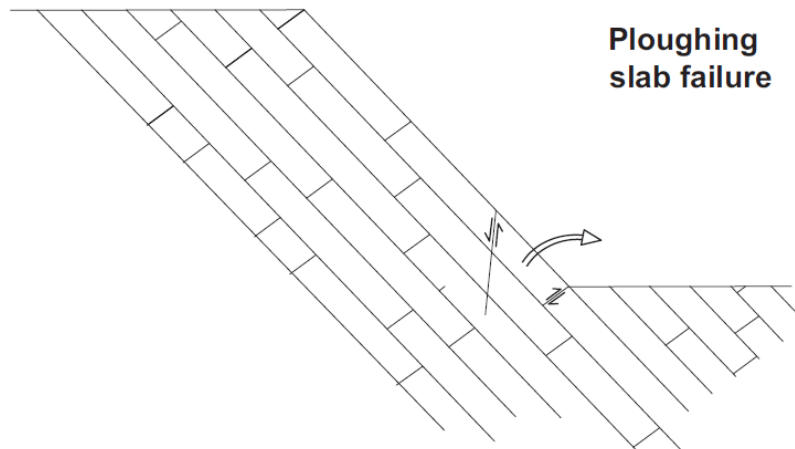


Figure 12.1: Ploughing Slab Failure (Alejano et al., 2011)

12.3. Geometry and Properties

Table 12.1: Material Properties

Slope Height (m)	Slope Angle (deg)	Joint Angle (deg)	ϕ' joint (deg)	Bedding Spacing (m)	ϕ' Bedding (deg)	γ (kN/m ³)
25	60	85	40	1.5	30	25.0

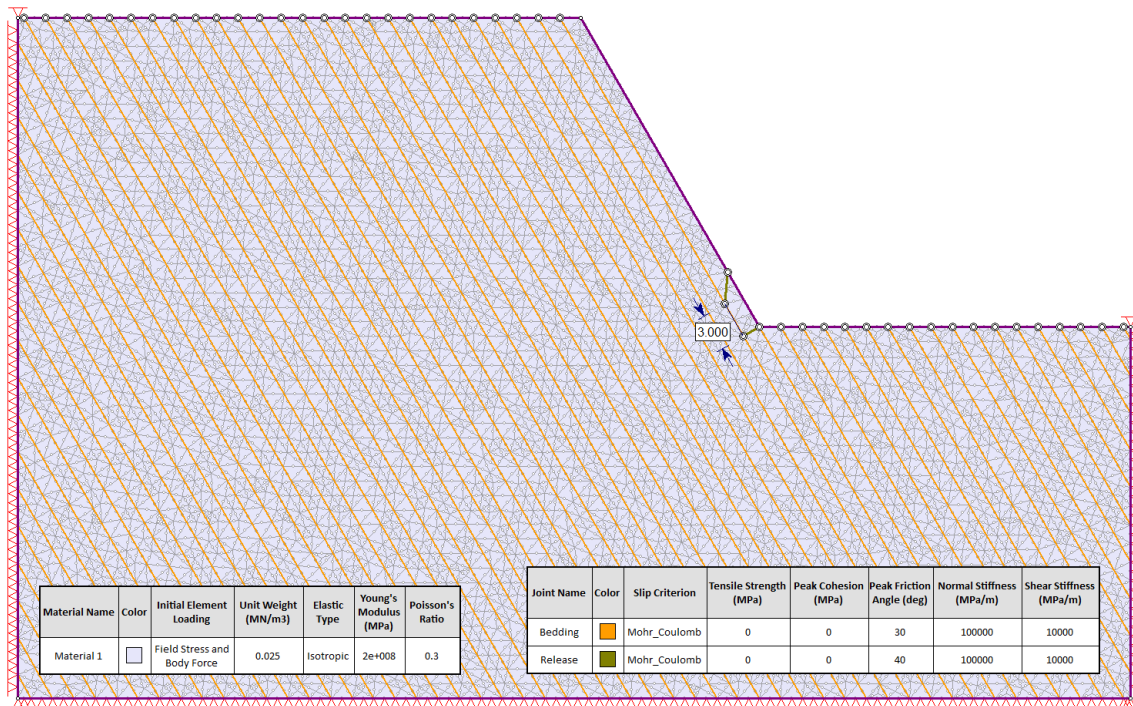


Figure 12.2: RS2 Geometry and Properties

12.4. Results

Table 12.2: Factor of Safety

Factor of Safety – RS2 with joint improvement	Factor of Safety – RS2 without joint improvement	Factor of Safety – UDEC	Factor of Safety – LE
1.75	1.39	1.78	2.0

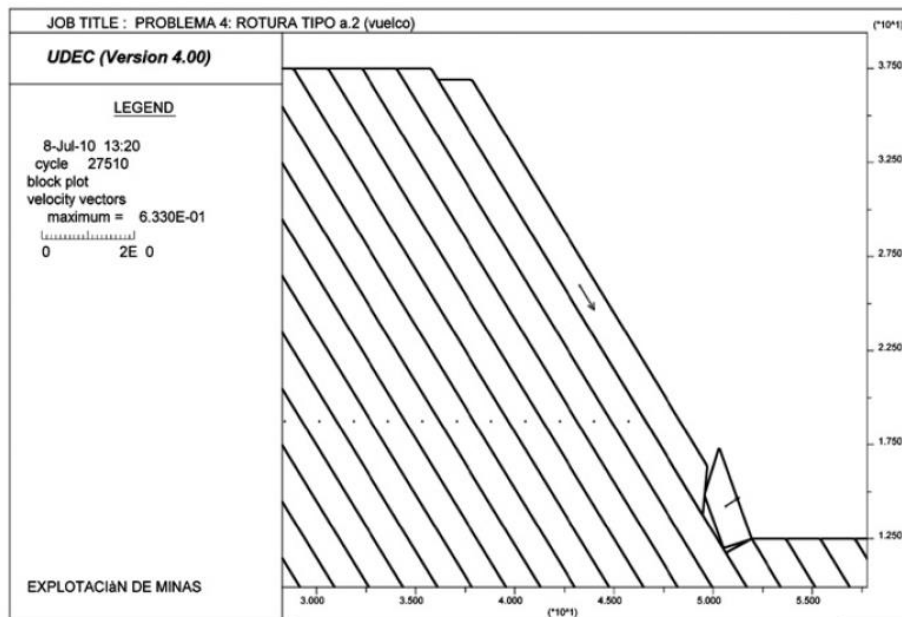


Figure 12.3: UDEC Model and Results (Alejano et al., 2011)

Critical SRP: 1.39

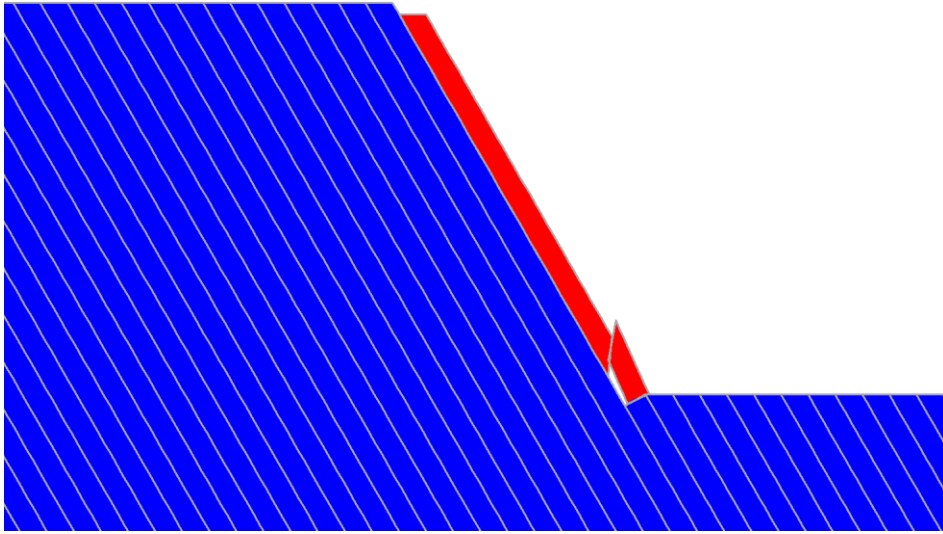


Figure 12.4: RS2 Deformed Shape

Critical SRP: 1.75

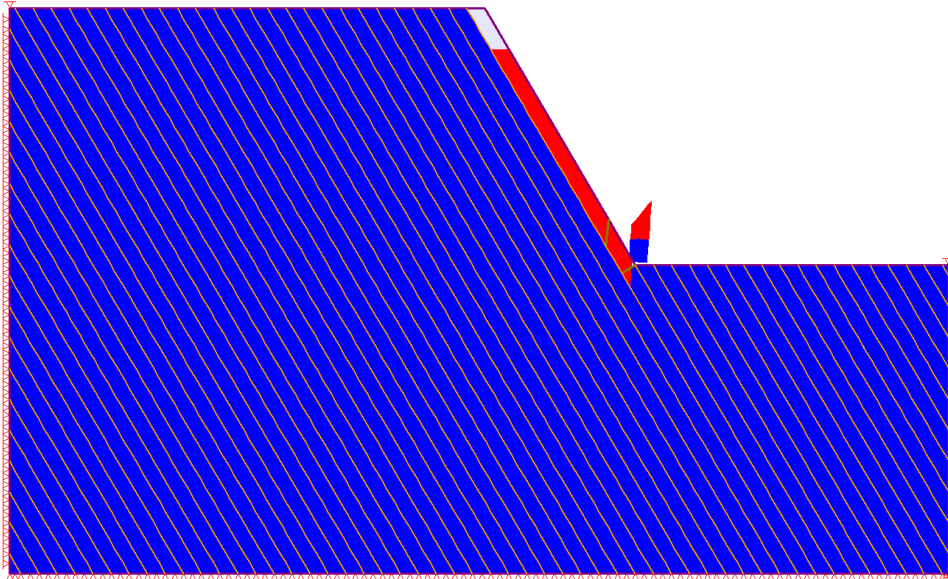


Figure 12.5: RS2-Joint convergence improved Deformed Shape

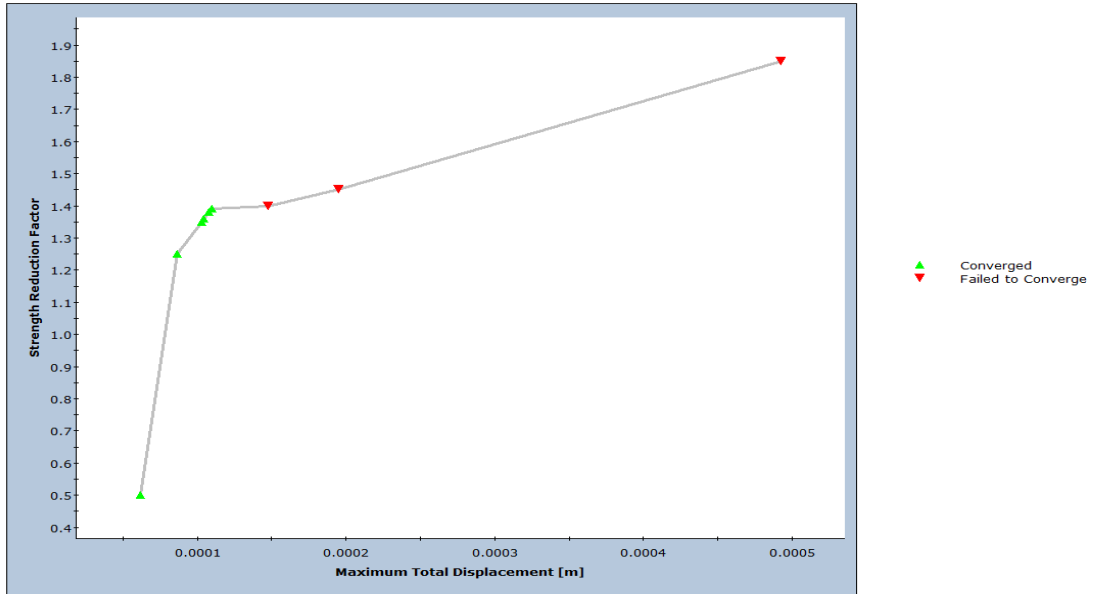


Figure 12.6: Shear Strength Reduction Plot (RS2)

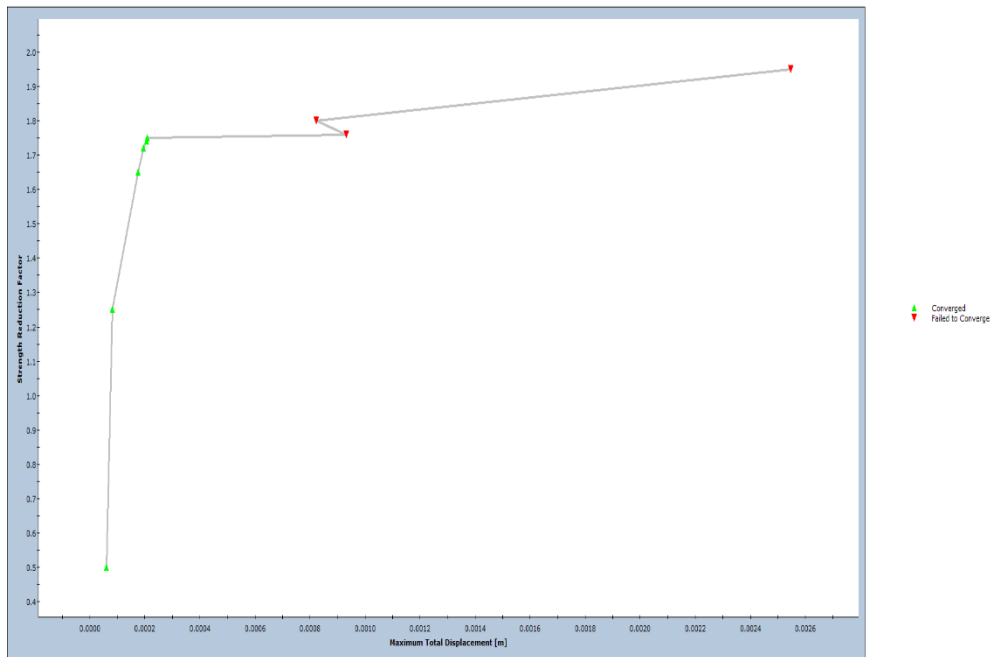


Figure 12.7: Shear Strength Reduction Plot (RS2-Joint convergence improved)

13. Alejano et Al. Ploughing Sliding Slab Failure

13.1. Introduction

This verification looks at the ploughing slab failure example from:

Alejano, L. R., Ferrero, A. M., Ramirez-Oyanguren, P., & Alvarez Fernandez, M. I. (2011). Comparison of Limit-Equilibrium, Numerical and Physical Models of Wall Slope Stability. *International Journal of Rock Mechanics and Mining Sciences*, 16-26.

13.2. Problem Description

An analysis of ploughing sliding slab failure was performed using RS2 and was verified using limit-equilibrium and UDEC-SSRT results provided in example 4 of section 4.2.4 in the reference. Ploughing slab failure takes place when sliding along a primary discontinuity combines with sliding along a joint striking sub-parallel to the slope face, causing the toe block to be lifted and eventually rotated out of the slope. Note that rigid blocks were used in the UDEC model. To reproduce this model in RS2, an artificially high modulus of 2×10^8 MPa was given to the material. With such a high modulus, the tolerance for convergence also had to be reduced.

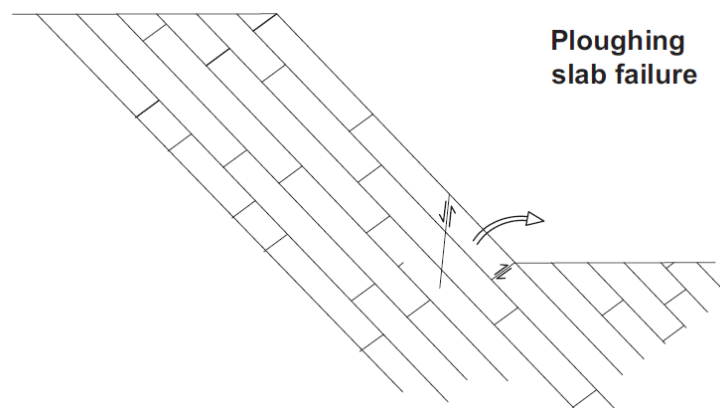


Figure 13.1: Ploughing Slab Failure (Alejano et al., 2011)

13.3. Geometry and Properties

Table 13.1: Slope Geometry and Material Properties

Slope Height (m)	Slope Angle (deg)	Joint Angle (deg)	ϕ' joint (deg)	Bedding Spacing (m)	ϕ' Bedding (deg)	γ (kN/m ³)
25	55	95	20	1.5	25	25.0

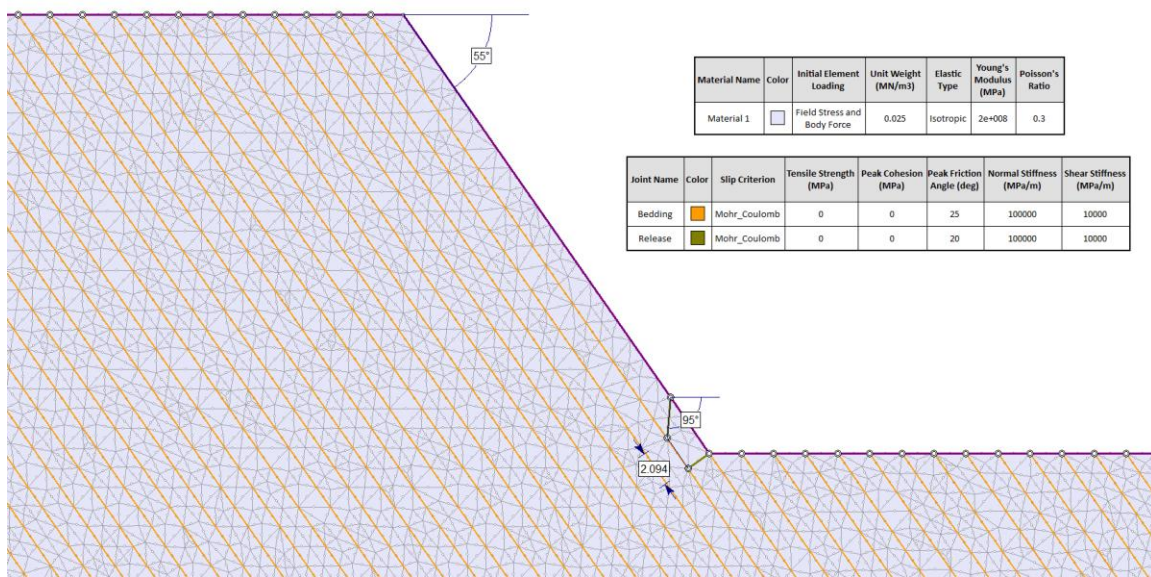


Figure 13.2: RS2 Geometry and Properties

13.4. Results

Table 13.2: Factor of Safety

Factor of Safety – RS2 with joint improvement	Factor of Safety – RS2 without joint improvement	Factor of Safety – UDEC	Factor of Safety – LE
1.05	1.0	1.0	1.0

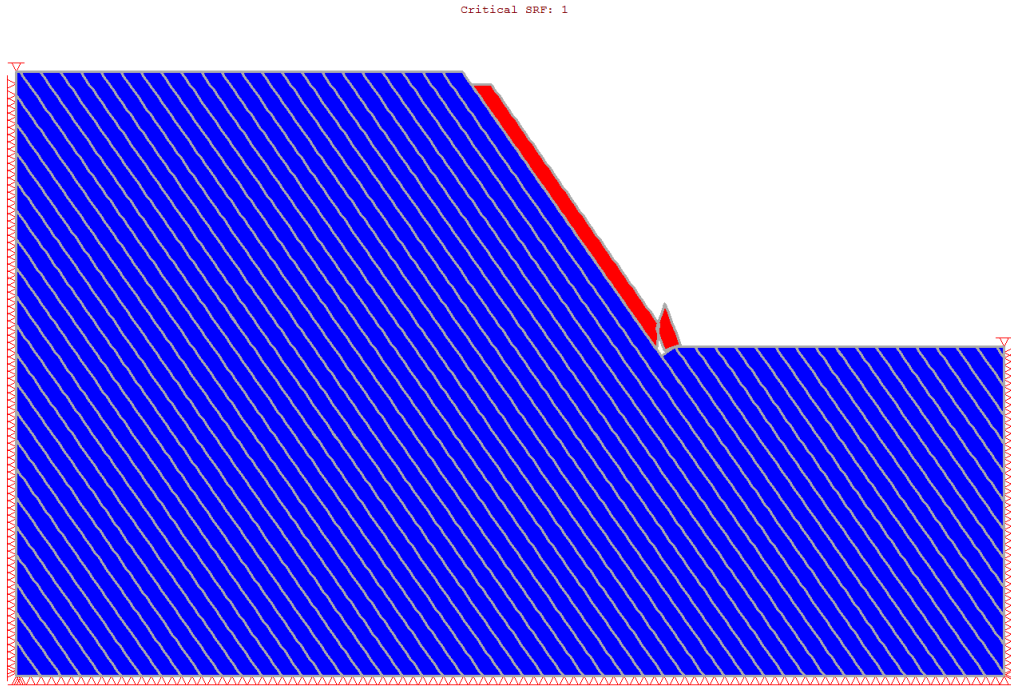


Figure 13.3: RS2 Deformed Shape

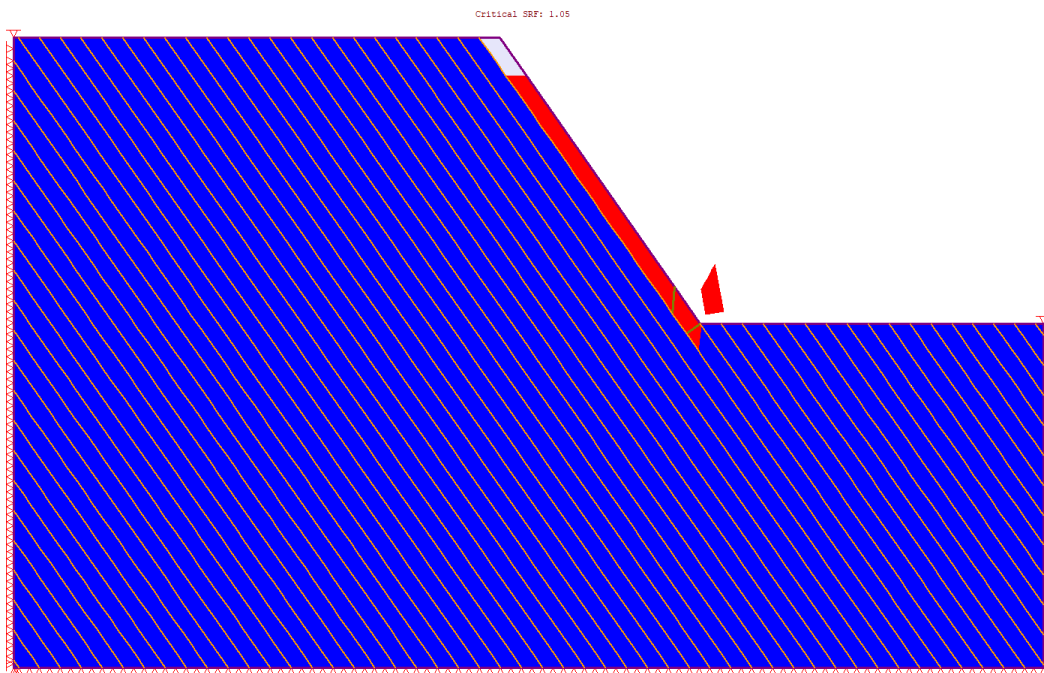


Figure 13.4: RS2-Joint convergence improved Deformed Shape

14. Alejano et al. Ploughing Sliding Slab Failure

14.1. Introduction

This verification looks at the ploughing slab failure example from:

Alejano, L. R., Ferrero, A. M., Ramirez-Oyanguren, P., & Alvarez Fernandez, M. I. (2011). Comparison of Limit-Equilibrium, Numerical and Physical Models of Wall Slope Stability. *International Journal of Rock Mechanics and Mining Sciences*, 16-26.

14.2. Problem Description

An analysis of ploughing sliding slab failure was performed using RS2 and was verified using limit-equilibrium and UDEC-SSRT results provided in example 5 of section 4.2.4 in the reference. Ploughing slab failure takes place when sliding along a primary discontinuity combines with sliding along a joint striking sub-parallel to the slope face, causing the toe block to be lifted and eventually rotated out of the slope. Note that the rigid blocks were used in the UDEC model. To model this in RS2, an artificially high modulus of 2×10^8 MPa was given to the material. With such a high modulus, the tolerance for convergence also had to be reduced.

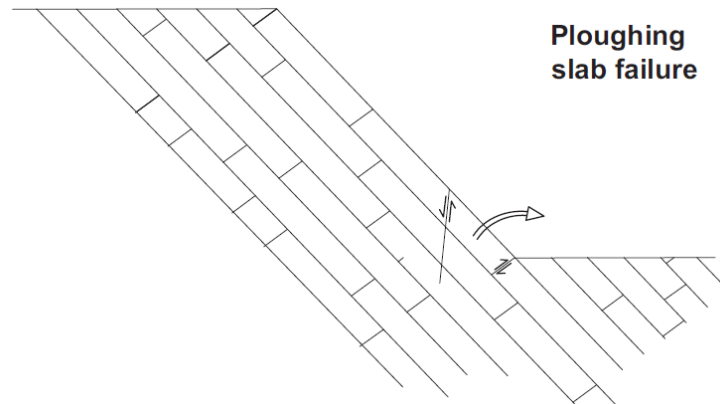


Figure 14.1: Ploughing Slab Failure (Alejano et al., 2011)

14.3. Geometry and Properties

Table 14.1: Slope Geometry and Material Properties

Slope Height (m)	Slope Angle (deg)	Joint Angle (deg)	ϕ' joint (deg)	Bedding Spacing (m)	ϕ' Bedding (deg)	γ (kN/m ³)
25	60	95	30	1.5	20	25.0

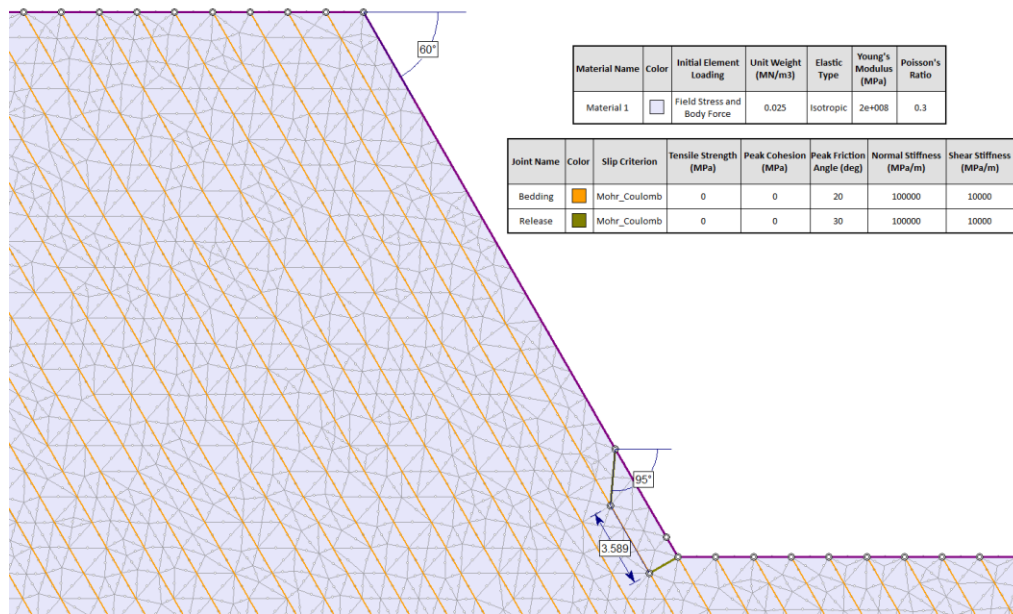


Figure 14.2: RS2 Geometry and Properties

14.4. Results

Table 14.2: Factor of Safety

Factor of Safety – RS2 with joint improvement	Factor of Safety – RS2 without joint improvement	Factor of Safety – UDEC	Factor of Safety – LE
1.09	0.89	0.9	1.0

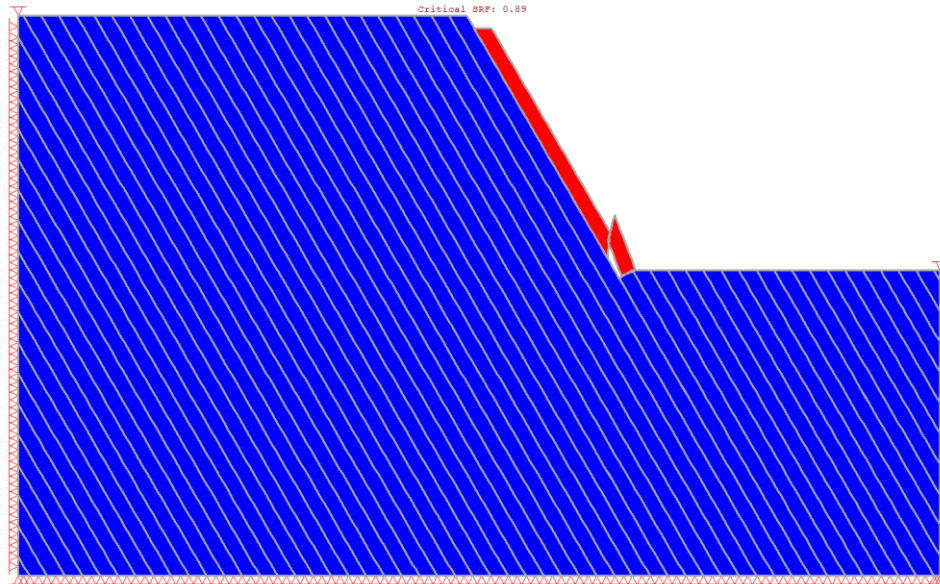


Figure 14.3: RS2 Deformed Shape

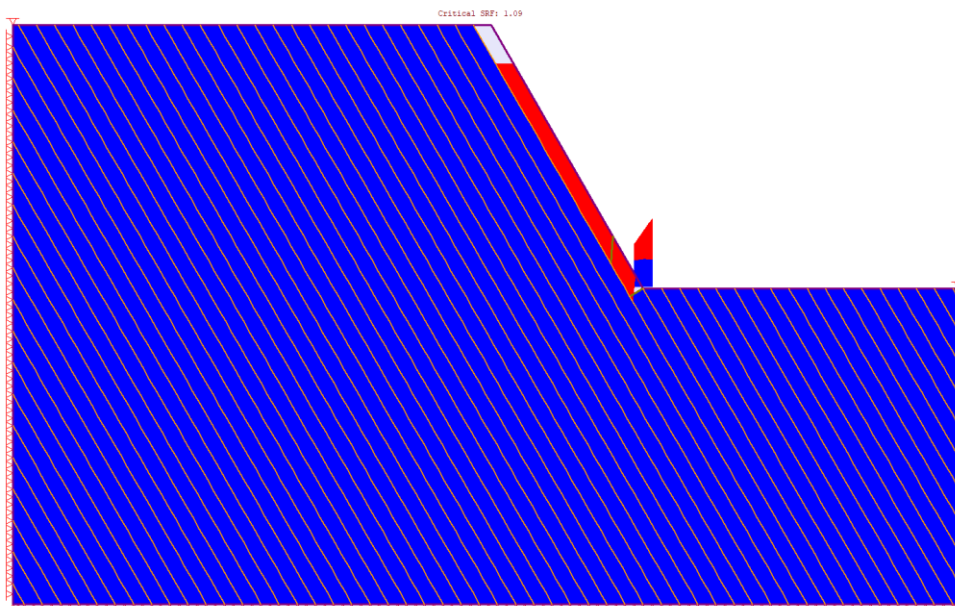


Figure 14.4: RS2-Joint convergence improved Deformed Shape

15. Alejano et Al. Partially Joint - Controlled Footwall Slope Failure

15.1. Introduction

This verification looks at the partially joint-controlled slope failure example from:

Alejano, L. R., Ferrero, A. M., Ramirez-Oyanguren, P., & Alvarez Fernandez, M. I. (2011). Comparison of Limit-Equilibrium, Numerical and Physical Models of Wall Slope Stability. *International Journal of Rock Mechanics and Mining Sciences*, 16-26.

15.2. Problem Description

An analysis of partially joint-controlled slope failure was performed using RS2 and was verified using limit-equilibrium and UDEC-SSRT results provided in example 6 of section 4.2.5 in the reference. A joint set dips in the same direction and angle as the slope. The mechanism of failure is one of joint slip coupled with break-through failure of the rock mass at the toe of the slope.

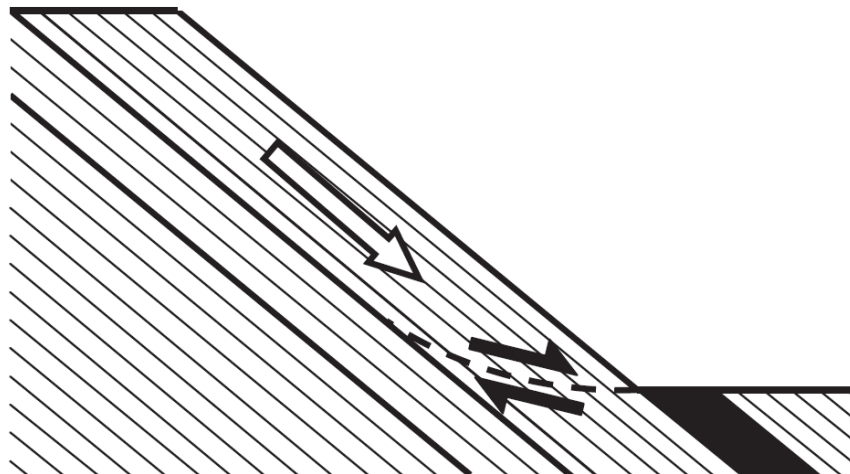


Figure 15.1: Partially Joint-Controlled Slope Failure (Alejano et al., 2011)

15.3. Geometry and Properties

Table 15.1: Slope Geometry and Material Properties

Slope Height (m)	Slope Angle (deg)	Rock Cohesion (MPa)	ϕ' Rock (deg)	Bedding Spacing (m)	ϕ' Bedding (deg)	γ (kN/m ³)
25	40	0.2	35	2	25	28.0

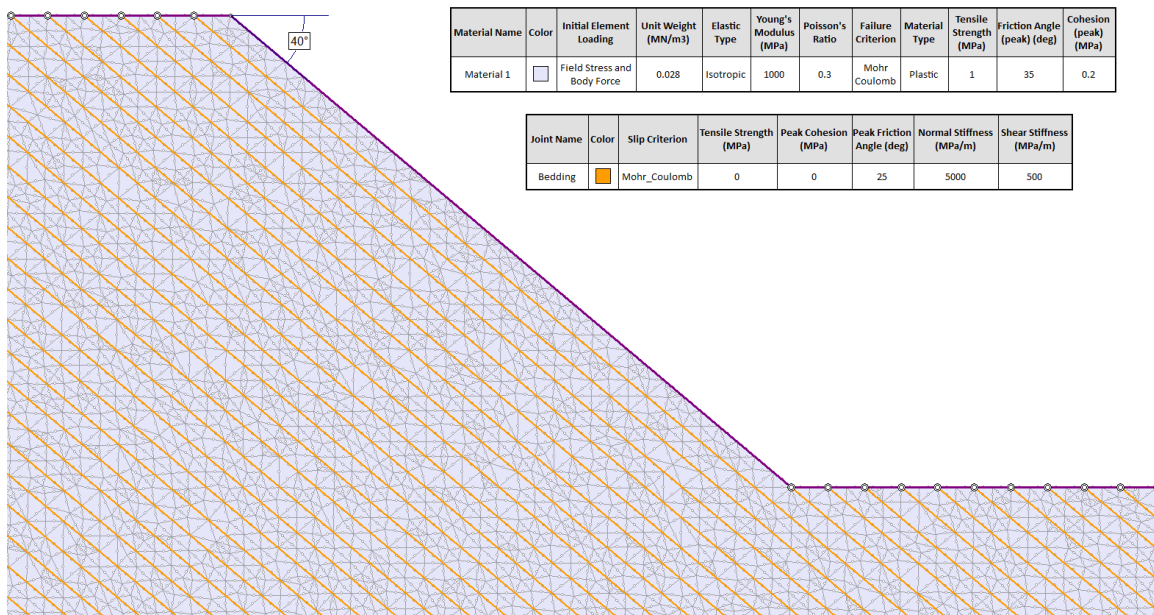


Figure 15.2: RS2 Geometry and Properties

15.4. Results

Table 15.2: Factor of Safety

Factor of Safety - RS2 with joint improvement	Factor of Safety - RS2 without joint improvement	Factor of Safety Slide LEM	Factor of Safety UDEC	Factor of Safety LE (Alejano)
1.42	1.28	1.25	1.6	1.72

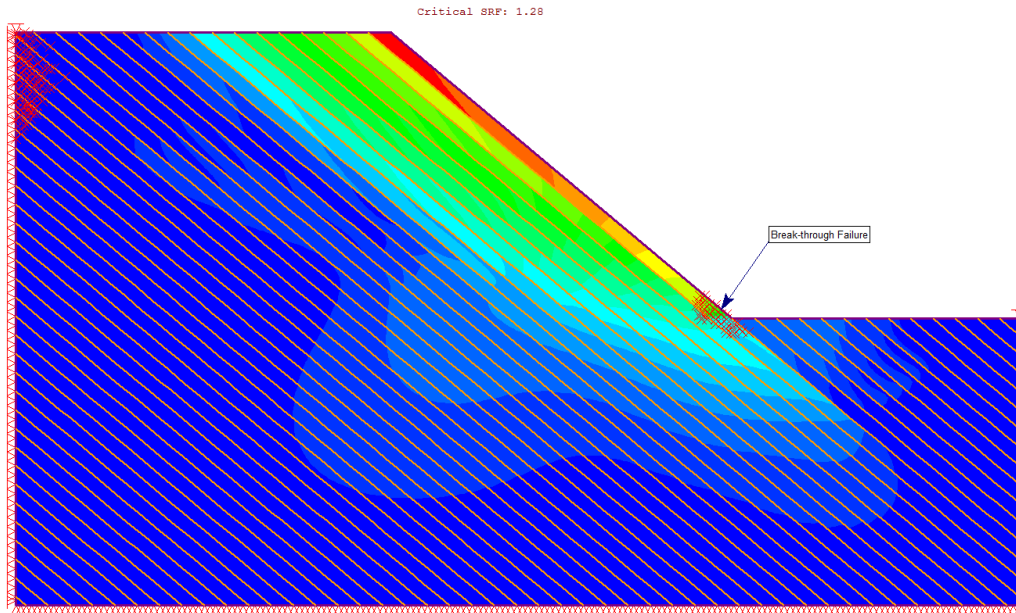


Figure 15.3: RS2 Displacement Contours with Failure

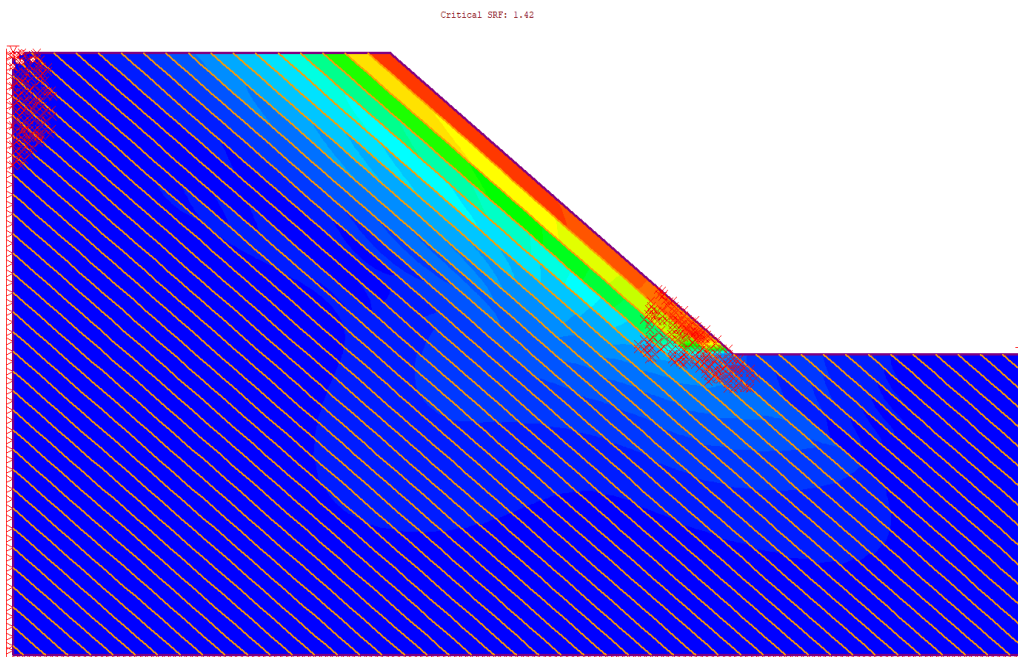


Figure 15.4: RS2-Joint convergence improved Displacement Contours with Failure

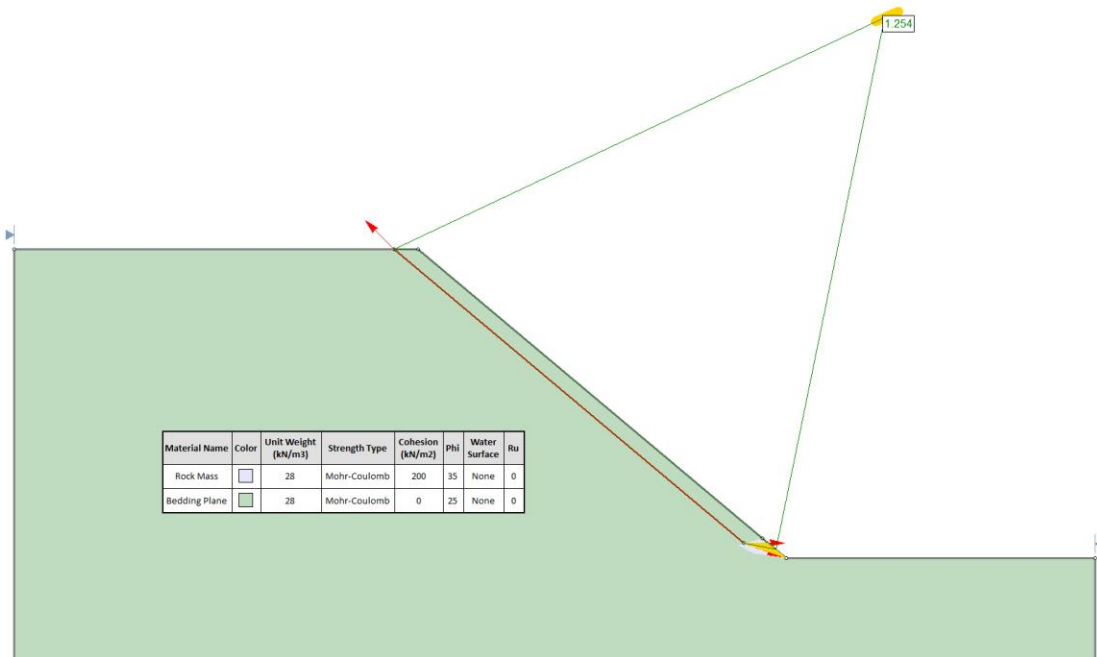


Figure 15.5: Spencer Factor of Safety Results from Slide

16. Barla et al. Partially Joint - Controlled Footwall Slope Failure

16.1. Introduction

This verification looks at a lab test performed in:

Barla, G., Borri-Brunetto, M., Devin, P., & Zaninetti, A. (1995). Validation of a Distinct Element Model for Toppling Rock Slopes. *8th International Congress on Rock Mechanics*, (pp. 417-421). Tokyo, Japan.

Lanaro, F., Jing, L., Stephansson, O., & Barla, G. (1997, April - June). D.E.M. Modelling of Laboratory Tests of Block Toppling. *International Journal of Rock Mechanics and Mining Sciences*, pp. 173e1 - 173e15.

16.2. Problem Description

A series of 9cm square blocks is stacked on a tilt plate in order to produce a 63° slope (Figure 17.1). The system of blocks is then rotated until the blocks topple. The angle at which the blocks topple, and the displacement of the crest block in a direction parallel with the base, are measured. A UDEC model was also built for the purpose of modeling the experiment. A comparison of RS2, UDEC and experimental results are provided below.

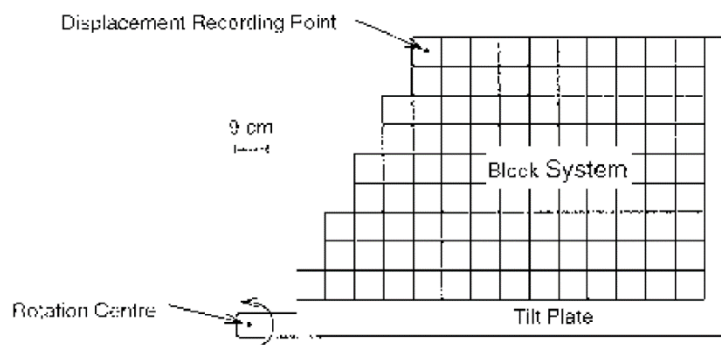


Figure 16.1: Lab Test Geometry (Lanaro et al., 1997)

16.3. Geometry and Properties

Table 16.1: Material Properties

Block Modulus (MPa)	Joint K_n (GPa/m)	Joint K_s (GPa/m)	ϕ' Joint (deg)	γ (kN/m ³)
350	5	0.5	38	28.0

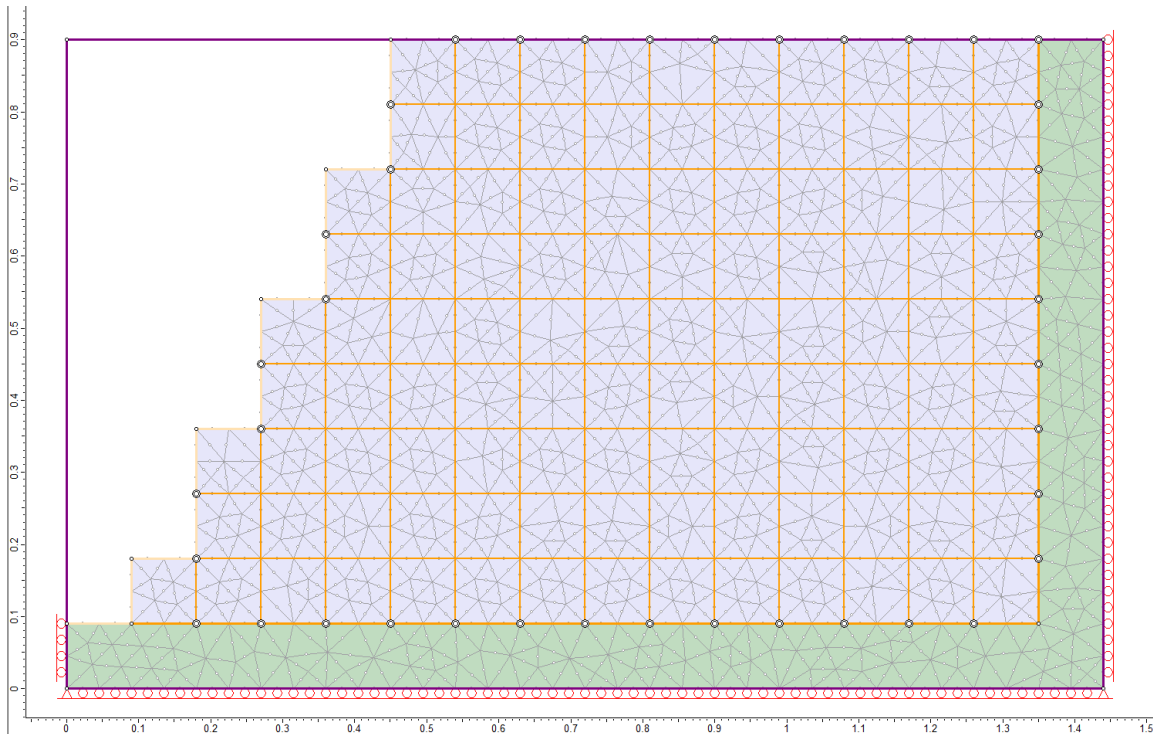


Figure 16.2: RS2 Geometry

16.4. Results

Table 16.2: Tilt Angle at Failure

Tilt Angle at Failure RS2 (deg)	Tilt Angle at Failure Experiment (deg)	Tilt Angle at Failure RS2 (deg)	Tilt Angle at Failure UDEEC (deg)
7	9	9	11

9 Degrees

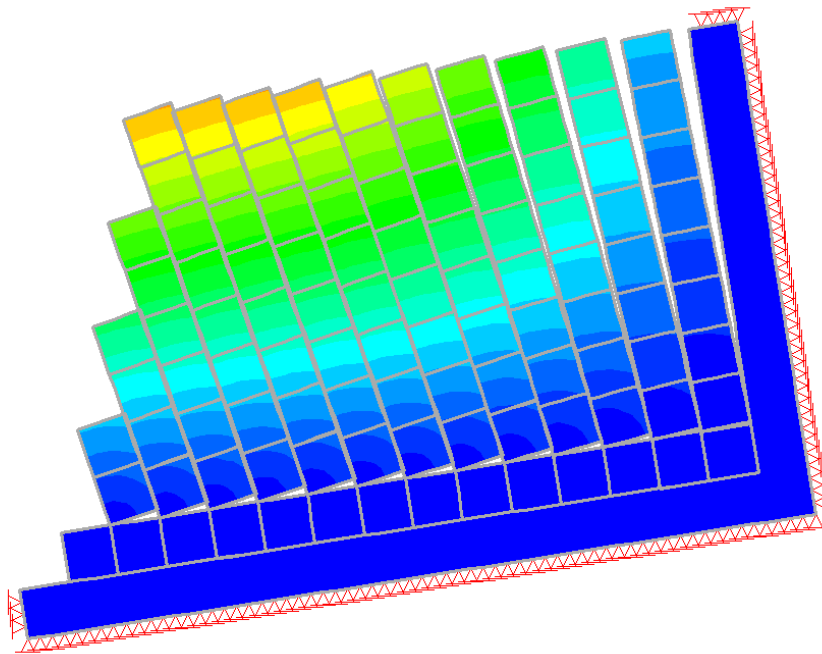


Figure 16.3: Displacement Contours and Deformed Shape at 9° (RS2)

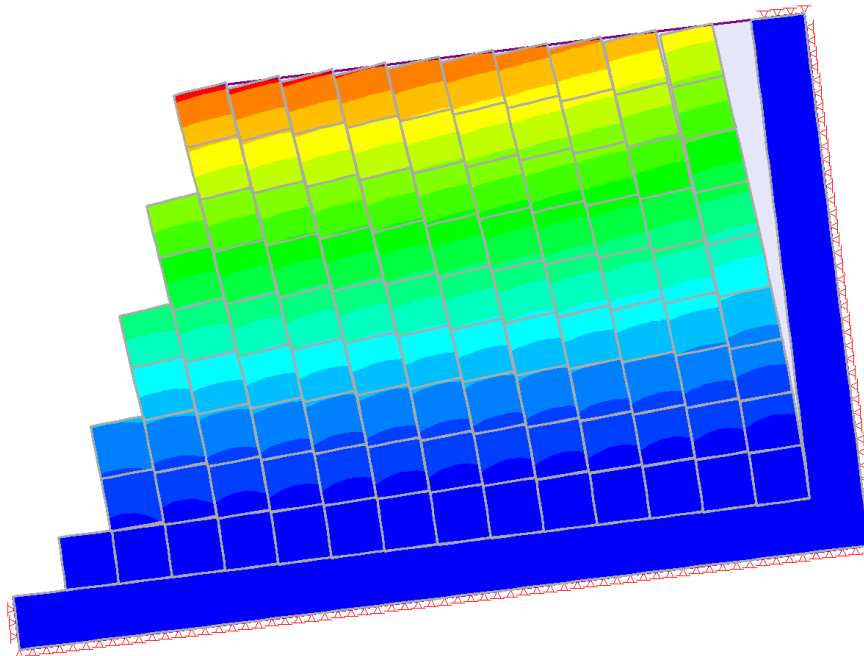


Figure 16.4: Displacement Contours and Deformed Shape at 7° (RS2-Joint convergence improved)

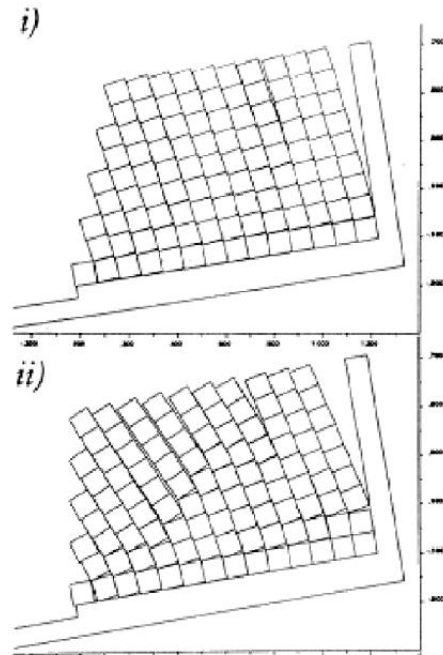


Figure 16.5: Evolution of Toppling using UDEC (Lanaro et al., 2011)

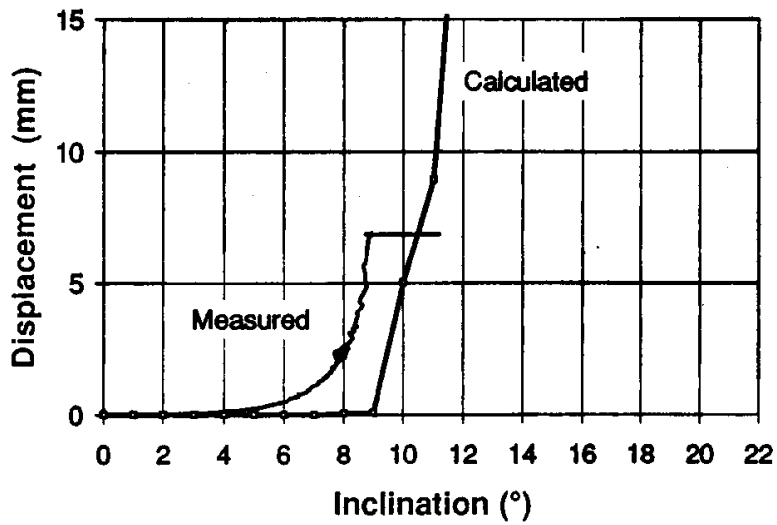


Figure 5. Comparison of results from physical and mathematical model. Displacements of the crest block. Model with 2:1 slope (63°).

Figure 16.6: Experimental and UDEC Displacement Results (Barla et al., 1997)

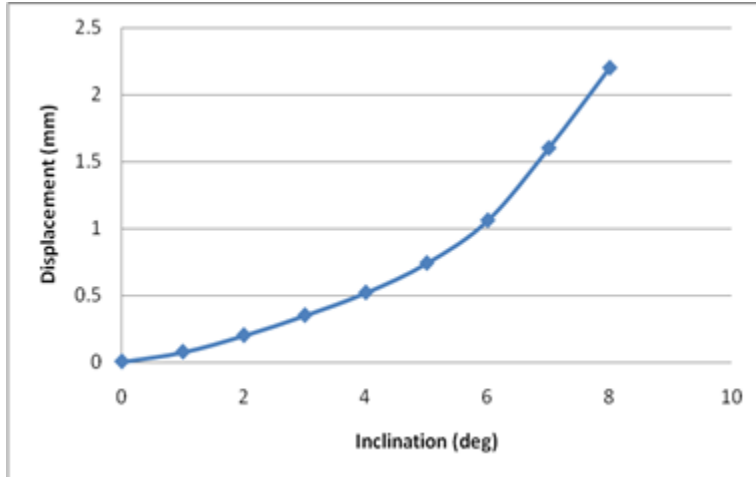


Figure 16.7: RS2 Displacement Results

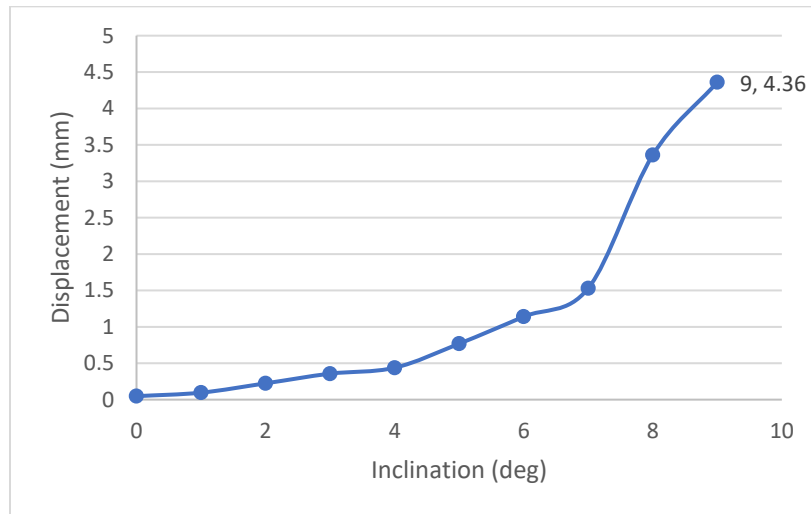


Figure 16.8: RS2-Joint convergence improved Displacement Results

17. Step-Path Failure with En-Echelon Joints

17.1. Introduction

This verification looks at an example application in:

Itasca Consulting Group Inc. (2011). Step-Path Failure of Rock Slopes. In I. C. Inc., *UDEC Version 5.0 Example Applications* (pp. 13-1 to 13-9). Minneapolis.

17.2. Problem Description

RS2 was used to analyze the step-path failure in a rock slope containing three non-continuous en-echelon joints. Step-path failure occurs when shear failure along joints combines with shear and tensile failure in the intact rock bridging between joints. RS2 results are compared to the UDEC results provided in the reference.

17.3. Geometry and Properties

Table 17.1: Slope Geometry and Properties

Slope Height (m)	Slope Angle (deg)	Joint Angle (deg)	ϕ' joint (deg)	Bedding Spacing (m)	γ (kN/m ³)
11.8	50	36.1	35	1.0	19.62

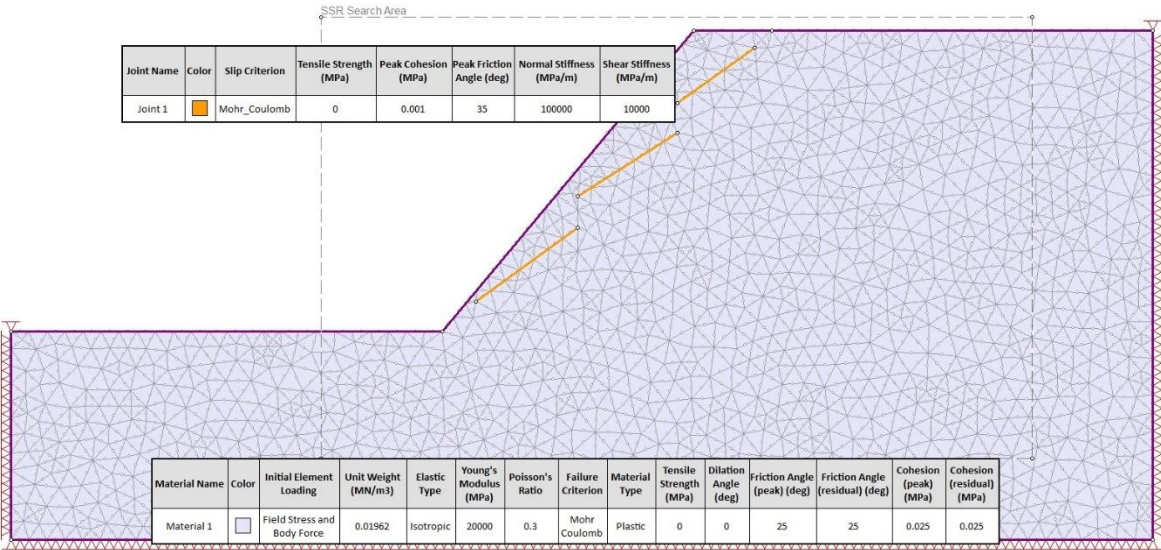


Figure 17.1: RS2 Slope Geometry and Material Properties

17.4. Results

Table 17.2: Factor of Safety

Factor of Safety – RS2 with joint improvement	Factor of Safety – RS2 without joint improvement	Factor of Safety – UDEC
1.2	1.24	1.29

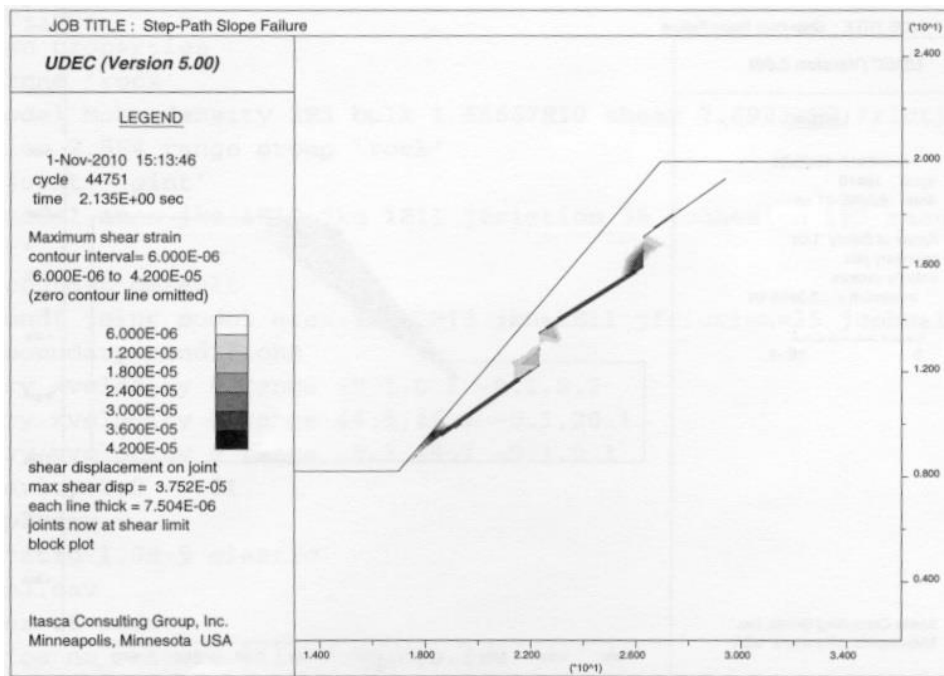


Figure 17.2: Joint Maximum Shear Displacement and Rock Maximum Shear Strain (UDEC, 2011)

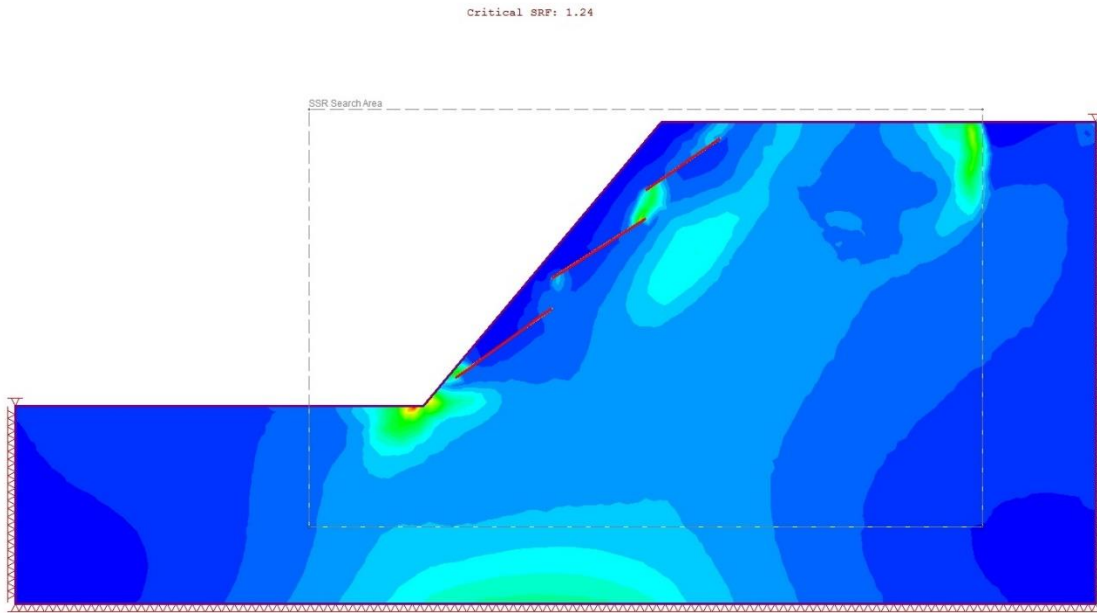


Figure 17.3: Maximum Shear Strain and Joints Yielding at SRF = 1.24(RS2)

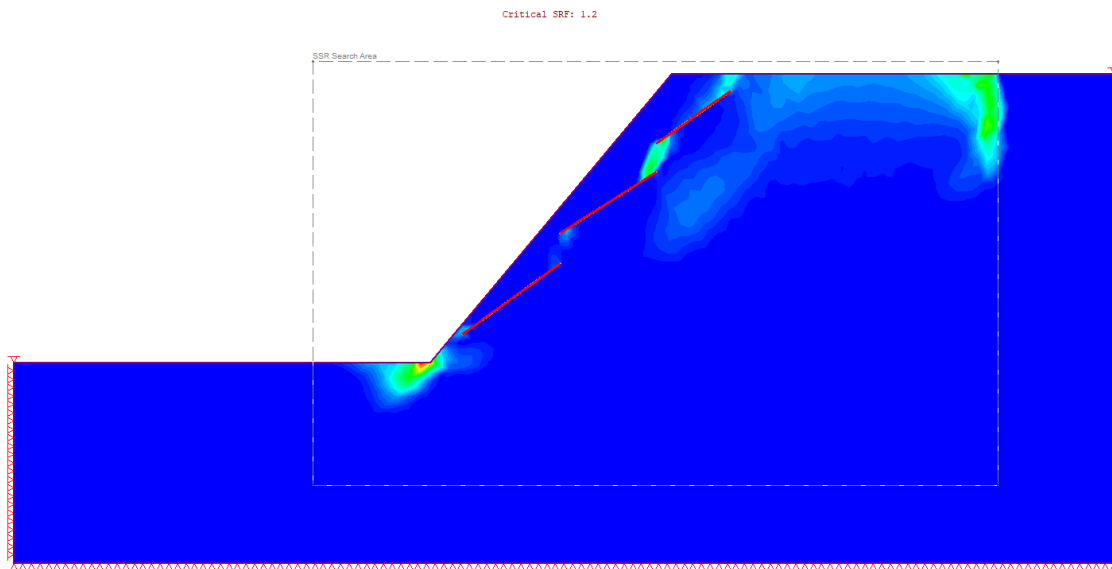


Figure 17.4: Maximum Shear Strain and Joints Yielding at SRF = 1.24(RS2-Joint convergence improved)

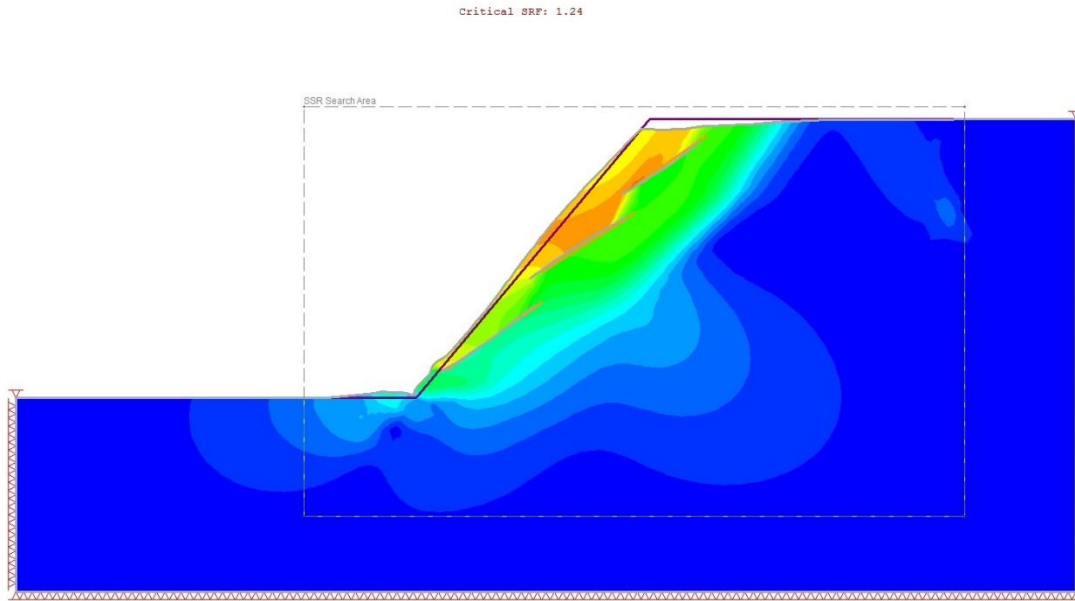


Figure 17.5: Total Displacement in RS2

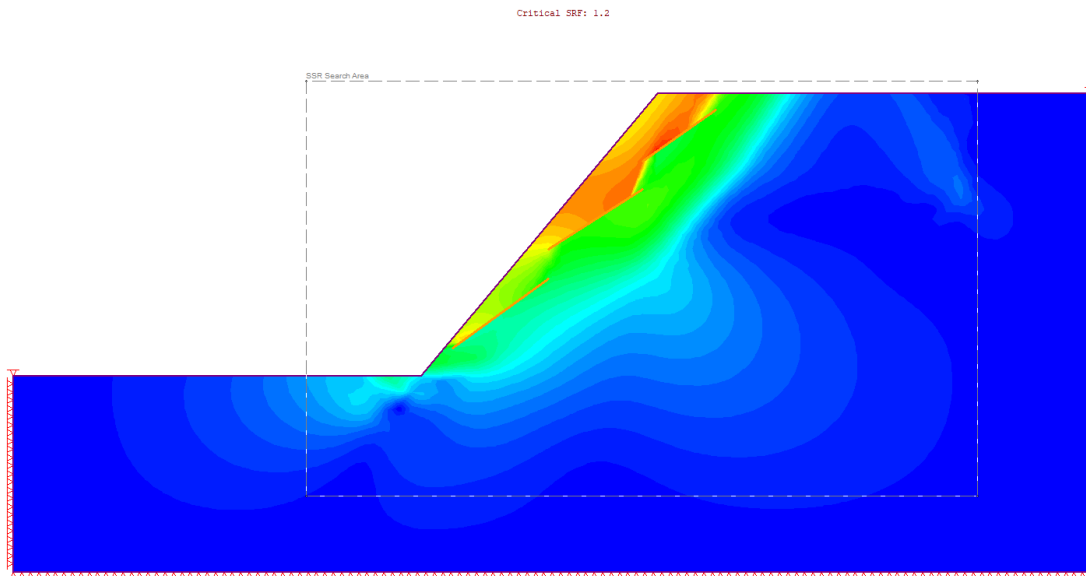


Figure 17.6: Total Displacement in RS2-Joint convergence improved

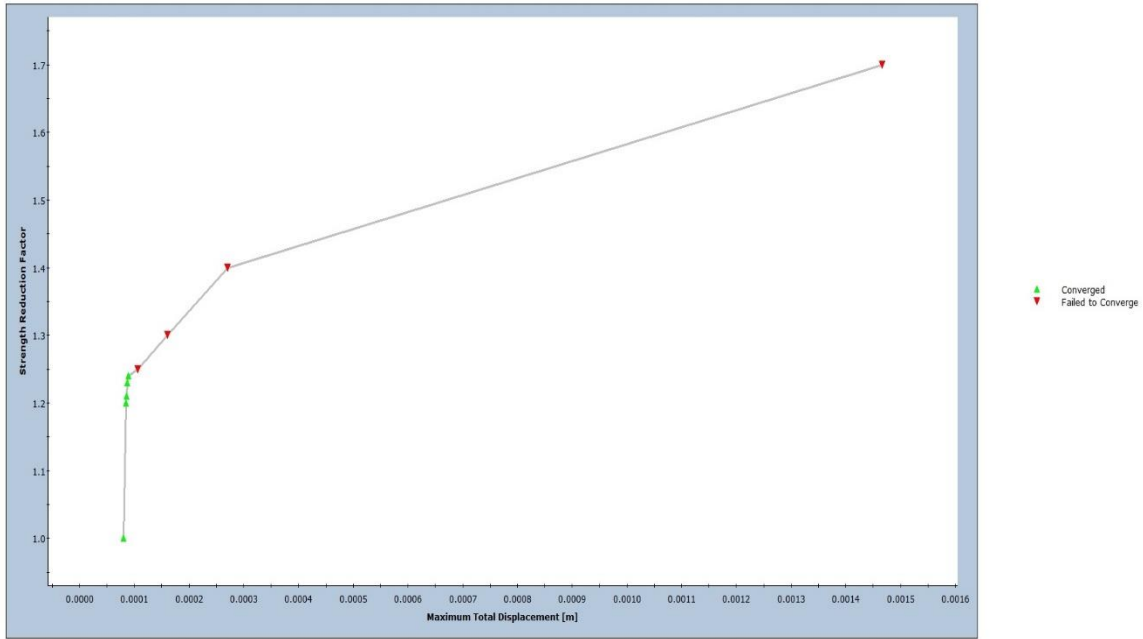


Figure 17.7: Shear Strength Reduction Plot (RS2)

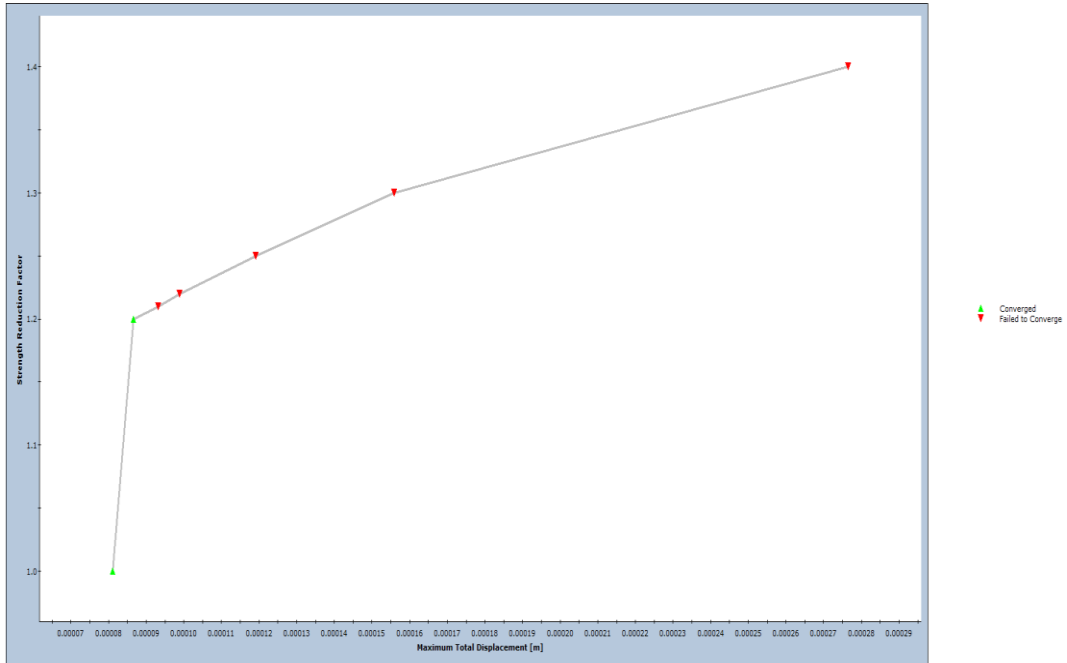


Figure 17.8: Shear Strength Reduction Plot (RS2-Joint convergence improved)

18. Step-Path Failure with Continuous Joints

18.1. Introduction

This verification looks at an example application in:

Itasca Consulting Group Inc. (2011). Step-Path Failure of Rock Slopes. In I. C. Inc., *UDEC Version 5.0 Example Applications* (pp. 13-1 to 13-9). Minneapolis.

18.2. Problem Description

RS2 was used to analyze the step-path failure in a rock slope containing three continuous joints. Step-path failure occurs when shear failure along joints combines with shear and tensile failure in the intact rock bridging between joints. RS2 results are compared to the UDEC results provided in the reference.

18.3. Geometry and Properties

Table 18.1: Slope Geometry and Properties

Slope Height (m)	Slope Angle (deg)	Joint Angle (deg)	ϕ' joint (deg)	Joint Spacing (m)	γ (kN/m ³)
11.8	50	36.1	35	0.883	19.62

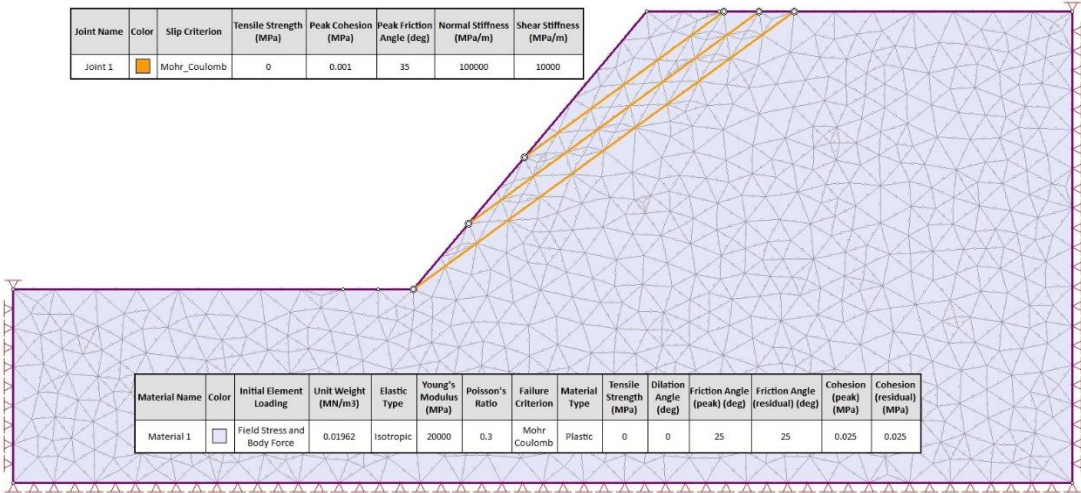


Figure 18.1: RS2 Slope Geometry and Material Properties

18.4. Results

Table 18.2: Factor of Safety

Factor of Safety – RS2 with joint improvement	Factor of Safety – RS2 without joint improvement	Factor of Safety – UDEC
1.0	1.01	1.01

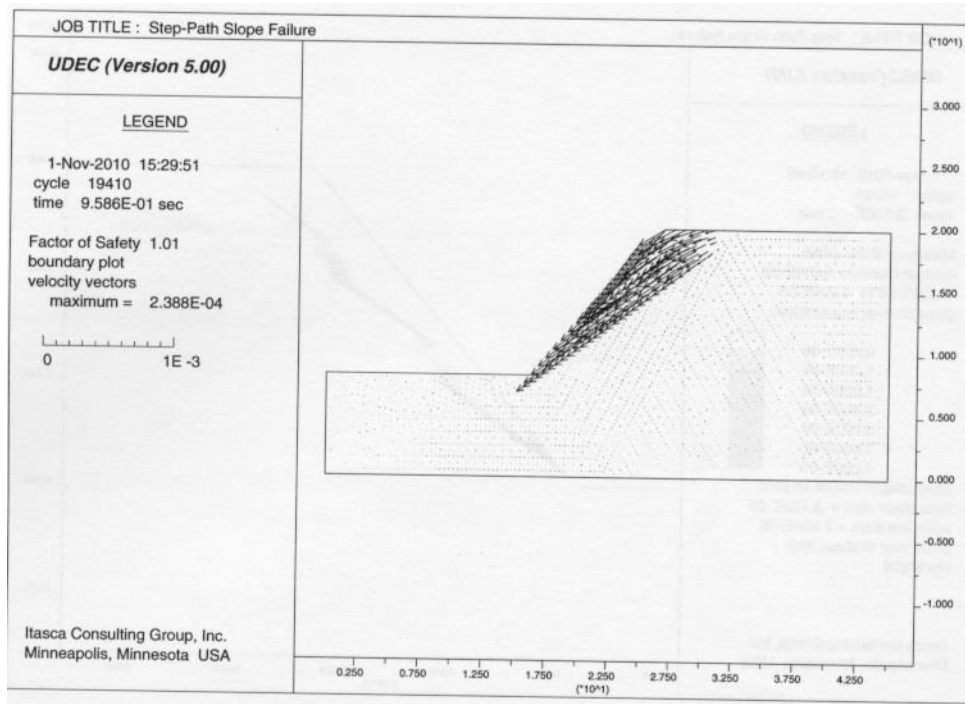


Figure 18.2: Velocity Vectors (UDEC, 2011)

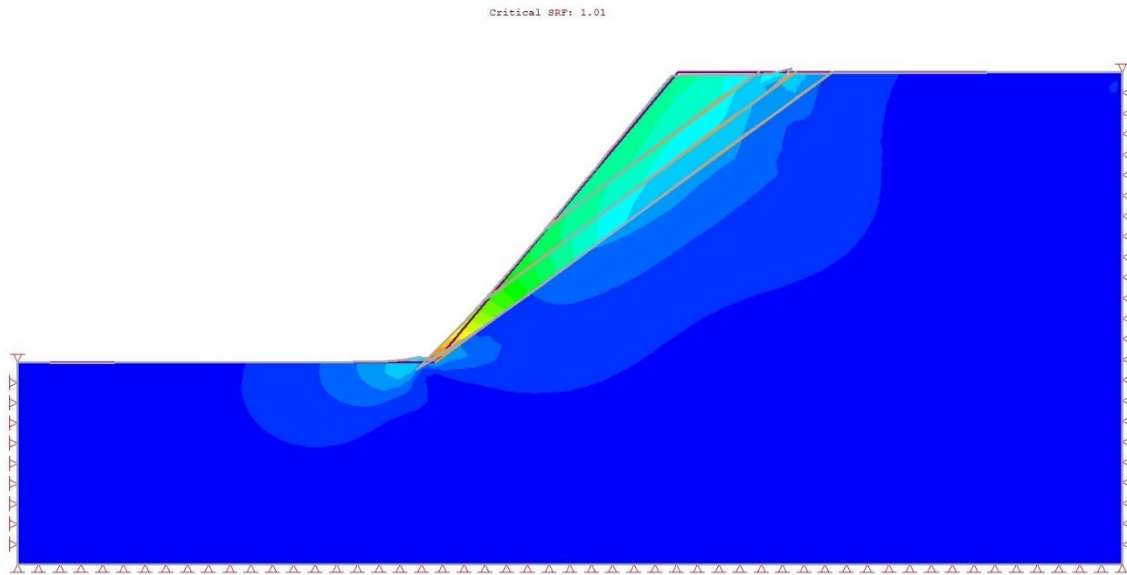


Figure 18.3: Total Displacement at SRF = 1.01(RS2)

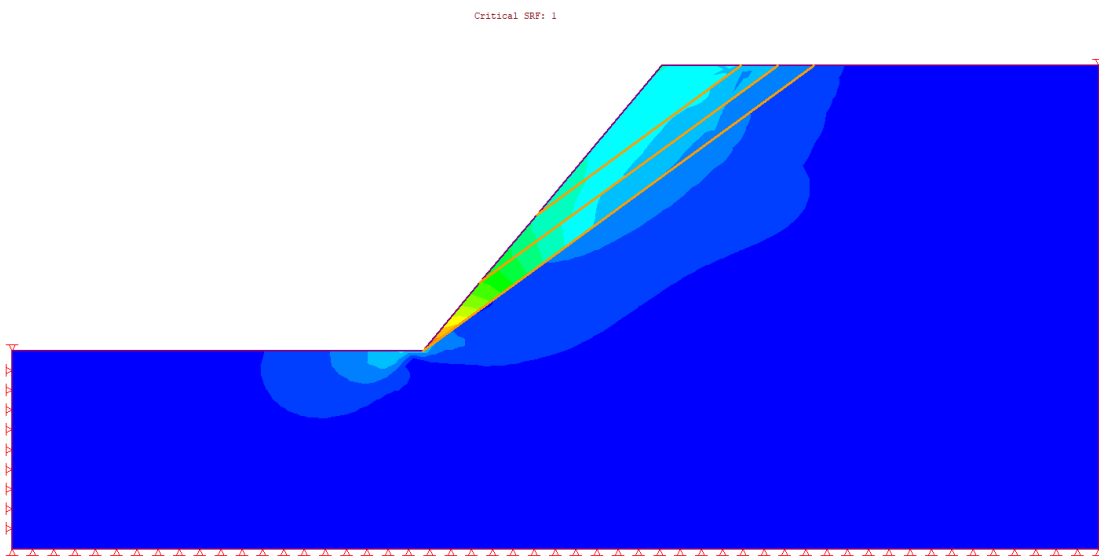


Figure 18.4: Total Displacement at SRF = 1.0(RS2-Joint convergence improved)

19. Bi-Planar Step-Path Failure

19.1. Introduction

This verification looks at an example application in:

Yan, M., Elmo, D., & Stead, D. (2007). Characterization of Step-Path Failure Mechanisms: A Combined Field-Based Numerical Modelling Study. In E. Eberhardt, D. Stead, & T. Morrison, *Rock Mechanics Meeting Society's Challenges and Demands Volume 1: Fundamentals, New Technologies and New Ideas* (p. 499). London, U.K.: Taylor and Francis Group.

19.2. Problem Description

RS2 and UDEC were used to analyze the step-path failure in a rock slope containing two discontinuous joints. Step-path failure occurs when shear failure along joints combines with shear and tensile failure in the intact rock bridging between joints. Given the same material properties, RS2 results are compared to UDEC results.

19.3. Geometry and Properties

Table 19.1: Slope Geometry and Properties

Slope Height (m)	Slope Angle (deg)	Joint Angle (deg)	ϕ' joint (deg)	γ (kN/m ³)
50	50	59	40	27

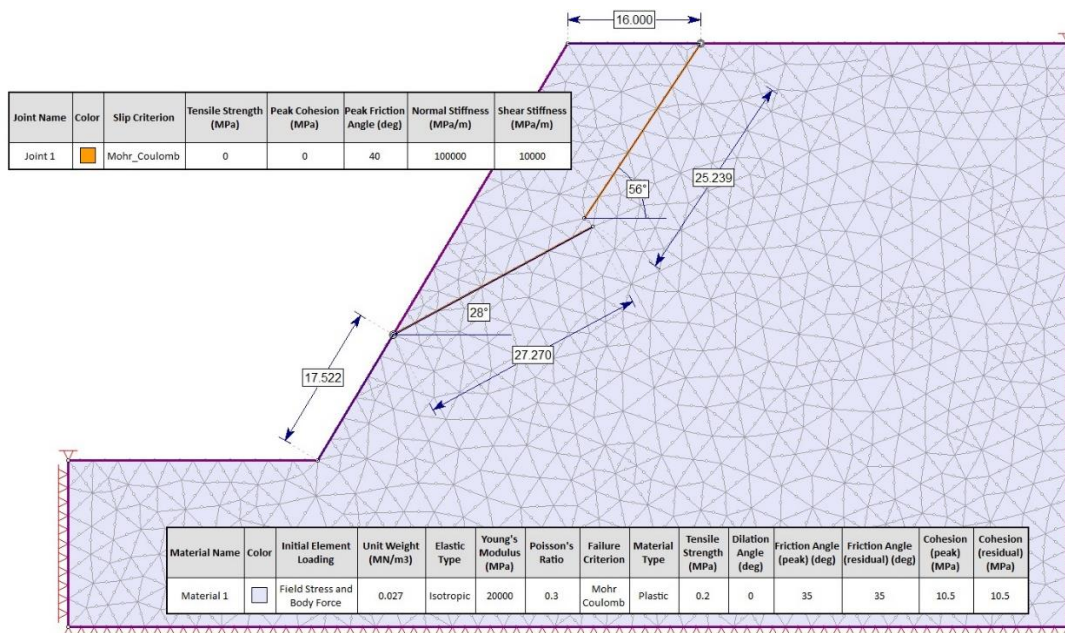


Figure 19.1: RS2 Slope Geometry and Material Properties

19.4. Results

Table 19.2: Factor of Safety

Factor of Safety – RS2 with joint improvement	Factor of Safety – RS2 without joint improvement	Factor of Safety – UDEC
1.41	1.5	1.46

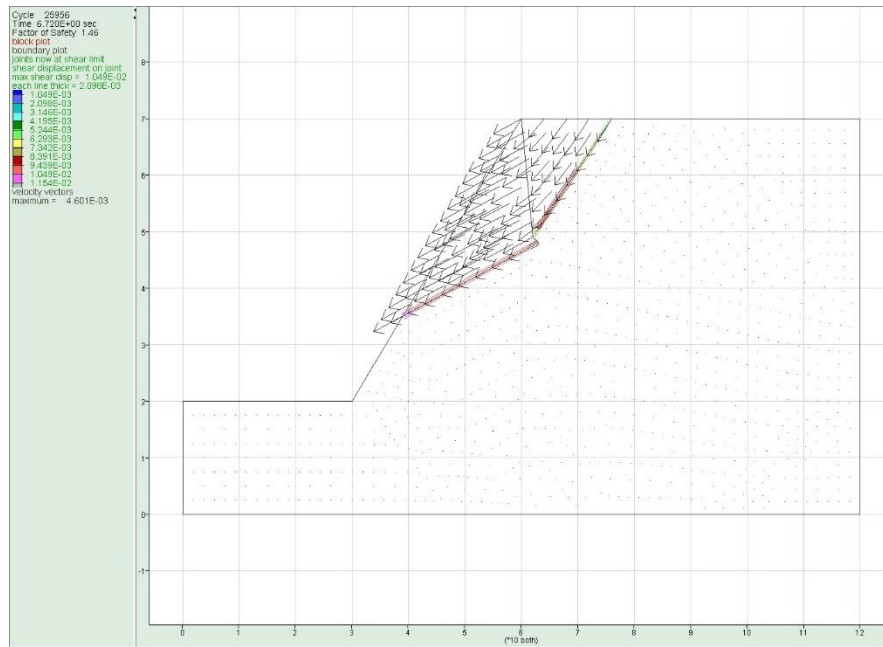


Figure 19.2: Velocity Vectors and Shear along Joints (UDEC)

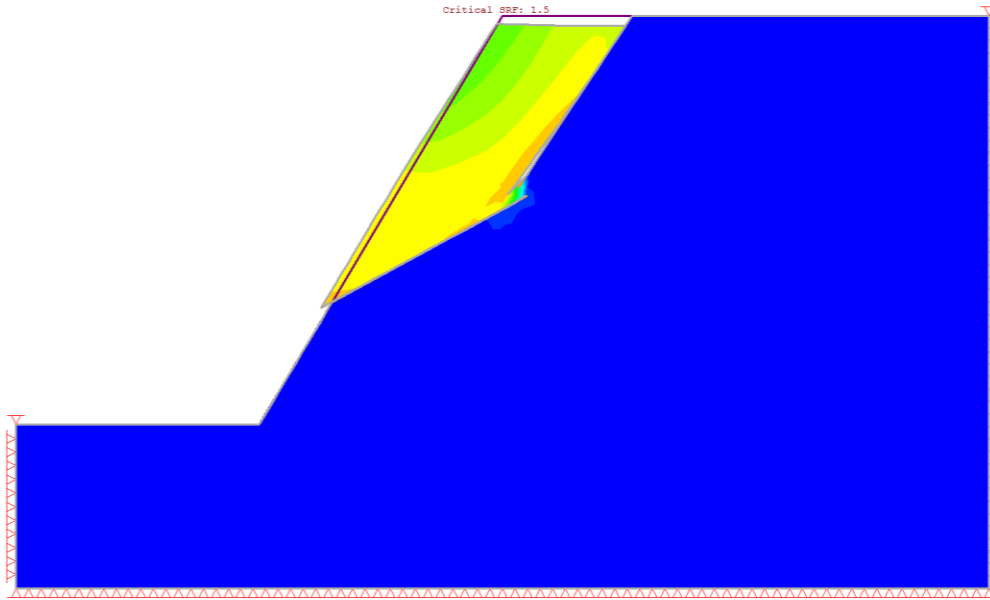


Figure 19.3: Total Displacement at SRF = 1.5 (RS2)

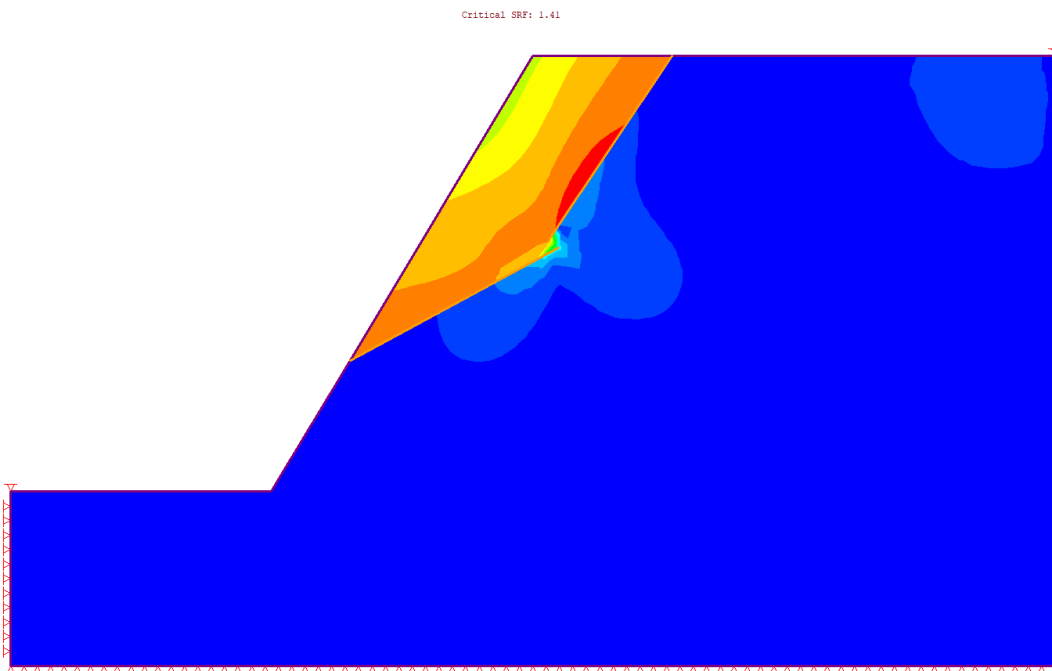


Figure 19.4: Total Displacement at SRF = 1.41 (RS2-Joint convergence improved)

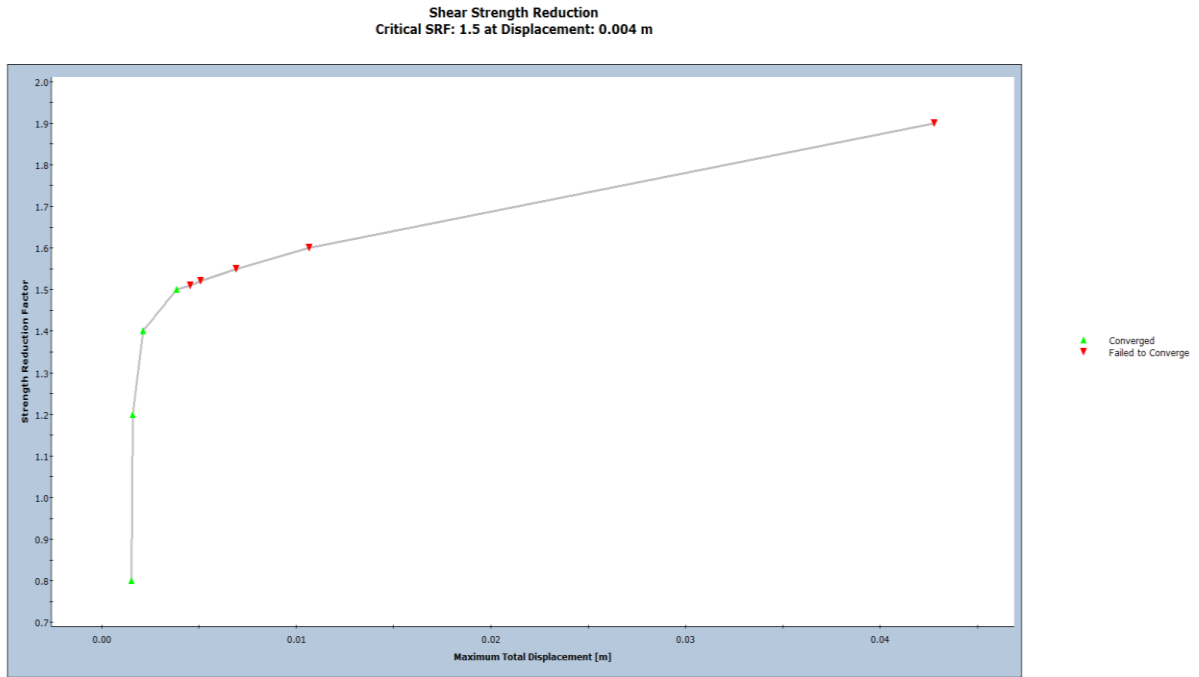


Figure 19.5: Shear Strength Reduction Plot (RS2)

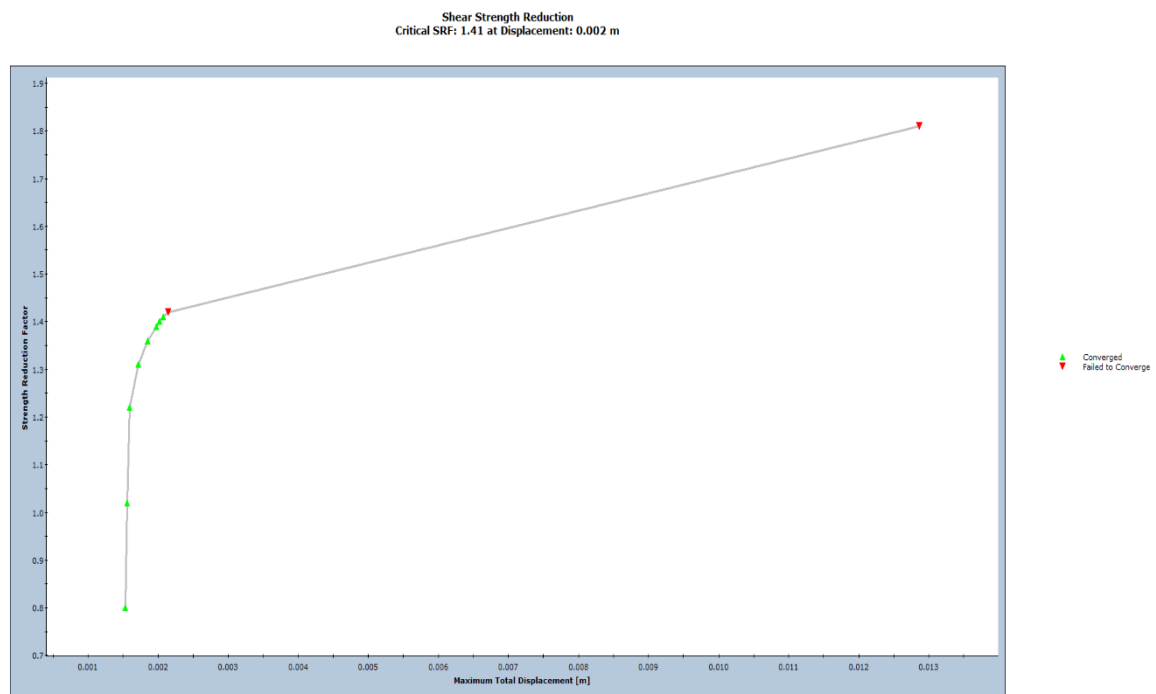


Figure 19.6: Shear Strength Reduction Plot (RS2-Joint convergence improved)

20. Hammah and Yacoub Slope with Voronoi Joints

20.1. Introduction

This verification looks at an example in:

Hammah, R. E., Yacoub, T., & Curran, J. H. (2009). Variation of Failure Mechanisms of Slopes in Jointed Rock Masses with Changing Scale. *Proceedings of the 3rd CANUS Rock Mechanics Symposium*, (pp. 1-8). Toronto.

20.2. Problem Description

RS2 and UDEC were used to analyze the mode of failure in a slope with blocky rock masses. These blocks were modelled using the Voronoi tessellation. Voronoi joints were first generated in UDEC, and then the geometry was imported into RS2.

20.3. Geometry and Properties

Table 20.1: Model Geometry and Properties

Slope Height (m)	Slope Angle (deg)	Joint Cohesion (MPa)	ϕ' Joint (deg)	γ (kN/m ³)
60	71.6	0.5	20	27

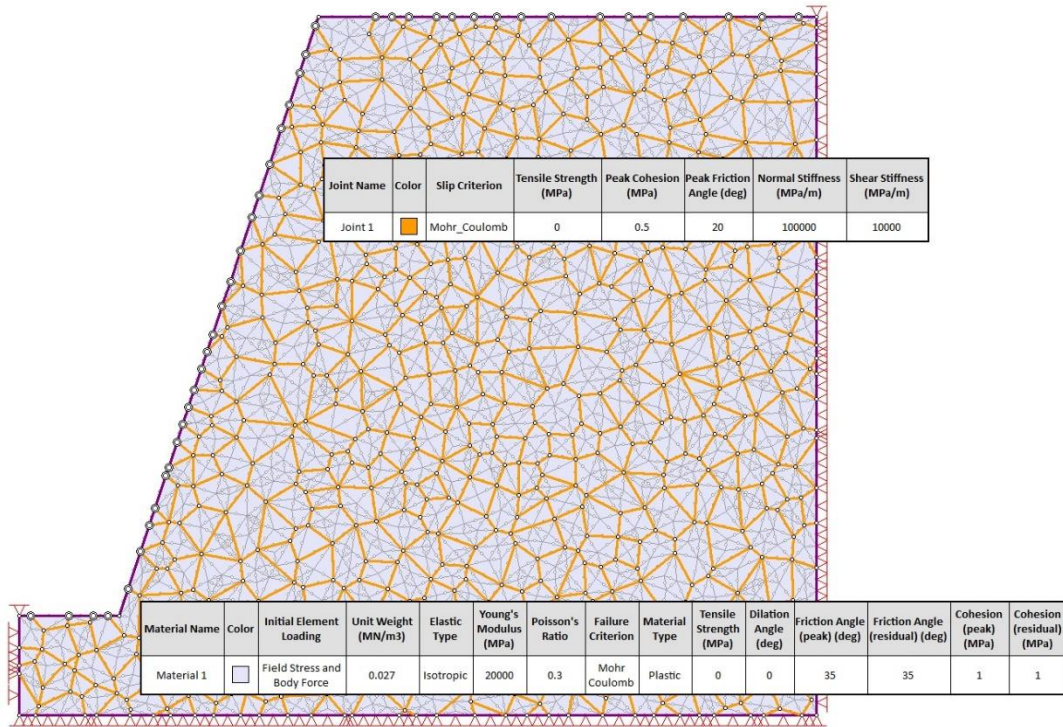


Figure 20.1: RS2 Model Geometry and Material Properties

20.4. Results

Table 20.2: Factor of Safety

Factor of Safety – RS2 with joint improvement	Factor of Safety - RS2 without joint improvement	Factor of Safety - UDEC
2.37	2.21	2.46

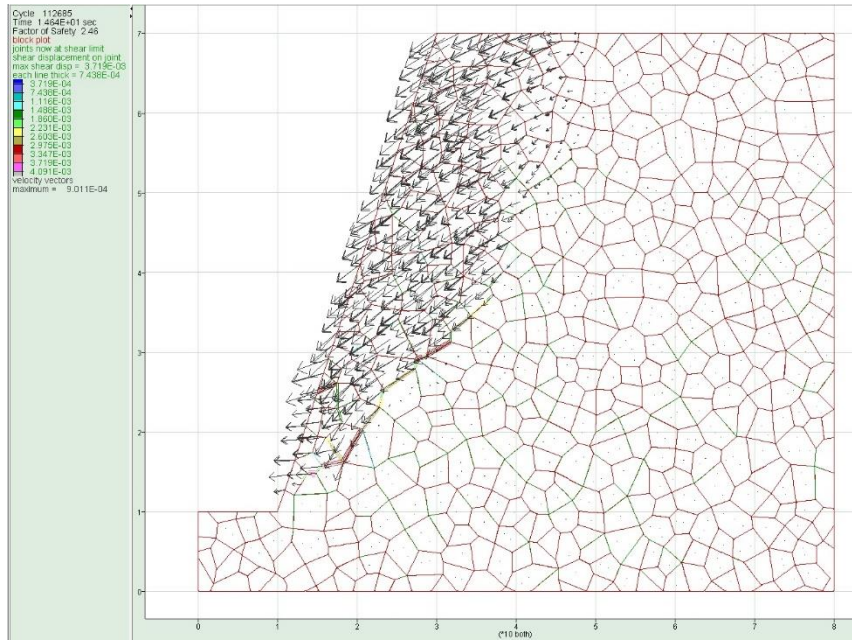


Figure 20.2: Velocity Vectors and Shear along Joints (UDEC)

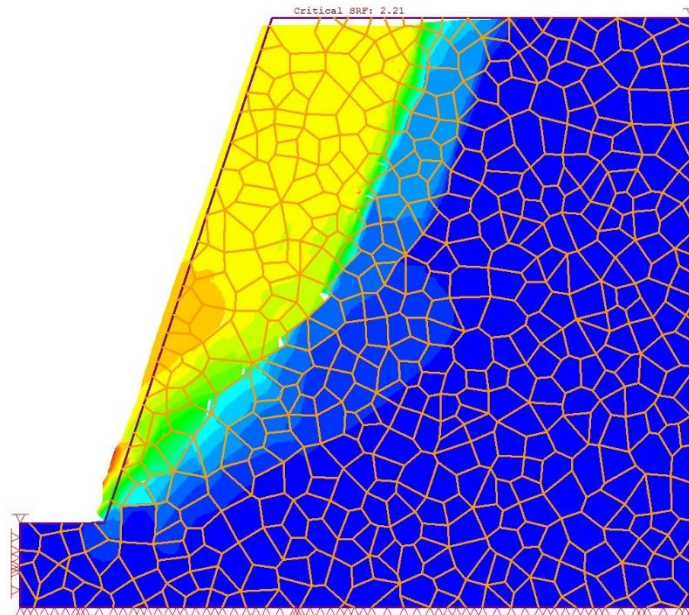


Figure 20.3: Velocity Vectors and Shear along Joints (UDEC)

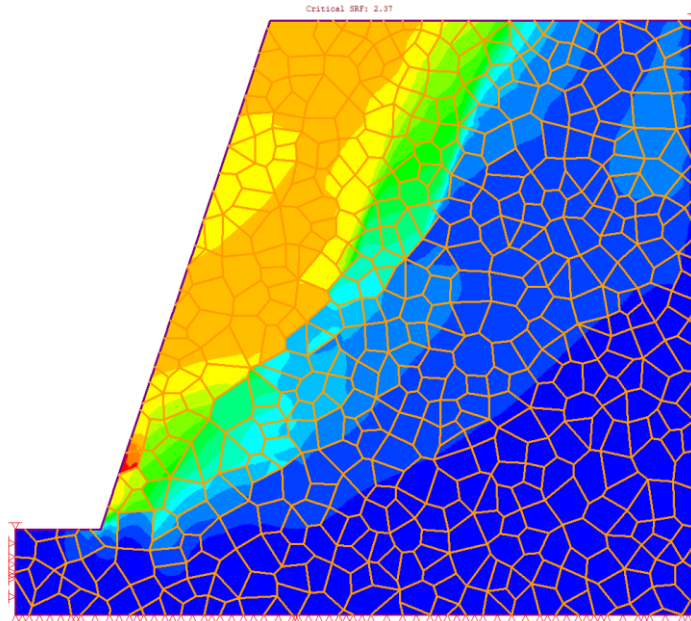


Figure 20.4: Total Displacement (RS2-Joint convergence improved)

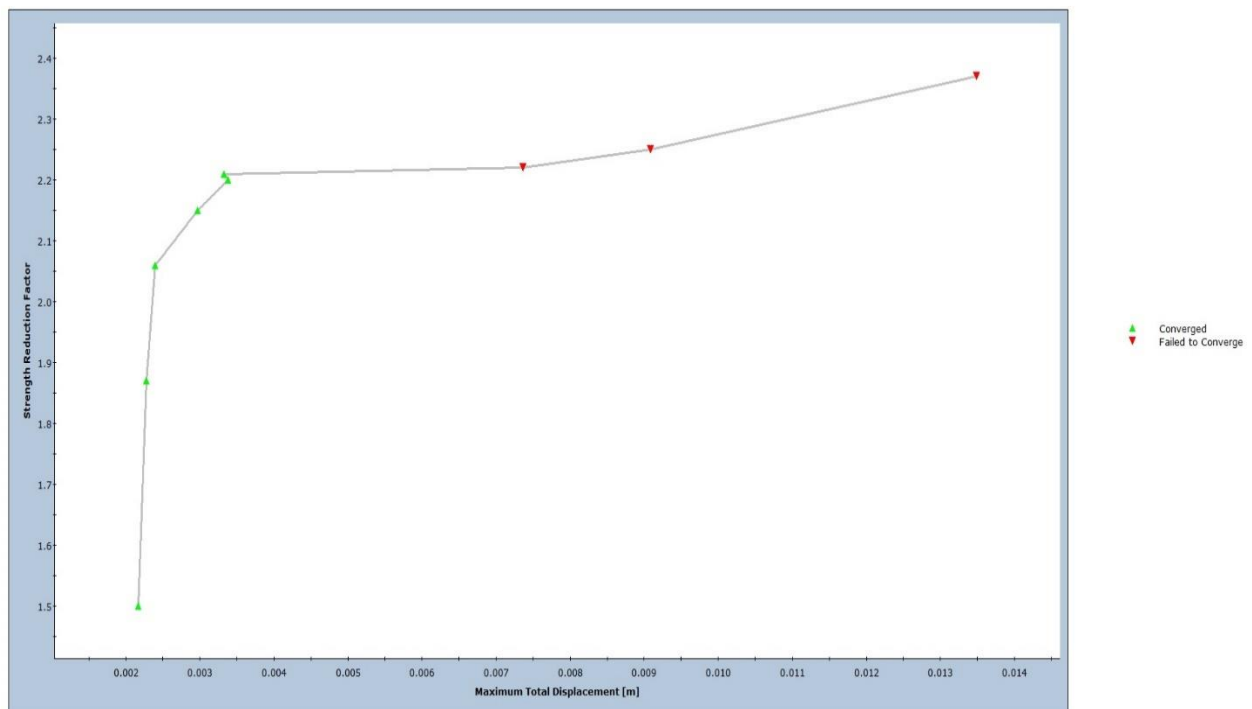


Figure 20.5: Shear Strength Reduction (RS2)

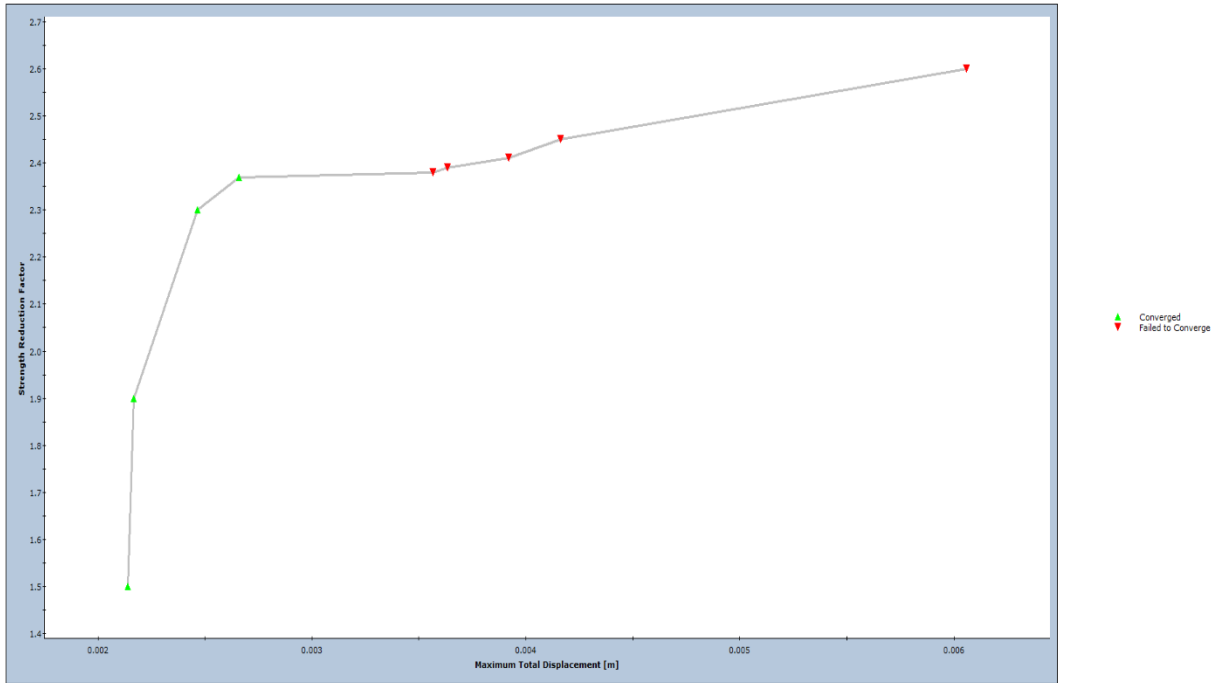


Figure 20.6: Shear Strength Reduction (RS2-Joint convergence improved)

21. Shallow Excavation - Tunnel

21.1. Introduction

This verification looks at a tutorial example in:

Itasca Consulting Group Inc. (2011). A Simple Tutorial - Use of GIIC. In I. C. Inc., *UDEC Version 5.0 User's Guide* (pp. 2-17 to 2-29). Minneapolis.

21.2. Problem Description

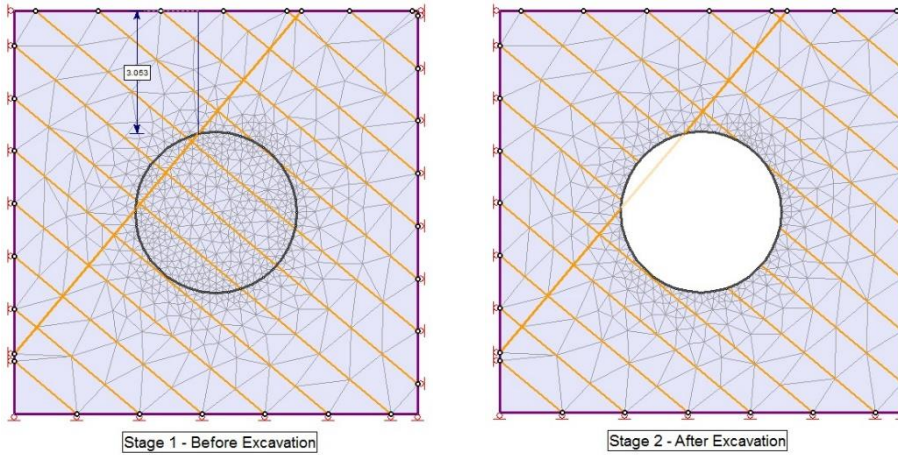
RS2 and UDEC were used to analyze the mode of failure in a tunnel at a shallow depth. The same material properties were applied in both software.

21.3. Geometry and Properties

Table 21.1: Model Geometry and Properties

Tunnel Radius (m)	Depth to Crown (m)	Bedding Angle (deg)	Fault Angle (deg)	γ (kN/m ³)
2	3	40	50	19.62

Joint Name	Color	Slip Criterion	Tensile Strength (MPa)	Peak Cohesion (MPa)	Peak Friction Angle (deg)	Normal Stiffness (MPa/m)	Shear Stiffness (MPa/m)
Joint 1		Mohr_Coulomb	0.1	0.1	40	10000	10000



Material Name	Color	Initial Element Loading	Unit Weight (MN/m3)	Elastic Type	Young's Modulus (MPa)	Poisson's Ratio	Failure Criterion	Material Type	Tensile Strength (MPa)	Dilation Angle (deg)	Friction Angle (peak) (deg)	Friction Angle (residual) (deg)	Cohesion (peak) (MPa)	Cohesion (residual) (MPa)
Material 1		Field Stress and Body Force	0.01962	Isotropic	17900	0.2	Mohr Coulomb	Plastic	0	0	35	35	10.5	10.5

Figure 21.1: RS2 Model Geometry and Material Properties

21.4. Results

Table 21.2: Factor of Safety

Factor of Safety – RS2 with joint improvement	Factor of Safety – RS2 without joint improvement	Factor of Safety – UDEC
8.5	8.27	8.16

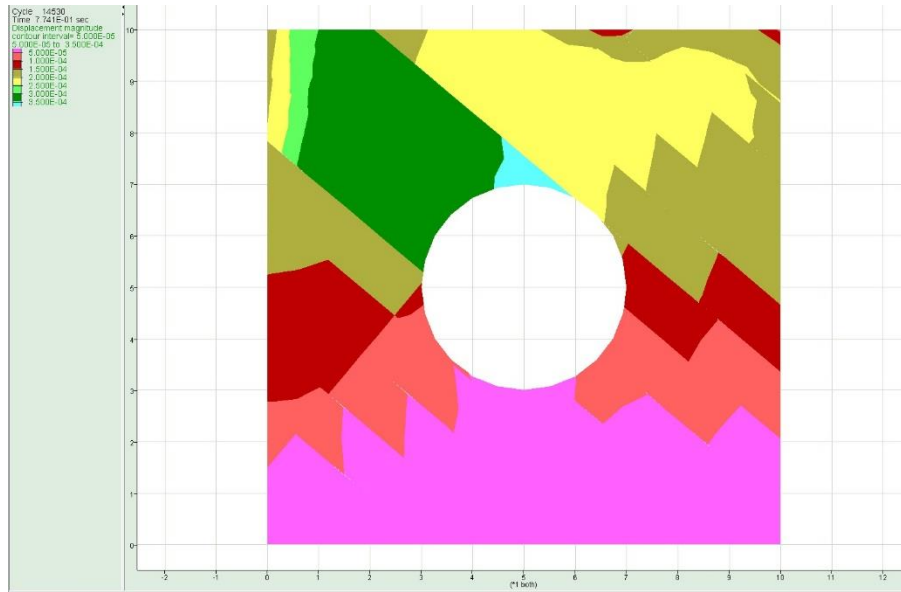


Figure 21.2: Total Displacement (UDEEC)

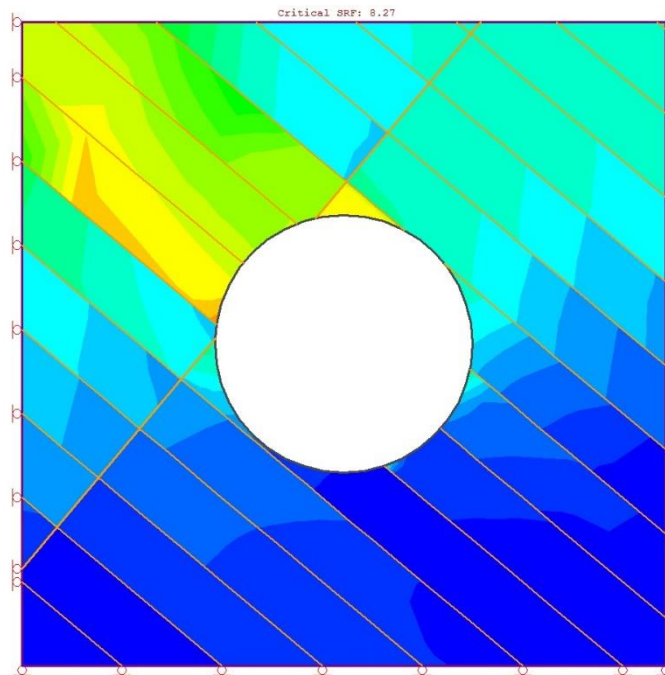


Figure 21.3: Total Displacement at SRF = 8.27 (RS2)

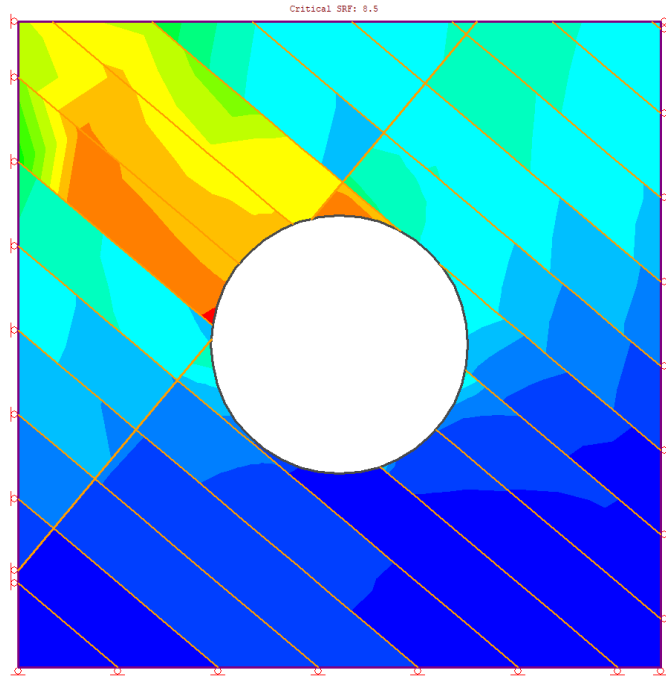


Figure 21.4: Total Displacement at SRF = 8.5 (RS2-Joint convergence improved)

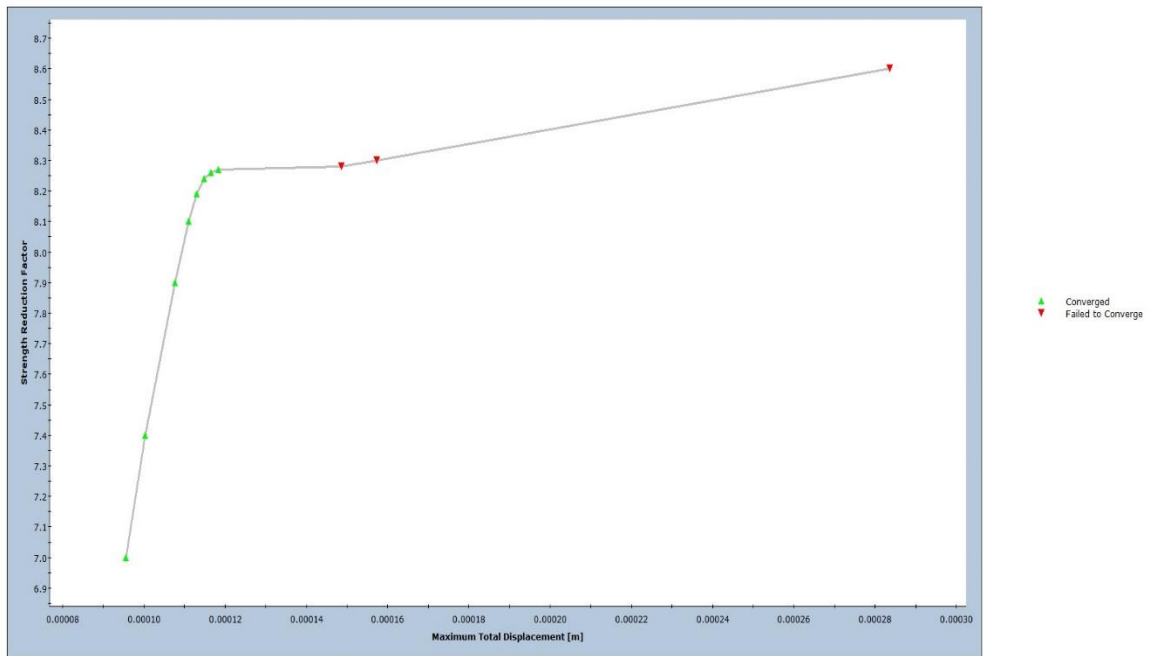


Figure 21.5: Shear Strength Reduction Plot (RS2)

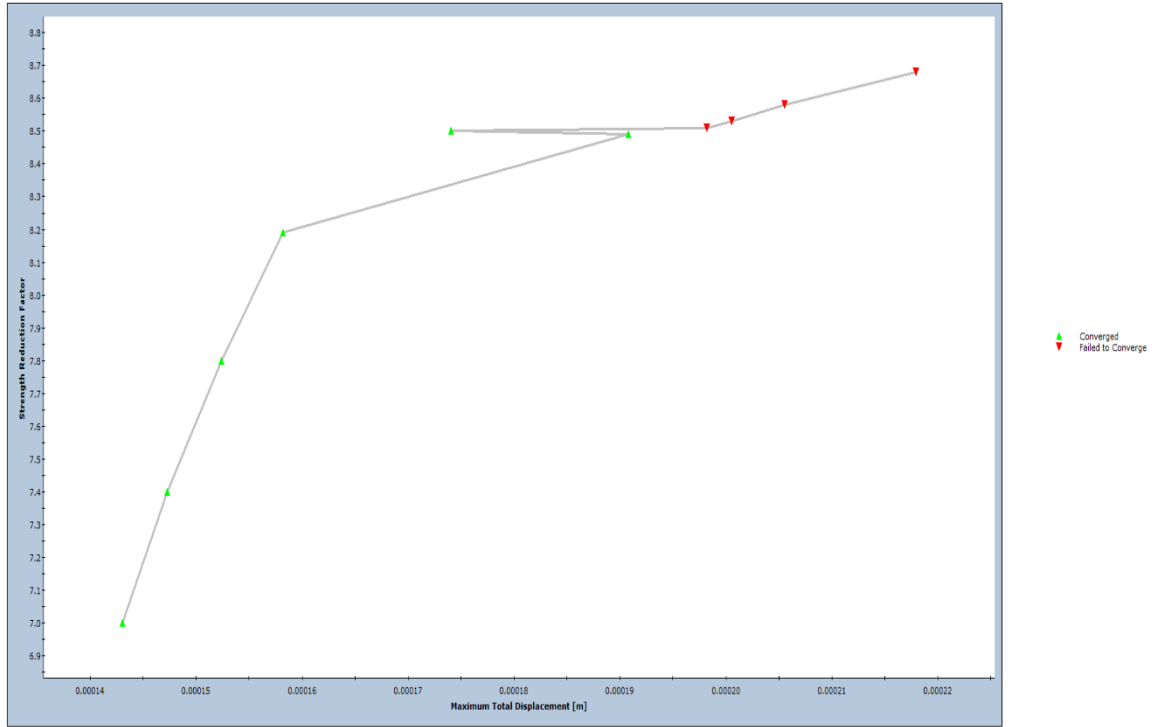


Figure 21.6: Shear Strength Reduction Plot (RS2-Joint convergence improved)

22. Joint Constitutive Model: Hyperbolic Softening

22.1. Introduction

This verification looks at an example in:

1. Deb, Debasis & Das. Kamal Ch (2010), "Extended finite element method for the analysis of discontinuities in rock masses". Geotech. Geol. Eng., Vol. 28, pp. 643-659
2. Esterhuizen, J., Filz, G.M. and Duncan, J.M., Constitutive Behaviour of Geosynthetic Interfaces, Journal of GeoTechnical and Geoenvironmental Engineering, October 2001, pp 834-840.

22.2. Formulation and Problem description

The Hyperbolic Softening joint model was developed based on the geosynthetic Hyperbolic slip criterion [2] which can be used for modeling the shear strength of the interface between a geosynthetic (e.g geotextile or geogrid) and soil. The model accounts for the softening of the geosynthetic by two methods: displacement softening and plastic work softening. Both methods were implemented in RS2. Generally, shear strength is defined by the following equation:

$$\tau = \frac{\sigma_{\infty} \sigma_n \tan \phi_0}{\sigma_{\infty} + \sigma_n \tan \phi_0}$$

where σ_n is normal stress; σ_{∞} is adhesion at $\sigma_n = \infty$; and ϕ_0 is the interface friction angle at $\sigma_n=0$.

In addition to mentioned parameters, the following parameters are required for the model: residual friction angle (ϕ_r), residual adhesion (σ_r), initial curve of the stress-strain displacement from experiment (k), and the plastic shear displacement that must take place to reach the residual strength (δ_r^p).

In order to verify the joint constitutive model, direct simple shear tests with large displacement in [2] were simulated. Displacement was applied to one face of the joint and stress was measured with the corresponding displacement. Material properties used in the simulation are shown in *Table 22.1*. The direct shear tests were simulated in two cases: constant pressure $P = 345$ kPa and different pressures ($P = 35$ kPa and 345 kPa). Note that only in the cases of vertical pressure changed dramatically, the work softening method should be chosen in order to capture soil-geosynthetic behavior.

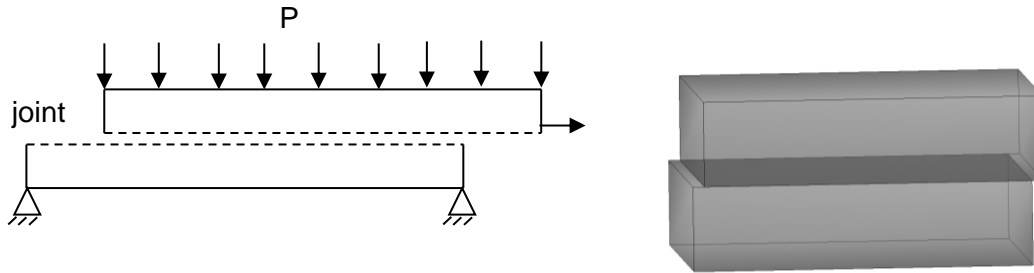


Figure 22.1: Problem description. a) Problem geometry; b) Representative mesh

Table 22.1: Input Parameters for Direct Shear Test

Parameter	Values
Peak adhesion (σ_{∞})	143 kPa
Residual adhesion (σ_r)	76 kPa
Peak friction angle (ϕ_0)	26.8 Degrees
Residual friction angle (ϕ_r)	18.4 Degrees
Initial stress strain curve slope (k)	20,000 MPa/m
Plastic shear displacement to reach residual strength (δ_r^p)	100 (mm)
Normal stiffness (K_n)	48,000 MPa/m
Shear stiffness (K_s)	48,000 MPa/m

22.3. Results

Results obtained from RS2 were compared with the experimental results [2] in 2 cases: constant vertical stress and varied vertical stresses. The results agree well with the experimental data. The displacement softening failed to capture the geosynthetic behavior when the applied pressure changed from 35 kPa to 345 kPa. Work softening can supplement for the displacement softening. The use of the work softening; however, is only recommended when the vertical stress varies considerably because of the computational load associated with the work softening.

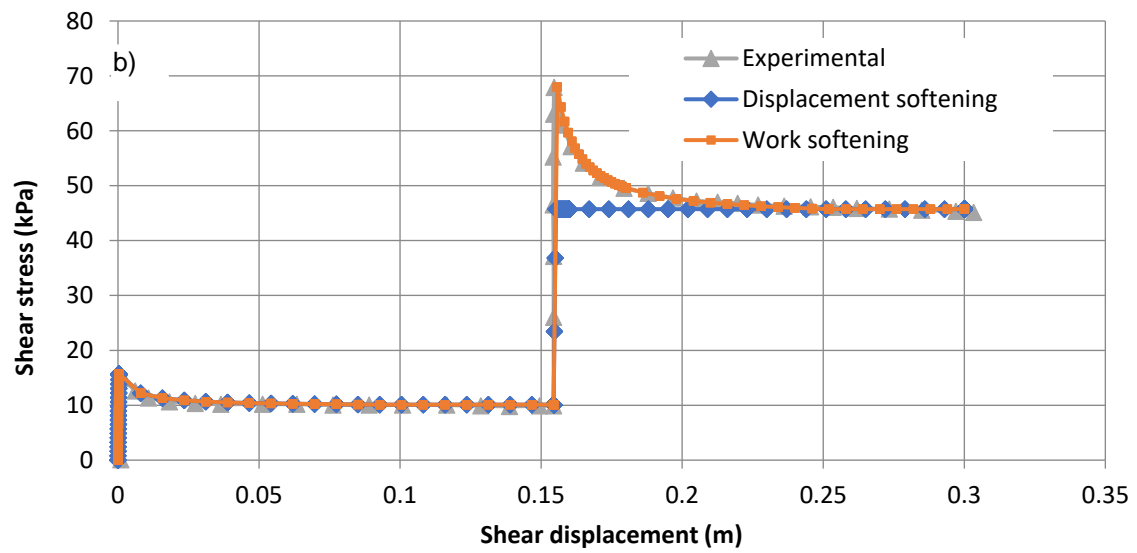
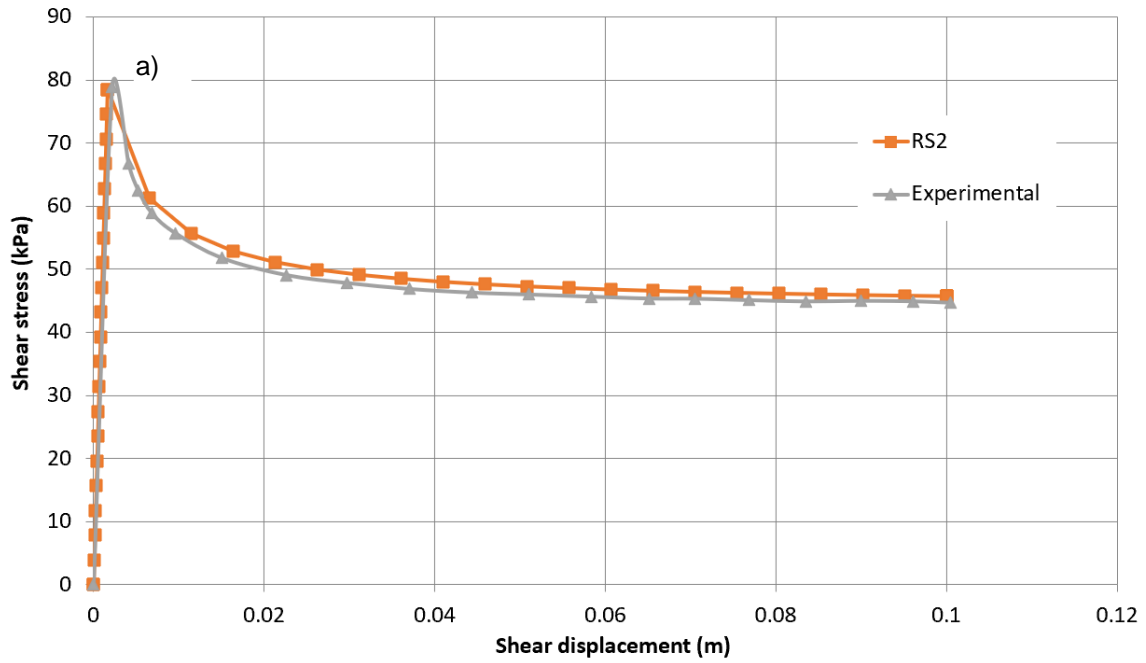


Figure 22.2: Stress-shear displacement curve; a) Constant pressure; b) Varied pressures.

23. Joint Constitutive Model: Mohr Coulomb with Residual Strength and Dilation

23.1. Introduction

This verification looks at a joint constitutive model with Mohr Coulomb slip criterion, where residual strength and joint dilation are also included. References are:

1. Deb, Debasis & Das. Kamal Ch (2010), "Extended finite element method for the analysis of discontinuities in rock masses". Geotech. Geol. Eng., Vol. 28, pp. 643-659
2. Esterhuizen, J., Filz, G.M. and Duncan, J.M., Constitutive Behaviour of Geosynthetic Interfaces, Journal of GeoTechnical and Geoenvironmental Engineering, October 2001, pp 834-840.

23.2. Formulation and Problem Description

23.2.1. Formulation

The joint constitutive model is the generalization of the Coulomb friction law. Both shear and tensile failure are considered, joint dilation and residual strength are also included.

In the elastic range, the behavior is governed by the joint normal and shear stiffnesses, k_n and k_s (Compression is negative).

The contact displacement increments are used to calculate the elastic force increments. The normal force increment and the shear force increment are updated using the following equations:

$$\Delta\sigma_n = k_n\Delta u_n \quad (23.1)$$

$$\Delta\tau = k_s\Delta u_s \quad (23.2)$$

The instantaneous loss of strength approximates the "displacement-weakening" behavior of a joint. The new forces are corrected by

$$\text{For tensile failure} \quad \text{if } \sigma_n > T_{max}, \sigma_n = T_{residual}$$

$$\text{For shear failure} \quad \text{if } \|\sigma_s\| > S_{max}, \|\sigma_s\| = S_{residual}$$

where $S_{max} = c - \sigma_n \tan\phi$ and $S_{residual} = c_{residual} - \sigma_n \tan\phi_{residual}$

Dilation takes place only when the joint is at slip. The plastic shear displacement magnitude (Δu_s) is then calculated and the dilation displacement in the normal direction is then calculated by

$$\Delta u_{n(dil)} = \Delta u_{s(plastic)} \tan\gamma \quad (23.3)$$

where γ is the dilation angle.

The normal force must be corrected to account for the effect of dilation

$$\sigma_n = \sigma_n - k_n\Delta u_n \quad (23.4)$$

In RS2, directional dilation can be accounted for or can be ignored (i.e. joint will shrink if slipped in the opposite direction). User can also specify min and max shear displacement (d_{min} and d_{max}) when the dilation is activated.

23.2.2. Problem Description

In order to verify the joint constitutive model, direct simple shear tests with large displacement in were simulated (see Figure 23.1). Displacement was applied to one face of the joint and stress was measured with the corresponding displacement.

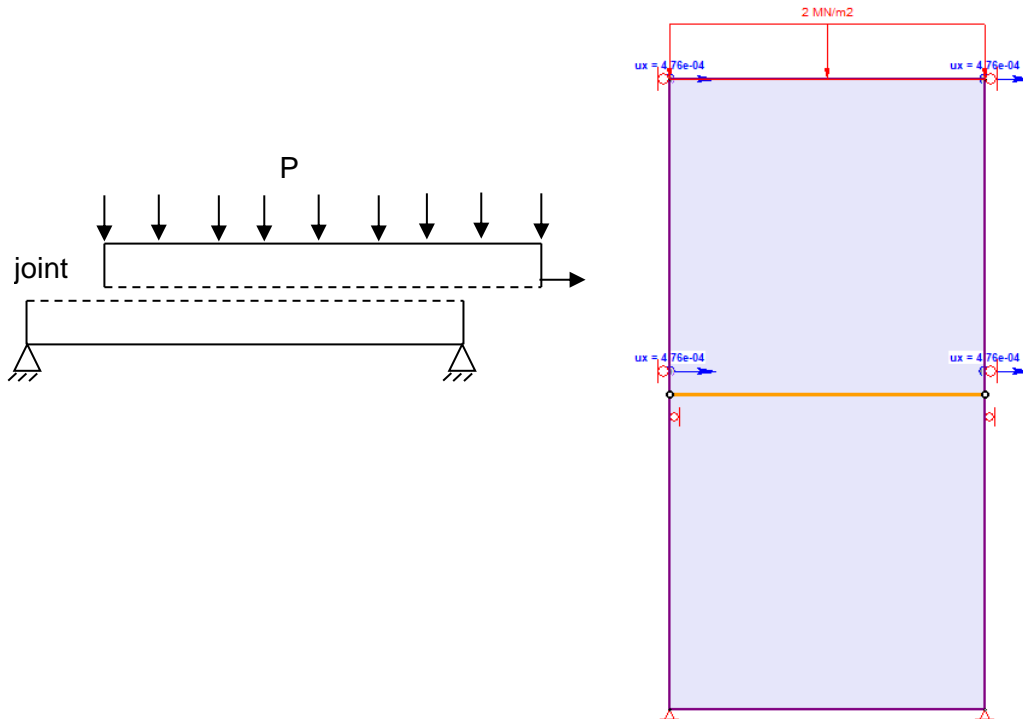


Figure 23.1: Problem description. a) Problem geometry; b) Representative mesh

23.2.3. Dilation

To verify the dilation angle, the shear test was simulated with four stages. At the first stage, a normal pressure of 3 MPa was applied to the surface. The direct shear test was performed until the shear displacement reached the value of 1mm. And then the normal pressure was increased to 9 MPa. The shear test was then continued until the shear displacement reach 2mm. Four simulations were performed with different values of dilation angles (0, 10, 20 and 30 degrees) Material properties are shown in Table 23.1.

Table 23.1 Input parameters for one-dimensional rock column model

Parameter	Value
Poisson's ratio	0.01
Cohesion	10 kPa

Friction angle	30 degrees
Normal stiffness (k_n)	10 GPa/m
Shear stiffness (k_s)	10 GPa/m
Dilation angle	0, 10, 20 and 30 degrees
Residual cohesion	10 kPa
Residual friction angle	30 degrees

23.2.4. Directional Dilation

In order to compare the different when accounting for directional dilation, a direct shear test was performed with a directional option on and off. Similar direct shear test with previous section was performed. The only difference is that when the shear displacement reaches 1 mm, the sample was sheared in the opposite direction until it reached the value of 1mm in that direction. Material properties are shown in Table 23.2.

Table 23.2: Input parameters for one-dimensional rock column model

Parameter	Value
Poisson's ratio	0.01
Cohesion	10 kPa
Friction angle	30 degrees
Normal stiffness (k_n)	30 GPa/m
Shear stiffness (k_s)	3 GPa/m
Dilation angle	20 degrees
Residual cohesion	10 kPa
Residual friction angle	30 degrees

23.3. Result and Discussion

23.3.1. Dilation

As shown in Figure 23.2, the angle between line of shear and normal displacement and the horizontal line is the dilation angle. At the first stage, the joint shrunk in the normal direction due to applied compressive pressure. As the joint slipped in stage 2, the dilation happened and the normal displacement was proportional to the shear displacement.

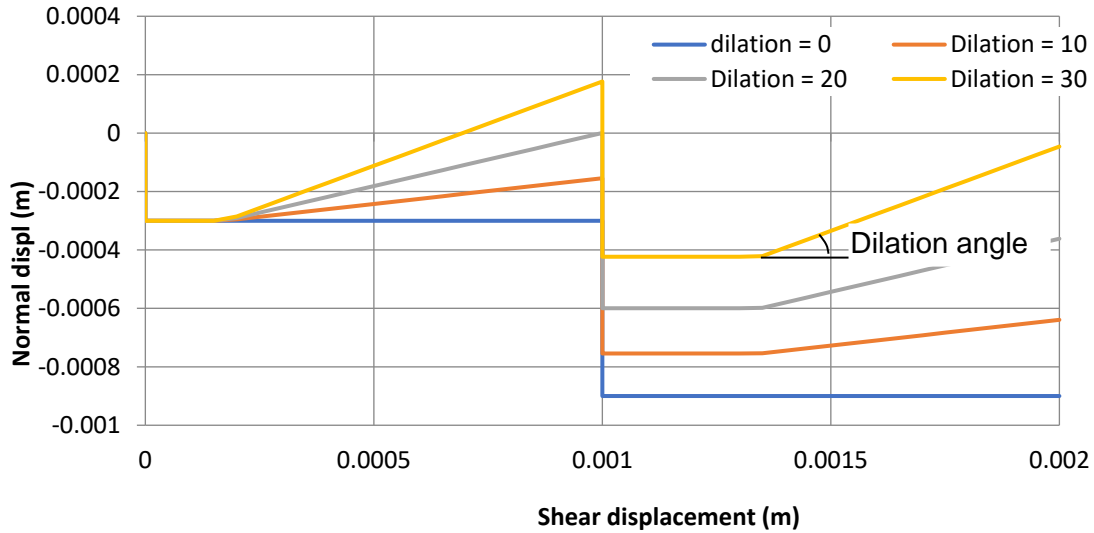


Figure 23.2: Mohr Coulomb model: Dilation angle

23.3.2. Directional Dilation

Joint responses corresponding to directional and non-directional dilation are shown in Figure 23.3. At the beginning, both options exhibited the same behavior until the shear displacement in the opposite direction was carried out. If the directional option was turned on, the joint shrunk if plastic shear displacement occurs in opposite direction. As long as the plastic shear displacement in the opposite direction balanced to the plastic shear displacement in the previous direction, the joint dilated again. However, if the option was turned off, the joint kept dilating without considering the direction of the shear displacement.

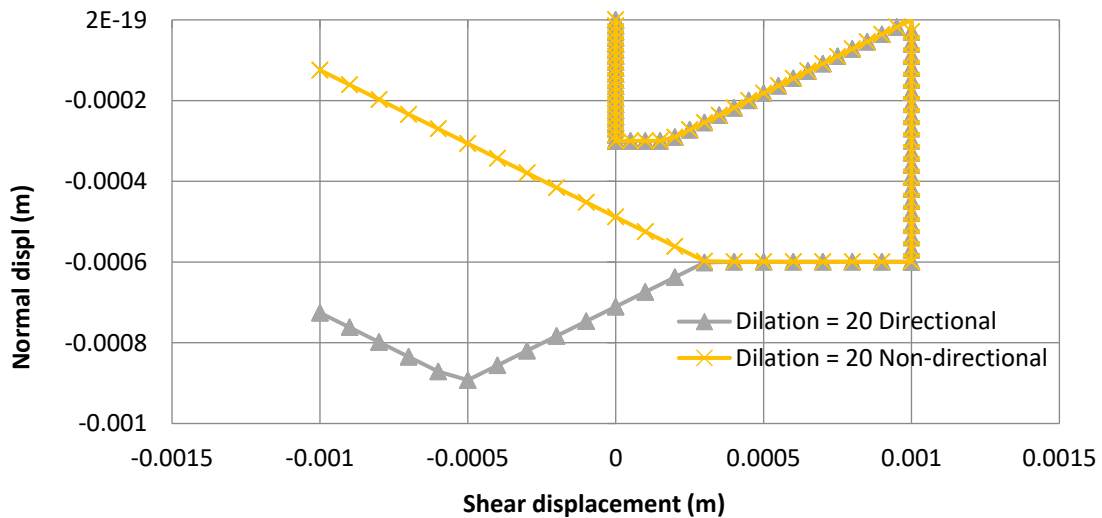


Figure 23.3: Mohr Coulomb model: Directional dilation

Bibliography

Alejano, L. R., & Alonso, E. (2005). Application of the 'Shear and Tensile Strength Reduction Technique' to Obtain Factors of Safety of Toppling and Footwall Rock slopes. *Eurock: Impact of Human Activity on the Geological Environment*.

Alejano, L. R., Ferrero, A. M., Ramirez-Oyanguren, P., & Alvarez Fernandez, M. I. (2011). Comparison of Limit-Equilibrium, Numerical and Physical Models of Wall Slope Stability. *International Journal of Rock Mechanics and Mining Sciences*, 16-26.

Alzo'ubi, A. K., Martin, C. D., & Cruden, D. (2010, June 18). Influence of Tensile Strength on Toppling Failure in Centrifuge Tests. *International Journal of Rock Mechanics and Mining Sciences*, pp. 974-982.

Barla, G., Borri-Brunetto, M., Devin, P., & Zaninetti, A. (1995). Validation of a Distinct Element Model for Toppling Rock Slopes. *8th International Congress on Rock Mechanics*, (pp. 417-421). Tokyo, Japan.

Deb, Debasis & Das. Kamal Ch (2010), "Extended finite element method for the analysis of discontinuities in rock masses". *Geotech. Geol. Eng.*, Vol. 28, pp. 643-659

Esterhuizen, J., Filz, G.M. and Duncan, J.M., Constitutive Behaviour of Geosynthetic Interfaces, *Journal of GeoTechnical and Geoenvironmental Engineering*, October 2001, pp 834-840.

Goodman, R. E., & Bray, J. W. (1976). Toppling of Rock Slopes. *Rock Engineering for Foundations and Slopes* (pp. 201 - 234). New York: American Society of Civil Engineers.

Hammah, R. E., Yacoub, T., & Curran, J. H. (2009). Variation of Failure Mechanisms of Slopes in Jointed Rock Masses with Changing Scale. *Proceedings of the 3rd CANUS Rock Mechanics Symposium*, (pp. 1-8). Toronto.

Itasca Consulting Group Inc. (2011). A Simple Tutorial - Use of GIIC. In I. C. Inc., *UDEC Version 5.0 User's Guide* (pp. 2-17 to 2-29). Minneapolis.

Itasca Consulting Group Inc. (2011). Step-Path Failure of Rock Slopes. In I. C. Inc., *UDEC Version 5.0 Example Applications* (pp. 13-1 to 13-9). Minneapolis.

Lanaro, F., Jing, L., Stephansson, O., & Barla, G. (1997, April - June). D.E.M. Modelling of Laboratory Tests of Block Toppling. *International Journal of Rock Mechanics and Mining Sciences*, pp. 173e1 - 173e15.

Lorig, L., & Varona, P. (2004). Plane Failure - Daylighting and Non-Daylighting. In D. C. Wyllie, & C. W. Mah, *Rock Slope Engineering Civil and Mining 4th Edition* (pp. 233-235). New York: Spon Press Taylor & Francis Group.

Lorig, L., & Varona, P. (2004). Toppling Failure - Block and Flexural. In D. C. Wyllie, & C. W. Mah, *Rock Slope Engineering Civil and Mining 4th Edition* (pp. 234-238). New York: Spon Press Taylor & Francis Group.

Pritchard, M. A., & Savigny, K. W. (1990). Numerical Modelling of Toppling. *Canadian Geotechnical Journal*, 823-834.

Yan, M., Elmo, D., & Stead, D. (2007). Characterization of Step-Path Failure Mechanisms: A Combined Field-Based Numerical Modelling Study. In E. Eberhardt, D. Stead, & T. Morrison, *Rock Mechanics Meeting Society's Challenges and Demands Volume 1: Fundamentals, New Technologies and New Ideas* (p. 499). London, U.K.: Taylor and Francis Group.